Ligated and Metal Free Initiating Systems for the Living Anionic Polymerization of Alkyl (meth)acrylates

A Thesis
Submitted to the University of Pune
in Partial Fulfillment of the Requirements
for the Degree of

Doctor of Philosophy
in Chemistry

by

D. Baskaran

Division of Polymer Chemistry
National Chemical Laboratory
Pune- 411 008
India

December 1996

கற்க கசடறக் கற்பவை கற்றபின்
நிற்க அதற்குத் தக.

- திருவள்ளுவர், *திருக்குறள்*, 40-391.

Study thoroughly cleansing your mind with whatever you learn;
After learning, follow in life what you have learnt.

- Thiruvalluvar, *Thirukkural*, 40-391.

Declaration

Certified that the work incorporated in the thesis **" Ligated and Metal Free Initiating Systems for the Living Anionic Polymerization of Alkyl (meth)acrylates"** submitted by Mr. Durairaj Baskaran was carried out by the candidate under my supervision, such material as has been obtained from other sources has been dully acknowledged.

S. Sivaram

26th December 1996
Pune- 411 008

Dr. S. Sivaram
(Supervisor)

Acknowledgments

First of all I would like to acknowledge gratefully the German Academic Exchange Services (DAAD), Bonn, Germany as well as the Council of Scientific and Industrial Research (CSIR), India for the graduate fellowship through which I could complete my studies at the Institute of Physical Chemistry, University of Mainz, Germany.

A basic ground for my curiosity to do research on this most challenging and demanding field was the freedom I experienced with Dr. S. Sivaram, my guide and a man who considers the development of the students and their scientific training above any material goal. I would like to record my deep sense of gratitude to him for giving me encouragement, emotional support, understanding and character.

I am extremely grateful to Prof. Dr. Axel Müller who acted as my adviser for the research I carried out at the Institute for Physical Chemistry, University of Mainz, Germany. He introduced me to the art of kinetics of anionic polymerization, but more importantly the research methodology. A special thanks is extended to him for his personal friendship in and out of the laboratory and his continuous support to my scientific motivation.

It was a great pleasure to work with Dr. S. Chakrapani and I learnt synthetic techniques of inert atmosphere chemistry from him. I also thank him for the stimulating scientific arguments and discussions we had during the course of the work. I express my sincere thanks to Dr. H. Kolshorn, Institute for Organic Chemistry, University of Mainz, Germany for his extra efforts to the NMR investigations which we conducted during weekends. I also thank him for making me to understand the difficult topics of NMR in a simpler way.

Some of the ideas regarding the interpretation of the mysterious results of metal-free anionic polymerization spawned from a fruitful discussion that I had with Prof. Thieo E. Hogen-Esch, University of Southern California, Los Angeles, during his short visit to Germany.

I take this opportunity to extend my thanks to the members of Polymer Chemistry Division, National Chemical Laboratory, India and Anionic Working Group (AAK), Institute of Physical Chemistry, University of Mainz, Germany for their cooperation and friendship during the period of the research.

I am forever grateful to my parents and to my wife for their support, sacrifice and inspiring patience that served to lighten the moments of frustration, during the study. A special appreciation is due to all my friends both in Germany as well as in India with whom I interacted intellectually during this investigation.

24th December 1996,
Pune- 411 008.

(D. Baskaran)

Contents

Chapter 6
Metal Free Anionic Polymerization of Methyl Methacrylate Using Tetraphenylphosphonium as Counterion **99**

Chapter 7

Metal Free Anionic Polymerization of Alky (meth) acrylates 138

Ligated and Metal Free Initiating Systems for the Living Anionic Polymerization of Alkyl (meth)acrylates

A thesis submitted to the University of Pune by D.Baskaran

Abstract

The efficacy of living anionic polymerization of alkyl (meth)acrylate is decided by the selection of optimum conditions such as bulky initiator, polar solvent, low temperature, and the nature of counterion, as well as, the dynamics of the ion pair association equilibria. The main objective of this investigation is to develop new initiator systems for the controlled living anionic polymerization of alkyl (meth)acrylate using ligands in conjunction with classical anionic initiators and new initiators consisting of non-metal counterions, such as, tetrabutylammonium, tetramethyldiethylguanidinium and tetraphenylphosphonium cations.

The ligands used in the study are N,N,N',N'-tetramethylethylenediamine (TMEDA) and lithium perchlorate ($LiClO_4$). The first part of the work deals with the anionic polymerization of methyl methacrylate (MMA) in the presence of TMEDA as well as $LiClO_4$ in THF at -78 °C and -40 °C.

- Benzyllithium and 1,1-diphenylhexyllithium (DPHLi) were used as initiators. Poly (methyl methacrylate)s with predetermined molecular weights and narrow molecular weight distribution were obtained using benzyllithium as initiator at -78 °C in THF in the absence of TMEDA. Interestingly, even at -40 °C, DPHLi in conjunction with TMEDA, provided PMMAs with polydispersity values less than 1.2 and without oligomer contamination.

- The kinetics of the anionic polymerization of MMA in presence of TMEDA are investigated in THF using DPHLi as initiator in a flow-tube reactor between -20 and 0 °C. The rate constants of propagation determined in the presence of TMEDA are compared to those obtained in the absence of chelating agent. For propagation, the reaction order with respect to active center concentration is found to be 0.5 in both cases indicating the chelation of the lithium cation which does not effectively perturb the aggregation of the enolate ion pairs. The rate constant

of propagation via non-aggregated ion pairs, $k_{\pm}$, and the equilibrium constant of aggregation, K_a, are not significantly affected by TMEDA or the effects compensate each other. Lower rate constant of propagation and no termination were observed in presence of cyclic tertiary polyamine ("crown amine") such as 1,4,8,11-tetramethyltetraazocyclotetradecane at -20 °C.

- Anionic polymerization of MMA proceeds in a living manner at -40 °C in THF and at -78 °C in toluene/THF (9:1 v/v) using DPHLi as initiator in presence of $LiClO_4$ as additive. The polymerization of tert-butylacrylate (tBA) using DPHLi/$LiClO_4$ in THF at -78 °C produces PtBAs of controlled molecular weight with narrow molecular weight distribution ($M_w/M_n < 1.1$). The ratio of $LiClO_4$ to initiator has a greater influence in determining the control of the polymerization.

- The kinetic studies on MMA polymerization in presence and absence of $LiClO_4$ in flow-tube reactor show a fractional reaction order indicating the existence of associated ion pairs in equilibrium with non-associated species. The obtained fractional reacion order indicates that $LiClO_4$ does not effectively perturb the aggregation of enolate ion pairs. $LiClO_4$ has no influence on the absolute rate constant of propagation. However, the rate constant of propagation in presence of $LiClO_4$ is lower. This is attributed to the formation of less reactive mixed aggregates. The rate constants of termination in presence and absence of $LiClO_4$ are comparable.

The second part of the study involves metal-free anionic polymerization of methyl acrylate, n-butylacrylate, tert-butylacrylate and MMA in THF at ambient temperature, 0 and -40 °C using initiators such as tetraphenylphosphonium triphenylmethanide, tetrabutylammonium diethylphenylmalonate, tetrabutylammonium 9-ethylfluorenide, tetrabutylammonium fluorenide and tetra-n-butylammonium salts of 1,1'-diphenylhexane.

- The anionic polymerization of methyl methacrylate using tetraphenylphosphonium triphenylmethanide as an initiator proceeds in a living manner even at room temperature. The rate constants of propagation were measured between -20 °C and + 20 °C using a flow tube reactor. At 0 °C, the reaction half-lives range from 0.3

to 1 sec. The polymerization follows first-order kinetics with respect to monomer conversion and shows a linear dependence of the number-average degree of polymerization on conversion with high initiator efficiencies and narrow molecular weight distributions ($M_w/M_n < 1.1$). The dependence of the measured rate constants on the active center concentration is consistent with the coexistence of ion pairs and free ions. Arrhenius parameters were obtained in the temperature range from -20 °C to +20 °C. The activation energy, $E_a = 25 \pm 2$ kJ mol^{-1} and the frequency exponent, log A = 7.4. The determined rate constants for the ion pairs are one to two orders of magnitude smaller than those expected for such a large cation indicating a large fraction of dormant species. NMR studies of a model phosphonium ester enolate confirm the presence of a dormant ylide in equilibrium with a small amount of enolate ion pairs.

- Metal-free anionic polymerization of alkyl (meth)acrylates using tetrabutylammonium as well as tetramethyldiethylguanidinium counterion do not give control of molecular weight. The effect of counterion is clearly seen from the result of the polymerization carried out using lithium counterion under identical condition. The inconsistent results such as lower initiator efficiencies, broad and bi-modal distribution of the resulting polymers are attributed to the ion-pairing effects on the initiation processes of metal-free anionic polymerization.

List of Tables

List of Figures

Chapter 1: Living Anionic Polymerization of Alkyl (meth)acrylates

1.1 Introduction

Macromolecules possess a wide variety of applications and their suitability for a particular application is often controlled by their specific structural and molecular parameters such as molecular weight, molecular weight distribution and the nature and number of functional groups as well as its spatial location on the macromolecule. The synthesis of macromolecules with well defined structures has received significant attention from the polymer chemist because of their potential applications as advanced materials. It is well known that the properties of polymers are strongly influenced by their molecular weight and molecular weight distribution[1-2]. Commercially, acrylate and methacrylate polymers are prepared by radical polymerization processes which do not provide control over molecular properties. "Living" radical-initiated polymerization processes give certain degree of control on polymer molecular weight and its distribution[2]. Chain-end functionalization and block copolymer formation using free radical polymerization chemistry are in the early process of evolution[2c].

Living anionic polymerization is an attractive technique which offers an opportunity to tailor-make model macromolecules of well defined structure as well as polymers of technical interest such as graft, block, star, ω-functional polymers and macromonomers. These well-defined polymers possess diversified applications in many areas such as compatibilizers for polymer blends, additives for lubricating oil, general purpose resins, adhesives, impact modifiers, processing aids, textile, optical fibers etc.

Although the concept of living polymers was anticipated by Flory, the first homogeneous anionic polymerization of styrene free of termination and chain-transfer was reported by Szwarc[3] in 1956. Based on innumerable scientific studies, a good understanding of anionic polymerization of hydrocarbon non-polar monomers such as styrene and dienes in apolar and polar solvent has been achieved[4]. However, classical anionic initiators such as metal alkyls when used for alkyl (meth)acrylate monomers generally yield polymers of broad MWD and low conversion[5,7-11]. The non-ideal

behaviour of alkyl(meth)acrylates is basically due to the polar ester group of monomer which undergoes many side reactions with metal alkyl during both initiation and propagation.

1.2 Anionic Polymerization of Methylmethacrylate

The feasibility of anionic polymerization of methylmethacrylate (MMA) was first examined by Rembaum and Szwarc[5] in 1956. Polymerization of styrene[3] using sodium naphthyl as initiator provided the living polystyrene anion cabable of initiating further polymerization of styrene in THF at -78 °C. Unlike the polymerization of styrene, polymerization of MMA obtained by the same initiator does not further initiate polymerization of MMA and styrene. Szwarc concluded that the polymerization of MMA underwent rapid self-termination.

In 1958, Fox et al[6] reported stereospecific, crystalline poly (methylmethacrylate) (PMMA) prepared by anionic polymerization in highly solvating media such as 1,2-dimethoxyethane at -60 °C using 9-fluorenyllithium as initiator. In continuation, Glusker et al[7] demonstrated the mechanism and to some extent the living character of MMA polymerization using 9-fluorenyllithium in toluene by quenching the reaction with radio active tritiated acetic acid. The molecular weight distribution of these PMMA were very broad and deviated significantyl from the Poisson distribution. It was shown that increasing the solvent polarity causes decreasing isotacticity and narrower molecular weight distribution[8]. Although, the disappearance of the initiator was very fast, a larger percentage of the species initiated by the lithium compound did not propagate to yield high molecular weight polymer. Glusker[9] interpreted the lack of propagation of these species to high molecular weight polymer in terms of 'pseudo-termination.

1.2.1 Secondary Reactions

The polar side group of (meth)acrylate monomer plays an important role in termination mechanism. The ester group of the monomer gets solvated by the cation and thereby it becomes more susceptible to undergo nucleophilic attack by the base. The nucleophilic attack of ester group by initiator can take place in initiation step as

well as propagation step. Many such secondary reaction are proposed by Schreiber[10] and Goodes et al[11] which can be classified as shown in Scheme 1.1.

Occurrence of these side reactions has been experimentally confirmed by many authors[8,9,11-18]. All these undesirable reactions are basically due to the metal ion solvation and high nucleophilicity of the initiator. In all the proposed termination reactions, methoxide expulsion is common. According to Goodes[11], the major secondary reaction is the attack of propagating enolate anion to antepenultimate ester carbonyl group forming β-ketocyclic ester which they could identify by IR spectroscopy as a distinct band at 1712 cm^{-1}.

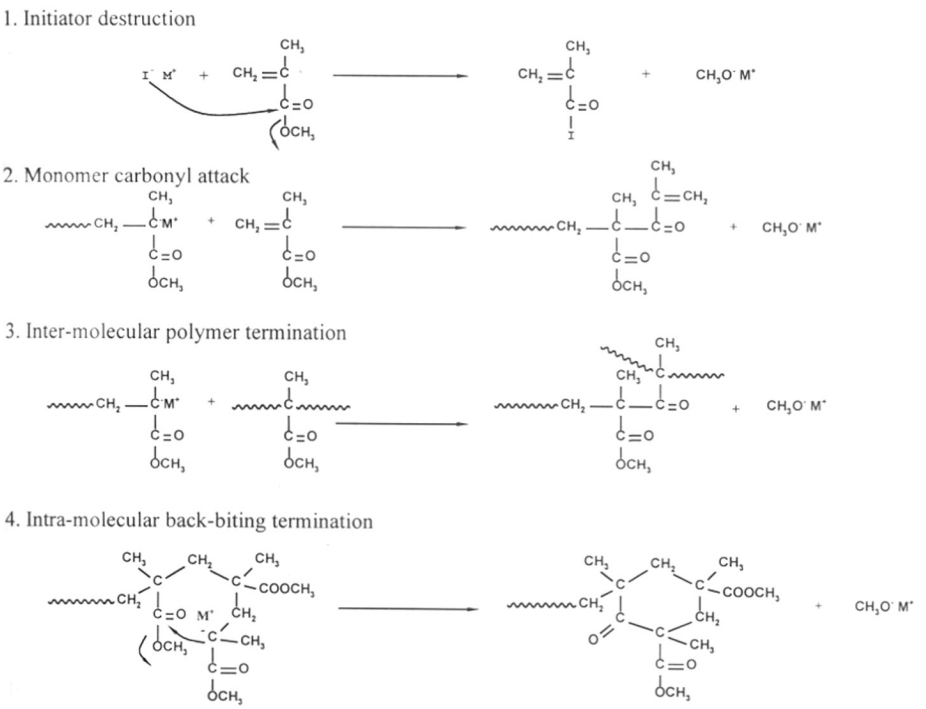

Scheme 1.1: Secondary reactions in methyl methacrylate polymerization

Subsequently, Glusker et al[8] also reported the intramolecular (back-biting) reaction. The first-order time-conversion plot of MMA polymerization in ether-toluene mixture (10:90) at -60 °C had an intercept at zero time. This indicated that the initial reaction was much more rapid and consumed approximately three moles of monomer per mole of initiator. The molecular weight of such a species is 466, which is very close to the

molecular weight of the lowest fraction obtained in their experiment. The IR spectra of the lowest molecular weight fraction showed carbonyl absorption at 1712 cm^{-1} which is characteristic of cyclic ketone derived from intramolecular termination.

The high nucleophilicity of initiator such as alkyl lithium can result in the attack of carbonyl group instead of vinyl unsaturation resulting in a vinyl ketone and lithium methoxide. This type of initiator destruction reaction was evident in all type of anionic initiator except in case of sterically hindered 1,1'-diphenylhexyllithium. It was also shown that most of the methoxide is formed during the initial steps of polymerization[12-14] although other sources of methoxide formation exist such as through an attack of a propagating oligomer chain end on the monomer carbonyl group resulting in the formation of a reactive keto functional end group. The evidence for such a termination of chain growth by transfer to acrylate monomer was seen in many cases where the obtained polymers has olefinic unsaturation[9]. Wiles and Bywater[13-15] reported the formation of considerable amount of lithium methoxide in n-butyllithium initiated polymerization of MMA in toluene. It has been shown that n-butyllithium and polystyryl anion[16] also reacts with ester group on both the monomer and carbonyl group of the propagating polymer chain.

Kitayama et al[17] have detected initiator fragment incorporation along the polymer chain by ^{1}H NMR when deutrated monomer was polymerized by undeutrated initiator. They found that the polymer and oligomer of MMA-d_8 produced in toluene using n-butyl lithium as an initiator had about one butylisoprophenyl ketone (BIPK) unit. This is due to the attack of n-butyllithium on to a polymer chain.

Reaction of the propagating anion with a carbonyl group of another polymer chain leading to chain coupling is rarely observed. This chain coupling would result in high molecular weight fraction. Since this intermolecular polymer termination is thermodynamically unfavourable, the appearance of the tailing in the high molecular weight side of GPC trace of the PMMA prepared by anionic method was not noticed[18].

1.2.2 Complexity of Anionic Polymerization of Acrylates

Anionic polymerization of acrylates pose a higher degree of complexity compared to methacrylates because of their higher reactivity towards nucleophiles and also the presence of acidic hydrogen at α-position to the carbonyl group[9,19,20]. Mode of reaction of n-butyllithium with methacrylate (MA) was investigated by Kawabata and Tsuruta[19]. It was shown that carbonyl addition takes place to a negligibly small extent in hexane whereas in THF, conjugate addition and n-butane formation occurs significantly in MA and MMA monomers.

Busfield and Methven[21] reported the mode of action of variety of sodiumaryl initiators towards MA in THF at -75 °C and -30 °C. It was shown that all sodiumaryl initiators such as anthracene, naphthalene, trityl, 1,1-diphenylethylene, biphenyl, fluorene and benzophenone yielded broad, bimodal PMA with low conversion (< 25 %). The low initiator efficiency was attributed to several side reactions accompanying initiation and propagation.

1.3 Factors Controlling Alkyl (meth)acrylate Polymerization

1.3.1 Selection of Initiator

Initial kinetic studies[13,22] of MMA polymerization with alkyl lithium initiator showed a very complex and variable dependence of rate on monomer and initiator concentration without any relation between molecular weight and the ratio $[M]_0/[I]_0$. Side reactions as described above were responsible for this complicated kinetics with the detection of lithium methoxide[15,20]. Rempp[16] and his coworkers attempted to prepare a block copolymer of (styrene-b-MMA) and encountered similar type of side reaction due to the reactivity of styryl carbanions towards the ester function of MMA monomer. In order to avoid such a side reaction, Rempp developed a procedure wherein few drops of 1,1'-diphenylethylene was added to a solution of living poly (styrene) before the addition of second block of MMA. Replacing styryl anion by diphenylmethyl carbanion provided a more sterically hindered and less reactive carbanion which gave quantitative initiation of MMA without reaction of initiator with the ester functionality.

Bywater[23] had described the use of 1,1'-diphenylhexyllithium (DPHLi) as initiator for the polymerization of MMA in toluene. The extensive attack of initiator on carbonyl group of monomer was reduced and the amount of lithium methoxide formed was also lower in case of DPHLi when compared to n-butyllithium initiator. DPHLi initiated PMMA has a broad unimodal distribution, unlike butyllithium initiated samples showing a bimodal distribution in toluene.

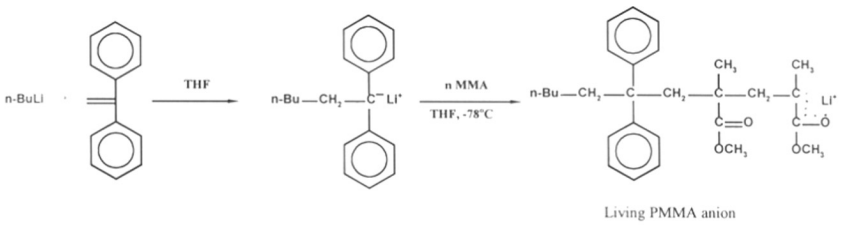

Living PMMA anion

Scheme 1.2: Polymerization of MMA using 1,1'-diphenylhexyllithium as initiator

1.3.2 Influence of the Nature of Solvent, Cation and the Temperature

It was established that the anion should be sterically hindered in order to avoid carbonyl attack of the alkyl (meth)acrylate monomer (Scheme 1.2). Termination reactions complicate the kinetics and broaden MWD of the PMMA in non-polar solvents whereas in polar solvent these side reactions are less pronounced. In polar solvent like THF, diphenyl sodium was used to prepare a monodisperse PMMA[24]. It was shown by Schulz[25] and Mita[26] that the anionic polymerization of MMA proceeds with insignificant or without termination in THF at T < -65 °C using Na^+ or Cs^+ as a counter ion. The rate of propagation is first order with respect to the monomer and the number average degree of polymerization is a linear function of conversion. The MWD of obtained PMMA are narrow. At higher temperatures, termination reactions gain in importance as indicated by deviation from the first-order kinetics, by broadening of the MWD[25] and by the generation of alkalimethoxide[26].

The nature of solvent and particularly the cation size also influences the alkyl (meth)acrylate polymerization. Solvent polarity largely affects the reactivity and identity of the propagating species. It is also known that the solvent polarity dictates the mode of addition in alkyl (meth)acrylate polymerization[27].

1.3.3 The Role of Solvated Contact Ion Pairs

In order to minimize side reactions, many approaches are documented in the literature. The external solvation of metal ion by polar medium at low temperature was suggested by Glusker et al[4,5] and Schulz et al[27] which helps in controlling ion-pair aggregation and minimizing secondary reactions. In polar solvent, such as 1,2-dimethoxyethane (DME) using benzyl-oligo-α-methylstyrylsodium as initiator, MMA polymerization proceeded without termination reactions. The first-order time-conversion plots were linear even at 0 °C and the obtained PMMA showed narrower (<1.01) molecular weight distribution when compared to the polymer obtained in THF. Schulz explained this observation by assuming the existence of an equilibrium between different types of contact ion pair as shown in Scheme 1.3.

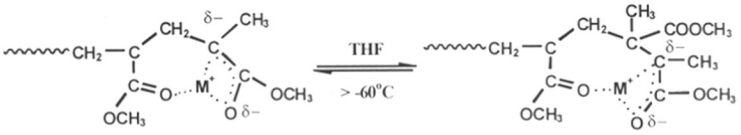

(A) intra-molecular solvated contact ion pair(B)

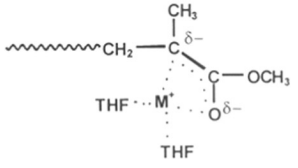

(C)

Sovated contact ion pair

Scheme 1.3: Propagation via contact ion pairs in MMA polymerization

Intramolecular solvated species (A) and (B) facilitates chain termination by back-biting reaction in solvents of low polarity. In solvents of high polarity like DME, the equilibrium shifts towards the solvated ion pair (C) and solvent-separated ion pairs. In solvents of medium polarity such as THF, the external solvation of the counter ion may exist in competition with intramolecular solvation (A,B). The low amount of termination reaction in DME in comparison with THF was, therefore, attributed to

low concentration of structure (B) which is a precursor for the intramolecular termination giving cyclic structure.

1.3.4 Effect of Alkyl Substitution in Alkyl (meth)acryates

Although the success of controlled anionic polymerization of alkyl (meth)acrylate depends largely on the type of ester functionality, methyl ester was subjected to important kinetic and mechanistic studies. Most of the published work in anionic polymerization of alkyl(meth)acrylate deals with MMA. Alkyl (meth)acrylate having bulky ester group such as t-butyl or trityl group undergoes controlled polymerization using alkyllithium as initiator even at higher temperature. The problem in MMA polymerization is essentially a selection of the experimental parameters such as choice of initiator, solvent and temperature of the reaction.

It was demonstrated by Müller[28] that anionic polymerization of t-butyl methacrylate in THF proceeded at room temperature with out side reaction using monofunctional initiator with Na^+ as cation. The kinetic results indicates that steric factor plays lesser role than the electronic effect of the t-butyl group. The positive inductive effect (+I) of t-butyl group decreases the reactivity of the monomer by the poor polarization of electron and in the propagating species, this +I effect increases the charge density at the carbon which provides the closer co-ordination of anion and counter ion in the ion-pairs and there by decreasing the propagating enolate reactivity. An attempt has been made to elucidate the interdependence of the ester alkyl group and a variety of synthetic parameters[28b].

1.4 Optimal Experimental Condition

Continuous studies in kinetics and mechanism of anionic polymerization of MMA during the last two decades has identified optimal experimental condition for living polymerization. The optimal conditions are the use of bulky monofunctional initiator such as diphenylmethyl, 1,1'-diphenylhexyl, 1,1'-diphenylmethyl, trityl, benzyl-oligo-α-methylstyryl salts or metallated esters with bulky counter ion ($Cs^+ > K^+ > Na^+ > Li^+$) in polar solvent (DME > THF) at low temperature (< -65 °C).

1.4.1 Purification of Monomers

Commercially available methacrylates contain considerable amount of residual alcoholic impurities. Although the effective drying agent such as CaH_2 reacts with the last traces of water, but it does not react appreciably with alcohols present in alkyl (meth)acrylates. Repeated fractional distillation is necessary to remove the traces of alcohol present in the commercial alkyl (meth)acrylate. It is possible to get pure acrylate monomer just by fractional distillation under vacuum in presence of inhibitor. However, McGrath[29] suggested the use of trialkylaluminum as effective drying agent for small scale purification of alky (meth)acrylate. Trialkylaluminum reacts vigorously with traces of moisture, alcohol and other protic impurities. The treatment with alkylaluminum removes the residual alcohol present in alkyl (meth)acrylates and the excess alkylaluminum then forms a complex with carbonyl group of acrylate monomer. This alkylaluminium-monomer complex has a characteristic bright yellow color which one can keep as an end point of impurity titration and immediate distillation under high vacuum renders extremely pure alkyl (meth)acrylate monomer.

1.5 Criteria for Living Anionic Polymerization

Control of molecular weight and molecular weight distribution in polymer synthesis is of primary importance for the molecular design of new polymeric materials. In order to obtain a living polymerization which will produce a narrow molecular weight distribution, uniform initiation and propagation with respect to all growing molecules is necessary, together with the absence of termination and chain transfer reactions. In order to get such a system for a living polymerization of methacrylates, the following criteria needs to be fulfilled.

1. The process should be free of termination and transfer reaction. This holds true only for anionic polymerization of hydrocarbon monomers and t-butyl methacrylate. This condition is fulfilled for MMA only in presence of special additives, especially at temperature above -75 °C.

2. Only one type of propagating species should exists or the rate of interconversion of different species should be much faster than the rate of polymerization. This

condition holds true for the polymerization of hydrocarbon monomers, and for methacrylate monomer in presence of an additive.

3. The rate of initiation should be higher or equal to the rate of propagation. This holds true for a great number of initiators.
4. The rate constant of propagation, k_p is independent of the degree of polymerization. It is assumed to hold true for higher degrees of polymerization. At the initial stages of polymerization the, k_p found to be dependent on the degree of polymerization[30].

1.5.1 Kinetics for Ideal Anionic Polymerization

The anionic polymerization of alkyl(meth)acrylate and also anionic polymerization of other monomers generally consist of three major reactions which can be represented as follows:

Initiation: $$I^* + M \xrightarrow{k_i} P_i^* \quad (1.1)$$

Propagation: $$P^* + M \xrightarrow{k_P} P_{i+1}^* \quad (1.2)$$

Termination: $$P_i^* (+X) \xrightarrow{k_t} P_i' \quad (1.3)$$

where I^* is initiator and M is monomer and P_i^*, P_i' is active and inactive (dead) polymer chain with degree of polymerization, i, respectively, and X is terminating agent. k_i, k_p and k_t are the rate constant for initiation, propagation and termination respectively.

The primary criteria for a living polymerization process is that the process should be free from termination and transfer reactions and the rate of initiation should be faster or atleast equal to the rate of propagation, i.e, $k_i \geq k_p$. In such a process, the number of active center, $[P^*]$ remains constant.

$$[P^*] = \sum [P_i^*] = \text{Const.} \quad (1.4)$$

Hence only propagation reaction is considered for the rate determination using pseudo-first-order kinetics. Thus, the rate of polymerization has a first-order dependence on monomer concentration and is represented as:

$$R_p = -\frac{d[M]}{dt} = k_p \cdot [M] \cdot [P^*] = k_{app} \cdot [M] \tag{1.5}$$

where k_{app} is the 'apparent' pseudo-first-order rate constant. Integration of equation 1.5 gives to:

$$\ln \frac{[M]_0}{[M]_t} = k_p \cdot [P^*] \cdot t = k_{app} \cdot t \tag{1.6}$$

$$k_{app} = -\frac{d \ln[M]}{dt} = k_p \cdot [P^*] \tag{1.7}$$

k_{app} can be determined from the constant slope of the first-order time-conversion plot provided that the, $k_i > k_p$ and $k_t << k_p$. If there is a slow initiation, then $[P^*]$ will increase initially and in presence of termination will decrease gradually during the polymerization. For a fast and complete initiation, $[P^*] = [I]_0$ and k_p can be determined directly from the first-order plot. However, due to aggregation and other factors (unavoidable quenching caused by impurites) most often the initiation is not complete. In such a case, $[P^*]$ can be determined indirectly from the number-average degree of polymerization, P_n, which is a linear function of monomer conversion, x_p as given below:

$$\overline{P}_n = \frac{number\ of\ polymerized\ monomers}{number\ of\ polymer\ chains} = \frac{[M]_0 \cdot x_p}{[P]_{tot}} \tag{1.8}$$

$$\text{and } [P^*] = K \cdot [P]_{tot} \tag{1.9}$$

where $[P]_{tot}$ is a total concentration of polymer chains including terminated ones which is equal to the initial initiator concentration for the polymerization without termination/transfer reaction and K is the number of active centers per polymer chain. A plot of P_n vs x_p gives a constant slope, $[M]_0/[P]_{tot}$. Any deviation from constancy indicates either the presence of slow initiation or transfer reaction. The presence of termination reaction will not change $[P]_{tot}$ and thus will not affect the linearity of the plot, P_n vs x_p. The presence of slow initiation result in an increase of $[P]_{tot}$ at the initial stages of reaction and the transfer reaction alters the number of active center per

polymer chain, K. These factors brings about a non-linearity in P_n vs x_p plot. In such a case, equation 1.9 becomes invalid and the following equation (1.10) can be used.

$$[P^*]_0 = K \cdot [P]_{tot.} = f \cdot [I]_0 \tag{1.10}$$

where $[P^*]_0$ is the initial concentration of active center just after initiation and f is the initiator efficiency which can be determined from the slope of P_n vs x_p plot in comparison with theoretical slope.

1.5.2 Rate Constant For Termination

The presence of unimolecular termination reactions such as back-biting decreases the active center concentration, $[P^*]$ gradually during polymerization, which can be represented by the following relationship:

$$-\frac{d[P^*]}{dt} = k_t \cdot [P^*] \tag{1.11}$$

Integration leads to,

$$-\ln\frac{[P^*]}{[P^*]_0} = k_t \cdot t \tag{1.12}$$

$$[P^*] = [P^*]_0 \cdot e^{-k_t \cdot t} \tag{1.13}$$

substituting $[P^*]$ in equation 1.5;

$$-\frac{d[M]}{dt} = k_p \cdot [M] \cdot [P^*]_0 \cdot e^{-k_t \cdot t} \tag{1.14}$$

and integration gives,

$$\ln\frac{[M]_0}{[M]_t} = \frac{k_p \cdot [P^*]_0}{k_t}\left(1 - e^{-k_t \cdot t}\right) \tag{1.15}$$

$$\ln\frac{[M]_0}{[M]_t} = \frac{k_{app}}{k_t}\left(1 - e^{-k_t \cdot t}\right) \tag{1.16}$$

$$\ln\frac{[M]_0}{[M]_t} = \frac{k_{app}}{k_t}\left(1 - e^{-k_t \cdot t}\right) \tag{1.16}$$

where $k_{app} = k_p[P^*]_0$. The rate constant of termination, k_t and k_p of the polymerization is determined using equation 1.16.

1.5.3 Molecular Weight Distribution

The molecular weight distribution (MWD) for a living polymerization was defined by Flory[31] in 1940 and follows the Poisson distribution. The polydispersity is given by:

$$D = \frac{\overline{P}_w}{\overline{P}_n} = 1 + \frac{1}{P_n} - \frac{1}{P_n^2} = \frac{P_n^2 + P_n - 1}{P_n^2} \text{ where } P_w = P_n + 1 - \frac{1}{P_n} \tag{1.17}$$

and the non-uniformity of chains (U) as introduced by Schulz[32] is:

$$U = \frac{\overline{P}_w}{\overline{P}_n} - 1 = \frac{P_n - 1}{P_n^2} \tag{1.18}$$

For higher degrees of polymerization $\overline{P}_n >> 1$; equation 1.17 and 1.18 can be simplified to $D \cong 1 + \frac{1}{\overline{P}_n} \approx 1$ and $U \cong \frac{1}{P_n}$, respectively. This shows the feasibility of obtaining polymers with narrow MWD by living anionic polymerization techniques.

1.5.4 Ions and Ion Pairs

The participation of different kind of active species like free anions and ion pairs in the polymerization of styrene in polar solvent was shown by Szwarc[33] and Schulz[34]. It was observed that the determined propagation rate constant, k_p decreases with increasing concentration of active center, $[P^*]$. This was attributed to free anions and ion pairs existing in equilibrium and contributing to propagation with two different rates (Scheme 1.4).

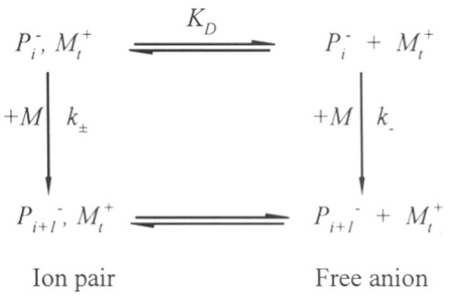

Scheme 1.4: Equilibrium of ion pairs and free anions in anionic polymerization

Thus, the experimental rate constant is given by,

$$k_p = \alpha \cdot k_- + (1-\alpha)\, k_\pm = k_\pm + (k_- - k_\pm)\cdot\alpha \qquad (1.19)$$

where α is the degree of dissociation. Due to the low dielectric constants of the ethereal solvents, the dissociation constants are very low ($K_D < 10^{-6}$ mol^{-1}) and consequently $\alpha << 1$. Thus, the mass action law can be simplified;

$$K_D = \frac{\alpha^2 \cdot [P^*]}{1-\alpha} \cong \alpha^2 \cdot [P^*] \qquad (1.20)$$

Therefore, $\alpha = (K_D / [P^*])^{1/2}$ leading to;

$$k_p = k_\pm + (k_- - k_\pm)\cdot K_D^{1/2} \cdot [P^*]^{-1/2} \qquad (1.21)$$

The plot of k_p vs $[P^*]^{-1/2}$ (Szwarc-Schulz plot) results in a linearity with slope of $(k_- - k_\pm) K_D^{1/2}$ and the positive intercept of $k_\pm$. Equilibrium constant, K_D can be determined by conductivity measurements[35]. K_D can also be determined by kinetic experiments in presence of large amount of common-ion salt which has much larger dissociation constant than that of the polymeric ion-pairs. This suppresses the degree of dissociation of polymeric ion-pairs. Tetraphenyl borates are suitable for this purpose.

The concentration of free ions is given by,

$$[P^-] = \frac{K_D \cdot [P^*]}{[Mt^+]} \tag{1.22}$$

Thus, the total $[Mt^+] = [Mt^+]_{add} + [Mt^+]_{pol} \approx [Mt^+]_{add}$ (1.23)

$[Mt^+]_{add}$ is calculated from the stoichiometric concentration of the salt and its dissociation constant[36].

The degree of dissociation now becomes;

$$\alpha = \frac{[P^-]}{[P^*]} = \frac{K_D}{[Mt^+]} \tag{1.24}$$

$$k_p = k_{\pm} + (k_- - k_{\pm}) \cdot \frac{K_D}{[Mt^+]} \tag{1.25}$$

and substituting α in equation 1.19 leads to an equation, 1.25 neglecting the effect of $[Mt^+]_{pol}$ on the dissociation of added salt. A plot of k_p vs $[Mt^+]^{-1}$ results $k_{\pm}$ as an intercept and K_D can be determined from the slope.

1.5.5 Other Types of Ion Pairs and Aggregates

The evidence for the existence of other kinds of ionpairs came from the anionic polymerization of styrene. The Arrhenius plot for the anionic polymerization of styrene in THF using Na^+ as counterion showed a significant deviation from linearity indicating the existence of two different types of ion pairs. i.e, tight or contact and loose or solvent-separated ion pairs[37]. Similarly, the active centers can also exist as various higher aggregates such as triple ions and associates[33,38].

1.5.6 Association Phenomenon in Alkyl (meth)acrylate Polymerization

The rate constant, k_p of the MMA polymerization was shown[39,40] to be strongly depend on the concentration of active centers. In THF, Li^+ as well as Na^+ counter ions causes a decrease in the propagation rate constant, k_p with increasing concentration of active centers, $[P^*]$, even in the presence of common-ion salt. This was attributed to the co-existence of associated and non-associated ion pair propagating at two different rate.

Müller and Lochmann[41] showed the existence of a possible association equilibrium between dimeric and non-associated ion pair in methacrylate polymerization as shown in Scheme 1.5.

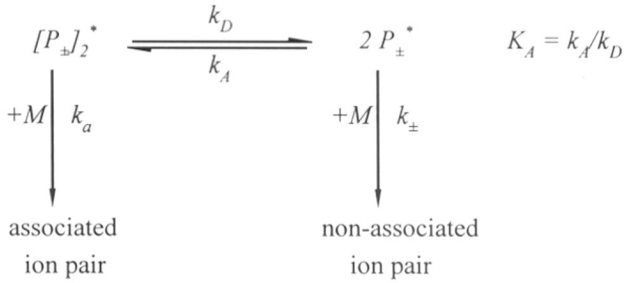

Scheme 1.5: Equilibrium between ion pairs and its associates

The over all rate constant of propagation, k_p is given by the rate constants of ion pair, $k_\pm$, the associates, k_a and the equilibrium constant, K_A (equation 1.26).

$$k_p = \alpha \cdot\cdot k_\pm + 1/2 \cdot (1-\alpha) \cdot k_a = 1/2 \cdot k_a + (k_\pm - 1/2 \cdot k_a) \cdot \alpha \qquad (1.26)$$

where the fraction of non-associated ion-pairs, α, is given[41a] by:

$$\alpha = \frac{[P_\pm^*]}{[P^*]} = \frac{\left(1 + 8 \cdot K_A \cdot [P^*]\right)^{1/2} - 1}{4 \cdot K_A \cdot [P^*]} \qquad (1.27)$$

and for $k_a \cdot [(P^*)_2] << k_\pm \cdot [P_\pm^*]$, the equation 1.26 becomes,

$$k_p = \alpha \cdot k_\pm = k_\pm \cdot \frac{\left(1 + 8 \cdot K_A \cdot [P^*]\right)^{1/2} - 1}{4 \cdot K_A \cdot [P^*]} \qquad (1.28)$$

For a limiting case (i) where $K_A \cdot [P^*] >> 1$, equation 1.27 and 1.28 becomes;

$$\alpha = \frac{1}{\sqrt{2 \cdot K_A \cdot [P^*]}} \qquad (1.29)$$

and $$k_p = \frac{k_\pm}{\sqrt{2 \cdot K_A \cdot [P^*]}} \qquad (1.30)$$

The apparent rate constant for propagation is given by $k_{app} = k_p \cdot [P^*]$; thus,

$$k_{app} = \frac{k_{\pm}}{\sqrt{2 \cdot K_A}} [P^*]^{1/2} \tag{1.31}$$

which leads to a reaction order of 0.5 with respect to $[P^*]$. For a case (ii) where $K_A \cdot [P^*] << 1$, equation 1.27 and 1.28 becomes;

$$\alpha = 1 - 2 \cdot K_A \cdot [P^*] \approx 1 \tag{1.32}$$

and $$k_p = k_{\pm} - 2 \cdot k_{\pm} \cdot K_A \cdot [P^*] \tag{1.33}$$

Thus, $$k_{app} = k_{\pm} \cdot [P^*] - 2 \cdot k_{\pm} \cdot K_A \cdot [P^*]^2 \cong k_{\pm} \cdot [P^*] \tag{1.34}$$

which leads to a reaction order of 1 with respect to $[P^*]$.

1.6 Enhanced Livingness of Anionic Polymerization of Acrylic Monomers: Strategies

Many attempts have been made to modify or hopefully to improve the anionic polymerization of alkyl (meth)acrylate in order to overcome the undersirable secondary reactions. Better control on the anionic polymerization of alkyl (meth)acrylate was obtained by merely changing the reactivity of either initiator or propagating species.

The use of ligands/additives in anionic polymerization is one of the tools to change the reactivity of anionic species and perturb the mechanism of propagation of polymerization. It is known that the activity of alkyllithium is increased by the addition of chelating amine. Langer[42] used BuLi complexed with tetramethylethylenediamine (TMEDA) to oligomerize ethylene through anionic mechanism. Polyethers and polyamines are the best ligands to increase the reactivity of carbanion pairs[43]. Alkyllithium is also known to form complex with other metal alkyl such as Mg, Zn, and Cd[44]. The use of other ligands such as solvating agents[59] (crown ethers, cryptands), alkalimetal alkoxides[51], alkalimetal alkoxyalkoxide[61], alkali halides[54] and aluminum alkyls[63,64] in anionic polymerization of alkyl(meth)acrylates improved the living character to a greater extent.

1.6.1 Complexation of Initiator By Metal alkoxides

In 1964, Bywater[45] studied the effect of lithium alkoxides in butyllithium initiated polymerization of MMA in toluene. He found that the addition of lithium methoxide increases the rate of polymerization in toluene. It was postulated that some of the growing ion-pairs in nBuLi initiated polymerization are associated or complexed with lithium methoxide. The complexed ion-pair appears to add monomer more rapidly than the uncomplexed form. In the case of nBuLi initiated styrene polymerization, both the initiation and propagation rates are decreased by the addition of lithium butoxide in benzene[46]. This observation was in agreement with that of Welch[47]. Subsequently, Trekovol and Lim[48] noticed that the action of nBuLi-lithium-t-butoxide towards initiation of MMA was quiet different from the behavior of the individual compounds.

Lochmann et al[49a] investigated the interaction of alkyl lithium compounds with lithium alcoholates. In their studies, they found that the equimolar mixture of lithium t-butoxide and n-butyl lithium form an adduct. Existence of a complex between the alkyl lithium and alcoholates was established by IR studies[49b]. The reactivity of alkyl lithium can be enhanced by complexing with potassium alkoxide. It is repoted that such complexes can metalate benzene and even add to ethylene at room temperature[49c]. The presence of potassium t-butoxide in butadiene polymerization initiated by nBuLi showed greater increase in rate of polymerization and vinyl unsaturation[50].

The growth center in anionic polymerization of MMA is an ester of α-substituted isobutyric acid metalated in the α-position. Lochmann et al[51a,b] prepared alkyl α-lithiosiobutyric acid esters as models for the propagating species in anionic polymerization of MMA esters and studied their interaction with lithium alkoxides. In order to find the mode of addition in MMA polymerization, these α-lithioesters were treated with methacrylates of corresponding esters[51c]. The course of the reaction

between MMA and methyl α-sodioisobutyrate was investigated with reaction time between 0.02 to 1.4 sec, as a function of solvent, effect of sodium-t-butoxide and temperature. The reaction yielded oligomers which underwent cyclizing self condensation consecutively. The rate of this cyclization was much higher in THF than in toluene. The addition of sodium-t-butoxide or lowering the temperature suppressed the cyclization[51d].

The rate of polymerization and cyclization and the equilibrium constant of polymerization of metaloester initiated MMA was reported by Müller[51e]. It was shown that these rates significantly depends on degree of polymerization[51f]. The rate constant for the reaction of methyl lithioisobutyrate with MMA (k_i) is higher than that of the subsequent propagation steps (k_p).

Addition of alkali-t-butoxide had a marked effect in decreasing both k_p and k_c. Dependence of the rate of cyclization on the chain length of the oligomers were also observed[51g]. These rate decreased by two orders of magnitude upon addition of lithium-t-butoxide. This indicates a lower tendency for cyclization of the enolate alkoxide adduct compared with the free enolate. In the presence of lithium-t-butoxide cyclization of the tetramer and the higher oligomer is so slow that hardly any cyclization of oligomers are observed. Although rate of cyclization drops ten times more than that of propagation, a considerable decrease in reactivity of the living dimer by formation of stable adduct with lithium-t-butoxide leads to slight broadening of MWD of the resulting MMA.

Thus, addition of lithium-t-butoxide leads to increased stability of the active centers which result in higher limiting conversions, comparatively narrow MWD and facilitating the preparation of block copolymers[51h].

1.6.2 Use of Alkalihalide as Additive

Alkyllithium compounds are known to form sold complexes with alkali halide[52]. The solid complex of n-butyllithium-lithium bromide was obtained and characterized by powder x-ray diffraction. Addition of ether apparently destroys this complex. The reactivity of alkyllithium-lithium halide complexes in a ternary complex

of alkyllithium, ether and lithium halide is quite different as has been observed by Talaeve and kocheshkov[53].

The use of alkali halide as an additive in alkali metal initiated alkyl(meth)acrylate polymerization was first reported by Teyssie and his co-workers[54] in 1987. They demonstrated the ability of inorganic salt to form a μ-type complex with the propagating ion pair. It was shown that the addition of an alkali halide, especially LiCl, changes the equilibrium between the different type of ion pairs in such a way that it results in a living nature in the polymerization of tert-butyl acrylate (tBA). The polymerization of tBA in either THF or THF-toluene mixture at -78 °C using α-methylstyryllithium as initiator in presence of lithium chloride as additive yielded polymer with narrow MWD (M_w/M_n < 1.1) whereas in the absence of lithium chloride, broad bimodal distribution (M_w/M_n >2) was obtained. Addition of 5 mole excess of LiCl improved the result further. It was observed that even in presence of excess LiCl, increase of reaction temperature from -78 °C to 0 °C resulted in a lose of control of molecular weight and broadening of polydispersity of PtBA from 1.1 to 1.65.

1.6.2.1 Influence of Solvent Polarity on LiCl System

The polymerization of MMA at -78 °C using α-methylstyryllithium as initiator in THF is essentially a living process and yields polymers with narrow molecular weight distribution (M_w/M_n = 1.2). LiCl influences the kinetics and mechanism of the polymerization of MMA giving raise very narrow molecular weight distribution (M_w/M_n > 1.08). In the presence of a mixture of solvents such as toluene-THF (9:1, v/v) of low polarity, polymerization of MMA does not proceed to completion. Incomplete conversion (50 %) or gel formation and polymers with broad and multimodal distributions were obtained indicating the occurrence of several side reactions during polymerization. Addition of LiCl does perturb this polymerization process to some extent and enables one to get at least unimodal PMMA of polydispersity 1.5 in toluene-THF (9:1 v/v) mixed solvent. Resumption experiment showed that in presence of LiCl in toluene-THF (9:1 v/v) mixed solvent, PMMA anion did not add fresh monomer quantitatively.

This indicated that LiCl addition gives only partial living character to MMA polymerization in toluene-THF particularly when toluene content is above 30% in the mixed solvent. It shows that the solvation of ion pairs of PMMA play an major role in enhancing the living character of the system which in turn is controlled by the polarity of the reaction medium. The presence of LiCl does not help in controlling the reactivity of propagating enolate anion in a solvent of low polarity.

1.6.2.2 Mechanistic Features of the LiCl System

Effect of LiCl in reactions involving lithium enolate-intermediate has been observed in many organic reactions[55]. It is known that the degree of aggregation of lithium enolates strongly depends on solvent and added complexing agent like LiCl, lithium-t-butoxide, or chelating agents rather than on a particular enolate structure[56]. The need for an excess of LiCl for obtaining control of anionic polymerization of alkyl (meth)acrylate indicates that the added salt is not only involved as a part of the stoichiometric complex but also strongly influences the aggregation phenomenon of propagating ion pairs. It is also observed that higher concentration of LiCl is needed (more than 10% excess with respect to $[I]_0$ when higher molecular weights were desired (2,50,000 g/mol)[57].

Detailed mechanistic study of alkyllithium/LiCl system was studied by Müller and his co-workers[41d]. They found that in the polymerization of MMA in THF with Li^+ as counter cation, the determined rate constants are higher when $R = [LiCl]/[P^*] < 1$ and it decreases gradually as the ratio R increases and reaches 50% of the initial value for R=10. This was explained by the assumption of the formation of at least two new species of different reactivity. Two new species of different reactivity could be a 1:1 and 2:1 adduct of the active center with LiCl when $[LiCl]/[P^*] > 1$.

The formation of LiCl-adduct with ion pairs actually decreases the aggregation as evidenced by viscometric measurment[41c]. This adduct formation disturbs the equilibrium between free and associated ion pair by the formation of complexed ion pairs. The position of multiple equilibria between non-associated, associated and complexed ion pairs determines the rate of polymerization and the dynamics of interconversion determines the polydispersity. Addition of LiCl, increases the rate of equilibrium between free and complexed ion pair than that of associated ions and

there by affects the rate of interconversion between dormant and active species. Thus the different species appears non-distinguishable to the monomers which is a prerequisite for obtaining Poisson distribution of molecular weights. This phenomenon leads to narrow MWD polyalkyl(meth)acrylates.

Using LiCl, block copolymers of MMA and tBA have been synthesized with predictable molecular weight and narrow molecular weight distribution irrespective of whichever monomer is first polymerized[54f]. The statistical copolymerization of a mixture of MMA and tBA in presence of LiCl failed due to a selective nucleophilic attack of penultimate methyl ester group of MMA by the propagating tert-butylacrylate anion leading to back-biting termination[54e].

1.6.3 Use of Crown-ethers and Alkali Alkoxyalkoxide

Chelation of metal cation offers one approach to bind the metal ion and thus create more steric hindrance around the propagating center. Attempts have been made to chelate the metal cation in the polymerization of butadiene[58a], isoprene[58b], styrene[58c] and also ethylene[42]. Intramolecular solvation of metal cation is the main cause for secondary reactions in anionic polymerization of alky(meth)acrylates. Hence, external chelation would probably minimize these secondary reactions due to strong binding and steric hindrance.

Teyssie and co-workers demonstrated the use of crown-ethers in the anionic polymerization of alkyl(meth)acrylates. MMA and tBA was polymerized in a living manner using diphenyl methylsodium (Ph_2CHNa) as initiator in presence of DB-18-CE-6 crown ether in toluene at temperatures as high as 0 °C[59a]. The living anionic statistical copolymerization of mixtures of MMA and tBA also proceeded without any side reaction[59b] such as the attack of methyl ester group of penultimate PMMA segment by the propagating PtBA anion in presence of DB-18-CE-6 at -78 °C. The determined reactivity ratios are for $r_{MMA} = 0.02$ and $r_{tBA} = 8.81$ indicating a tapered copolymer structure.

Another ligand used in the anionic polymerization of alky(meth)acrylates is alkali alkoxyalkoxides which were first employed in the MMA polymerization by Maruhashi and Takida in 1969[60a]. This family of ligands provides excellent control on

the living anionic polymerization of variety of alkyl(meth)acrylate as well as hydrocarbon monomers[60b]. They have a combination of properties associated with both alkali alkoxide as well as crown ethers. Recently, Teyssie and his co-workers[61] employed such a system and showed the efficiency of lithium 2-(2-methoxyethoxy ethoxide) (LiOEEM) ligand in promoting controlled anionic polymerization of MMA in non-polar solvent at -78 °C. They have also demonstrated living statistical copolymerization of MMA and tBA in presence of LiOEEM in THF at -78 °C[61a].

In presence of LiOEEM ligand, living polymerization of primary acrylate such as 2 -ethylhexylacrylate proceeds in a controlled manner in toluene-THF (9:1 v/v) mixed solvent at -78 °C[61b]. Block copolymers comprising 2EHA and MMA leading to the formation of acrylic thermoplastic elastomer have been successfully synthesized using LiOEEM ligand in toluene-THF (75:25 v/v) mixed solvent at -28 °C[61c]. Detailed NMR studies of the mixed complexation of a model compound, methyl-α-lithiosiobutyrate (MIBLi) with LOEEM showed increased charge density of the α-carbon of the MIBLi with ^{13}C resonances shifting 16 and 18 ppm upfield compared to tetrameric and dimeric MIBLi respectively. The enhanced living character brought by polydentate lithium alkoxide ligand was attributed to the formation of a sterically hindered single complexed species. A recent review provides an overview of the various ligands in the anionic living polymerization of alkyl(meth)acrylate[62].

1.6.4 Other Methods of Living Anionic Polymerization of Alkyl(meth)acrylates

1.6.4.1 Use of Alkylaluminum as Additive

Hatada[63] first reported the use of trialkylaluminum as an effective additive to give PMMA with narrow molecular weight distribution in toluene using t-butyllithium as initiator. Highly syndiotactic polymers (> 90 %) with controlled molecular weight and narrow MWD are obtained at Al/Li ratios higher than 3. Although the co-ordination of carbonyl group of MMA and aluminum does control the syndiotactic insertion of monomer, the living nature of chain ends is not fully controlled by this co-ordination. It has also been shown that the interaction between initiator and trialkylaluminum is essential to get a perfect control of reaction. Ballard and his co-worker[64] demonstrated the living nature of this polymerization at ambient temperature using sterically hindered trialkylaluminum.

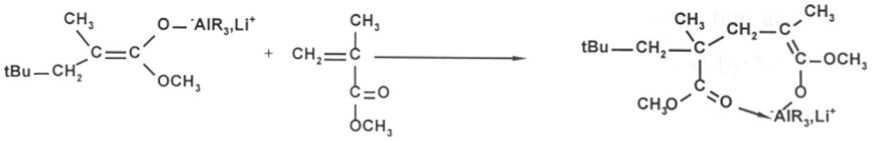

Scheme 1.6: Aluminum ate complex and its penultimate co-ordination

A detailed NMR investigation by Muller and his co-worker[65] on the propagating model ester enolate, i.e., ethyl-α-lithioisobutyrate, MMA with aluminumalkyl showed that the existence of an enol-aluminate complex as an active center for the polymerization. The first order time-conversion plot of the anionic polymerization of MMA in toluene at -78 °C showed a typical curvature at low conversions. This was explained as due to the coordination of the penultimate ester carbonyl group of the growing chain to the aluminate end-group of the living end (Scheme 1.6).

1.6.4.2 Metal Porphyrin as Initiators

Inoue and his co-workers[66] demonstrated the use of aluminum porphyrin such as (tetraphenylphorphinato)aluminum chloride, alkoxide, or carboxylate as excellent initiators for the living polymerization of wide variety of monomers especially for epoxides. Later, it was found that porphyrinatoaluminum methyl initiates living polymerization of alkyl(meth)acrylates upon irradiation by visible light[66e] (Scheme 1.7). Reaction was performed by just exposing the reaction mixture of MMA with (TPP)AlMe (100:1 ratio) to visible light and terminating the reaction mixture after 12 hours by adding excess methol. PMMA was obtained in quantitative conversion and had narrow molecular weight distribution ($1.06 < M_w/M_n < 1.2$). It was also found that the same reaction did not proceed in dark.

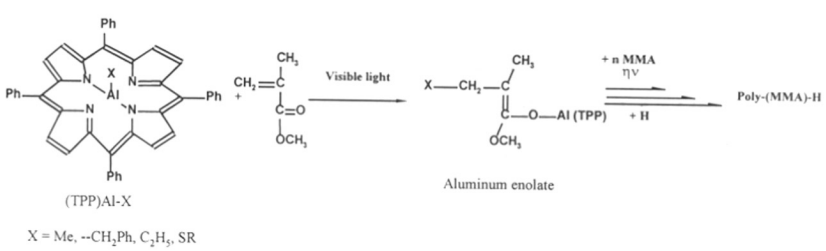

Scheme 1.7: Aluminum porphyrin initiated MMA polymerization

The effect of light is observed not only in the initiation step but also in the propagation steps. The course of this novel reaction was examined by NMR which confirmed that the polymerization proceeds via a concerted mechanism, where the MMA co-ordinates to the aluminum atom leading to the conjugate addition of methyl group of initiator to monomer to form an aluminum enolate. Aluminum enolate once again coordinates with MMA and propagation occurs through a Michael addition process. Visible light accelerates this initiation and propagation to yield quantitative conversion.

1.6.4.3 Lanthanide Complexes as Initiators

Another class of initiators for anionic polymerization of alkyl(meth)acrylates are bis[bis(trimethylsilylamino) tin II] or germanium II[67a] and lanthanides complexes[67b,c]. Polymerization of MMA, tBMA, BenzylMA with these initiators gave polymers with high molecular weight and comparatively narrow molecular weight distribution (M_w/M_n <1.32).

Lanthanide III complexes[67c] such as $((C_5Me_5)_2SmH)_2$ or the complexes derived from $(C_5Me_5)_2Yb(THF)_2$ and triethylaluminum showed high catalytic activity in the polymerization of MMA in toluene between 40 °C to -78 °C. The living nature of the chain ends was demonstrated by monomer resumption experiment carried out even after 1h of the first monomer addition. Yasuda and his co-workers have isolated an organolanthanide III intermediate coordinated by a penultimate Poly(MMA) unit. The 1:2 adduct of $((C_5Me_5)_2SmH)_2$ with MMA is an air-sensitive orange crystal whose melting point is 132 °C. It was shown by x-ray analysis that one of the MMA unit binding the metal in enolate form, and other MMA unit coordinates to the metal at its carbonyl group. The proposed initiation mechanism suggested that an attack of hydride at the α-carbon of MMA led to the formation of transient intermediate (A) which then undergoes further monomer insertion through 1,4-addition to form an eight membered ring intermediate (B) as shown in Scheme 1.8.

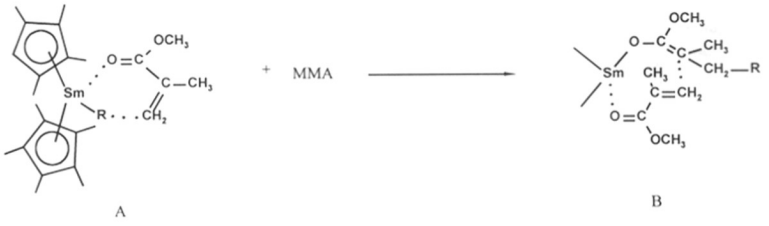

Scheme 1.8: Initiation of MMA with Lanthanide III complexes

The eight membered transition state undergoes coordinated anionic polymerization successfully with long living nature of active chain end. Complexes falling on the same class of organolanthanide III complexes such $YbMe(C_5Me_5)_2(OEt)_2$, $(YbMe(C_5H_5)_2)_2$, $SmMe_2AlMe_2(C_5Me_5)_2$, $SmMe(C_5Me_5)_2(THF)$, $YbMe(C_5H_5)_2(THF)$ and $LuMe(C_5Me_5)_2(THF)$ are also promote the living syndiotactic polymerization of alky(meth)acrylates in a controlled manner at -78 °C.

1.6.5 Metal-Free Anionic Initiators

The major problem in classical anionic initiators is the solvation of metal cation by monomer carbonyl group which leads to several side reaction such as back-biting and initiator destruction reaction. It is known[68] that the rate of propagation, k_p, is strongly influenced by the atomic characteristic of metal cation employed in the polymerization. Therefore, the use of non-metal cations in the anionic polymerization of alky(meth)acrylates is expected to change the course of the reaction significantly.

Reetz and his co-workers[69] first demonstrated the use of quaternary ammonium as counter ion in the anionic polymerization of acrylates. Quarternary ammonium salts of alkyl and aryl thiolates, malonates and malononitriles, etc., were used as initiators. Surprisingly they initiated polymerization at room temperature without any catalyst (Scheme 1.9) by repeated Michael addition of monomer via ammonium enolates.

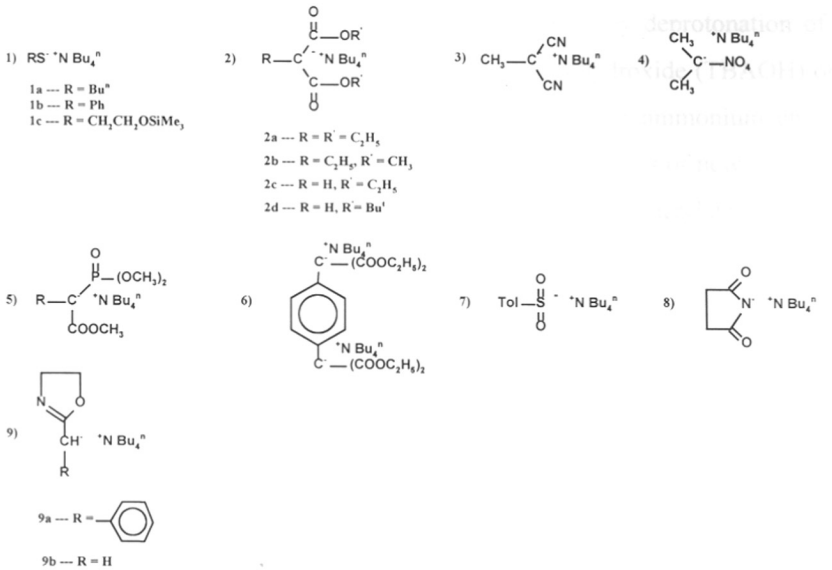

Scheme 1.9: Metal-free carbanions for alkyl(meth)acrylate polymerization

Poly (n-butylacrylate) (PnBA) with narrow molecular weight distribution ($1.11 < M_w/M_n < 1.2$) and predictable molecular weights were obtained at room temperature in polar solvents like MeCN, DMF, $PhNO_2$, and THF with metal free initiators. However, controlled initiation and propagation of acrylates using initiators like ammonium thiolates were limited. It gave oligoacrylates with controlled molecular weights upto 10 monomeric units only. When high molecular weight was targetted, the $M_{n(obs)}$ values were lower than $M_{n(calc)}$. This was attributed to a side reaction involving thiolate elimination at one end of the polymer chain by the basic propagating enolate ester. The eliminated thiolate initiates a new chain resulting in a lower M_n than expected.

Addition of n-butylacrylate to the solution of metal free carbon nucleophiles in THF at room temperature gave an exotherm which after the required time and termination followed by aqueous work up resulted in poly (n-butylacrylate). The polymer obtained by these ammonium methanides (**2a**,**3**,**4** in Scheme 1.9) initiators possessed comparatively narrow MWD of around 1.2. The initiators **2a,b** (Scheme 1.9) provided the synthesis of high molecular weight PnBA with good control.

These resonance stabilized carbanions are simply prepared by deprotonation of the corresponding thiols/CH acids by tetra-n-butylammonium hydroxide (TBAOH) or by treating the sodium salts of thiols/CH acids with tetra-n-butylammonium chloride. Subsequently, Sivaram and his coworkers[70] have reported a series of new ammonium methanide and demonstrated the oligomerization of methylacrylate (MA) and acrylonitrile (AN) using these initiators.

Reetz suggested that the mechanism of these reaction involves a strong electrostatic attraction between anion and ammonium ion. The positive charge on the nitrogen is not localized, but it is dispersed on four α-carbons so that the monomer approach easily and get inserted in a Michael fashion. The newly inserted monomer is now turned into the new enolate chain end. The backbiting reaction observed in classical anionic polymerization of acrylates and methacrylates arises due to the activation of the ester group by the solvation of metal ion such as Li^+ or Na^+ and the expulsion of alkoxide ion.

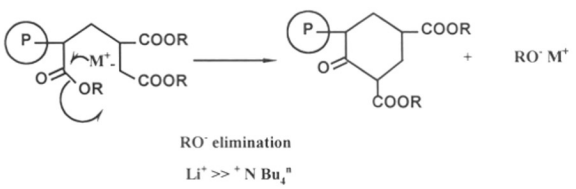

Scheme 1.10: The extent of alkoxide expulsion in anionic polymerization

In metal free system too, one can expect the similar reaction (Scheme 1.10). The alkoxide elimination may become insignificant because of the poor activation of ester group by bulky ammonium ion. The undesired alkoxide expulsion, $RONR_4$ is kinetically and thermodynamically less favorable than in the case of ROLi or RONa[69a]. However, the real mechanistic and kinetic aspects of this reaction are yet to be clarified and unequivocal proof for livingness needs to be provided. Recently, bulky phosphazene (P4-base)[71] and tetraphenylphosphonium cations[72] have also been used for the controlled polymerization of alkyl (meth)acrylates.

1.7 References

1. (a) Flory, P. J. *J. Am. Chem. Soc.* **1945**, 67, 2048. (b) Fox, T.G and Flory, P.J. *J. Am. Chem. Soc.***1948**, 70, 2384.
2. (a) Matyjaszewski, K. *Macromolecules,* **1993**, 26, 1787. (b) Matyjaszewski, K.; Szymanski, R.; Teodorescu, M. *Macromolecules,* **1994**, 27, 7565. (c) Hawker, C. J. *Angew. Chem. Int. Ed. Engl.* **1995**, 34, 1456 and Hawker, C. J.; Hedrick, J. H. *Macromolecules,* **1995**, 28, 2993.
3. Szwarc, M.; Levy, M.; Milkovich, R. *J. Am. Chem. Soc.***1956**, 78. 2656.
4. Szwarc, M. *Adv. Polym. Sci.* **1983**, 49, 108.
5. Rembaum, A. A .; Szwarc, M. *J. Polym. Soc.* **1956**, 22, 189.
6. Fox, T. G.; Garrett, B. S.; Goode, W. E.; Gratch, S.; Kincaid, J. K.; Spell, A.; Stroupe, D.J. *J. Am. Chem. Soc.* **1958**, 80, 1768.
7. Glusker, D.L.; Stiles, E.; Yoncoskie, S. *J. Polym. Sci.* **1961**, 49, 297.
8. Glusker, D.L.; Lyslofe, I.; Stiles, E. *J. Polym. Sci.* **1961**, 49, 315.
9. Glusker, D.L.; Galluccis, R. A.; Evans, R. A. *J. Am. Chem. Soc.* **1964**, 86, 187.
10. Schreiber, H.*Makromol. Chem.* **1956**, 36, 86.
11. Goodes, *J. Polym. Sci.* **1960**, 47, 75.
12. Müller, A. H. E.; Lochmann, L.; Trekoval, J. *Makromol. Chem.* **1986**, 187, 1473.
13. *Polymer* **1962**, 3, 175.
14. Wiles, D. M.; Bywater, S. *J. Phys. Chem.* **1964**, 68, 1938.
15. Wiles, D. M.; Bywater, S. *Chem. and Ind.* **1963**, 1209.
16. (a) Rempp, P.; Volkou, U. I.; Parrod, J.; Sadron, C. H. *Bull. Soc. Chim. France.* **1960**, 919. (b) Freyss, D.; Rempp, P.; Benoit, H. *J. Polym. Sci. Lett.* **1964**, 2, 217. (c) Freyss, D.; Leng, M.; Rempp, P. *Bull. Soc. Chim. France.* **1964**, 221.
17. *Polymer. J.* **1984**, 16, 925.
18. Gerner, F.J.; Hocker, H.; Müller, A. H. E.; Schulz, G. V. *Eur. Polym. J.* **1984**, 20(4), 439.
19. Kawabata, N.; Tsuruta, T. *Makromol. Chem.* **1965**, 86, 231.
20. Fait, B. A. *E. Polym. J.* **1967**, 3, 523.
21. Busfield, W. K.; Methven, J. M. *Polym. J.* **1973**, 14, 137.
22. Bywater, S. *Pure. Appl. Chem.* **1962**, 4, 319.
23. Wiles, D. M.; Bywater, S. *Trans. Faraday Soc.* **1965**, 61, 150.
24. Roig, A.; Figueruelo, J. E.; Llano, E. *J. Polym. Sci. Poly. Lett.* **1965**, 3, 173.
25. (a) Lohr, G.; Schulz, G. V. *Makromol. Chem.* **1973**, 172, 137. (b) Lohr, G.; Schulz, G. V. *Eur. Polym. J.* **1974**, 10, 121. (c) Lohr, G.; Müller, A. H. E.; Warzelhan, V.; Schulz, G. V. *Makromol. Chem.* **1974**, 175, 497.
26. Mita, I.; Watanabe, Y.; Akatsu, T.; Kambe, H. *Polym. J.* **1973**, 4, 271.
27. Kraft, R.; Müller, A. H. E.; Hocker, H.; Schulz, G. V. *Makromol. Chem., Rapid Commun.* **1980**, 1, 363.
28. (a) Müller, A. H. E. *Makromol. Chem.* **1981**, 182, 2863. (b) Long, T. E.; Allen, R. D.; McGrath, J. E. *Recent advances in mechanistic and synthetic aspects of polymerization, M. Fontanille and A. Guyot (eds),* **1987**, 79; R. Reidel Publishing company.

29. Allen, R. D.; McGrath, J. E. *Polym. Bull.* **1986**, 15, 127.

30. Tsvetanov, B. Ch; Müller, A. H. E.; Schulz, G. V. *Macromolecules*, **1985**, 18, 863.

31. Flory, P. J. *J. Am. Chem. Soc.* **1940**, 62, 1561.

32. Schulz, G. V. *Z. Phys. Chem. Abt. B* **1940**, 47, 155.

33. (a) Bhattacharyya, D. N.; Lee, C. L.; Smid, J.; Szwarc, M. *Polymer*, **1964**, 5, 54. (b) Bhattacharyya, D. N.; Lee, C. L.; Smid, J.; Szwarc, M. *J. Phys. Chem.* **1965**, 69, 612.

34. (a) Hostalka, H.; Figini, R. V.; Schulz, G. V. *Makromol. Chem.* **1964**, 71, 198. (b) Hostalka, H.; Schulz, G. V. *Z. Phys. Chem.(Frankfurt),* **1965**, 45, 286.

35. Accascina, F.; Fuoss, R. M.; '*Electrolytic Conductance'* Wiley, New York, **1965**.

36. Boileau, S.; Hemery, P.; Justice, J. C. *J. Solution Chem.* **1975**, 4, 873.

37. (a) Barnikol, W. K. R.; Schulz, G. V. *Z. Phys. Chem.(Frankfurt)* **1965**, 47, 89. (b) Shimomura, T.; Tolle, K. J.; Smid, J.; Szwarc, M. *J. Am. Chem. Soc.* **1967**, 89, 796.

38. (a) Bhattacharyya, D. N.; Smid, J.; Szwarc, M. *J. Am. Chem. Soc.* **1964**, 86, 5024. (b) Takaya, K.; Yamauchi, S.; Ise, N. *J. Chem. Soc., Faraday Trans.1,* **1974**, 70, 1330. (c) Ise, N. *J. Macromol. Sci., Chem.* **1975**, A9, 1047.

39. Johann, C.; Müller, A. H. E. *Makromol. Chem., Rapid Commun.* **1981**, 2, 687

40. Jeuck, H.; Müller, A. H. E. *Makromol. Chem., Rapid Commun.* **1982**, 3, 121.

41. (a) Kunkel, D.; Müller, A. H. E.; Janata, M.; Lochmann, L. *Macromol. Chem., Macromol. Symp.* **1992**, 60, 315. (b) Kunkel, D. *Dissertation, University of Mainz, Germany* **(1991)**. and also see ref. 12 and 30.

42. Langer, A.W. *Trans., New York, Acad. Sci.,* **1965**, 27, 741.

43. (a) Smid, J. *Anionic polymerizaton- ACS Symp. Series,* **1981**, 166, 79. (b) Boileau, S. *Anionic polymerization-ACS Symp. Series,* **1981**, 166, 283.

44. Seltz, L. M.; Little, G. F. *J. Organomet. Chem.* **1969**, 18, 227.

45. Wiles, D. M.; Bywater, S. *Polymer* **1962**, 3, 175 (also refereces 14 and 15).

46. Roovers, J. E. L.; Bywater, S. *Trans. Faraday Soc.* **1966**, 62, 1876.

47. Welch, F. J. *J. Am. Chem. Soc.* **1960**, 82, 6000.

48. Trekoval, J.; Lim, D. *J. Polym. Sci., Part C,* **1964**, 4, 333.

49. (a) Lochmann, L.; Pospisil, J.; Lim, D. *Tetra. Lett.* **1966**, 2, 257. (b) Lochmann, L.; Pospisil, J.; Vodnansky, J.; Trekoval, T.; Lim, D. *Coll. Czecho. Chem. Commun.* **1965**, 30, 2187. (c) Schosser, M. *J. Organomet. Chem.* **1967**, 8, 9.

50. Hsieh, L. H.; Wofford, C. F. *J. Polym. Sci. A-1,* **1969**, 7, 449.

51. (a) Lochmann, L.; Lim, D. *J. Organomet. Chem.* **1973**, 9, 50. (b) Halaska, V.; Lochmann, L. *Coll. Czech. Chem. Commun.* **1973**, 38, 1780.(c) Lochmann, L.; Rodova, M.; Petranck, J.; Lim, D. *J. Polym. Sci., Polym. Chem.* **1974**, 12, 2295. (d) Lochmann, L.; Pokorny, S.; Trekoval, J.; Adler, H. J.; Berger, W. *Makromol. Chem.* **1983**, 184, 2021. (e) Müller, A. H. E.; Lochmann, L.; Trekoval, J. *Makromol. Chem.* **1986**, 187, 1473. (f) Lochmann, L.; Janata, M.; Machova, L.; Vlcek, P. *Polym. Preprint.* **1988**, 29(2), 29. (g) Lochmann, L.; Müller, A. H. E. *Makromol. Chem.* **1990**, 191, 1657. (h) Lochmann, L.; Kolvarik, J.; Doskocilova, D.; Vozka, S.; Trekoval, J. *J. Polym. Sci., Polym. Chem.* **1979**, 17, 1727.

52. Glaze, W.; West, R. *J. Am. Chem. Soc.* **1960**, 82, 4437.

53. Talalaeva, T. V.; Kocheshkov, K. A. *Doklady. Akad., Nauk. SSSR,* **1955**,104, 260.

54. (a) Fayt, R.; Forte, R.; Jacobs, C.; Jerome, R.; Ouhadi, T.; Teyssie, Ph.; Varshney, S. K. *Macromolecules,* **1987**, 20, 1442. (b) Forte, R.; Ouhadi, T.; Fayt, R.; Jerome, R.; Teyssie, Ph. *J. Polym. Sci., Polym. Chem.* **1990**, 20, 2233. (c) Varshney, S. K.; Hautekeer, J. P.; Fayt, R.; Jerome, R.; Teyssie, Ph. *Macromolecules,* **1990**, 23, 2618. (d) Hautekeer et al *Macromolecules,* **1990**, 23, 3893. (e) Jacobs, J.; *Macromolecules,* **1990**, 23, 4024. (f) Varshney, S.K.; *Macromolecules,* **1991**, 24, 4997.

55. (a) Seebach, D.; Estermann, H. *Tetrahedron Lett.* **1987**, 28, 3103. (b) Narasaka, K.; Ukaji, Y.; Watanabe, K. *Chem. Lett.* **1986**, 1755.

56. Seebach, D. *Angew. Chem. In. Ed. Engl.* **1988**, 27, 1624.

57. Klein, J.W.; Gnanou, Y.; Rempp, P. *Polym. Bull.* **1990**, 24, 39.

58. (a) Davidjan, A.; Nikolaev, N. I.; Zgonnik, V.; Belenkii, B.; Nesterow, V.; Erussalimsky, B. *Makromol. Chem.* **1976**, 177, 2469. (b) Davidjan, A.; Nikolaev, N. I.; Zgonnik, V.; Belenkii, B.; Nesterow, V.; Krasikow, V.; Erussalimsky, B. *Makromol. Chem.* **1978**, 179, 2255. (c) Helary, G.; Fontanille, M. *Eur. Polym. J.* **1978**, 14, 345.

59. (a) Varshney, S. K.; Jerome, R.; Bayard, Ph.; Jacobs, C.; Fayt, R.; Teyssie, Ph. *Macromolecules,* **1992**, 25, 4457. (b) Wang, J. S.; Jerome, R.; Bayard, Ph.; Baylac, L.; Patin, M.; Teyssie, Ph. *Macromolecules,* **1994**, 27, 4615. (c) Johnann, C.; Müller, A. H. E. *Makromol. Chem., Rapid Commun.* **1981**, 2, 687.

60. (a) Maruhashi, M.; Takida, H. *Makromol. Chem.* **1969**, 124, 172. (b) use of alkylalkoxyalkoxide in styrene and 1,3-butadiene copolymerization, see in Narita, T.; Masaki, A.; Tsuruta, T. *J. Macromol. Sci., Chem.* **1970**, A4(2), 277 and A4(4), 885.

61. (a) Wang, J. S.; Jerome, R.; Bayard, Ph.; Patin, M.; Teyssie, Ph..; Vuillemin, B.; Heim, Ph. *Macromolecules,* **1994**, 27, 4635. (b) Wang, J. S.; Bayard, Ph.; Jerome, R.; Varshney, S. K.; Teyssie, Ph. *Macromolecules,* **1994**, 27, 4890. (c) Wang, J. S.; Jerome, R.; Bayard, Ph.; Teyssie, Ph. *Macromolecules,* **1994**, 27, 4908.

62. Wang, J. S.; Jerome, R.; Teyssie, Ph. *J. Phys. Org. Chem.* **1995**, 8, 208.

63. (a) Kitayama, T.; Shinozaki, T.; Masuda, E.; Yamamoto, M.; Hatada, K. *Polym. Bull.* **1988**, 20(6), 505. (b) Hatada, K.; Kitayama, T.; Ute, K.; Masuda, E.; Shinozaki, T.; Yamamoto, M. *Polym. Prepr.* **1988**, 29(2), 54. (c) Kitayama, T.; Shinozaki, T.; Sakamoto, T.; Yamamoto, M.; Hatada, K. *Makromol. Chem., Suppl.* **1989**, 167, 15.

64. (a) Ballard, D. G. H.; Bowlers, R. J.; Haddleton, D. M.; Richards, S. N.; Sellens, R.; Twose, D. L. *Macromolecules,* **1992**, 25, 5907. (b) Haddleton, D. M.; Muir A. V. G.; O'Donnell, J. P.; Richards, S. N.; Twose, D. L. *Macromol. Symp.* **1995**, 91,93.

65. Schlaad, H.; Müller, A. H. E. *Makromol. Chem., Rapid Commun.* **1995**, 16, 399.

66. (a) Takeda, N.; Inoue, S. *Makromol. Chem.* **1978**, 179, 1377. (b) Aida, T.; Mizuta, R.; Yoshida, Y.; Inoue, S. *Makromol. Chem.* **1981**, 182, 1073. (c) Yasuda, T.; Adia, T.; Inoue, S. *Macromolecules,* **1984**, 17, 2217. (d) Shimasaki, K.; Aida, T.; Inoue, S. *Macromolecules,* **1987**, 20, 3076. (e) Kuroki, M.; Aida, T.; Inoue, S. *J. Am. Chem. Soc.* **1987**, 109, 4737.

67. (a) Kobayashi, S.; Shoda, S.; Iwata, S.; Abe, M. *Polym. News.* **1990**, 5(1), 15. (b) Yasuda, H.; Yamamota, H.; Yamashita, M.; Yokata, K.; Nakamura, A.; Miyake, S.; Kai, Y.; Kanehisa, N. *Macromolecules,* **1993**, 26, 7134. (c) Yasuda, H.; Yamamoto, H.; Yokota, K.; Miyake, S.; Nakamura, A. *J. Am. Chem. Soc.* **1992**, 114, 4908.

68. Müller, A. H. E. in *Comprehensive Polymer Science, G. Allen, J.C. Bevington, Ed.* Pergamon, Oxford, **1988**, 3, 387.

69. (a) Reetz, M. T.; Ostarek, R. *J. Chem. Soc., Chem. Commun.* **1988**, 213. (b) Reetz, M. T.; Knauf, T.; Minet, U.; Bingel, C. *Angew. Chem., Int. Ed. Engl.* **1988**, 27, 1373. (c) Reetz, M. T.; Hütte, S.; Goddard, R. *J. Am. Chem. Soc.* **1993**, 115, 9339.

70. (a) Sivaram, S.; Dhal, P. K.; Kashikar, S. P.; Khisti, R. S.; Shinde, B. M.; Baskaran, D. *Macromolecules,* **1991**, 24, 1698. (b) Raj, D. J. A.; Wadgaonkar, P. P.; Sivaram, S. *Macromolecules,* **1992**, 25, 2774.

71. Pietzonta, T.; Seebach, D. *Angew. Chem., Int. Ed. Engl.* **1993**, 32, 716.

72. Zagala, A. P.; Hogen-Esch, T. E. *Macromolecules,* **1996**, 29, 3038.

Chapter 2: Objective and Scope of the Present Investigation

In recent years, considerable efforts have been made to polymerize alkyl(meth)acrylates using anionic initiators at relatively higher temperatures keeping all the advantages of a living polymerization technique. As detailed in chapter 1, the basic problem in obtaining living alky (meth)acrylates is associated with the ester group that plays a significant role in initiation, propagation and also in side reactions during polymerization. It is seen that establishing synthetic condition for a wide range of poly (alkyl methacrylates) requires manipulation of not only the synthetic parameters such as initiator, solvent and temperature but also the rigorous purification of monomers, particularly, considering each alkyl (meth)acrylate as a distinct one.

The stability of the propagating enolate is entirely different for each alkyl (meth)acrylates. In particular, the branched alkyl (meth)acrylates are inherently easier to polymerize due to the enhanced stability of the propagating species. Recently, several strategies have been developed and widely used for the living anionic polymerization of alkyl (meth)acrylates (Chapter 1.6). The use of several coordinating ligands with classical anionic initiator and the use of new initiator for alky (meth)acrylate polymerization enhances their living nature and enables one to form block, star and end-functionalised polymers. For higher alkyl methacrylates and for primary alkyl acrylates, the research is continuing for a better reaction conditions with various strategies such as the use of new additives in conjunction with classical anionic initiators, the metal-free anionic polymerization, and anionic coordination polymerization.

The living anionic polymerization of alkyl (meth)acrylates is characterized by the existence of peripherally solvated contact ion pairs and a dynamic equilibrium between aggregated and non-aggregated forms. The nature of ligands and counter ion plays a dominant role in controlling the efficiency of alky (meth)acrylate polymerization. The use of new ligands and metal-free cations has, therefore, attracted significant attention in the anionic polymerization of alky (meth)acrylates, as a means to obtain precise control on chain length and molecular weight distribution.

The research carried out in the present thesis was undertaken with a view:

- to examine the use of common chelating agent such as N,N,N',N'-tetramethylethylenediamine (TMEDA) as a ligand to enhance the degree of control of methyl methacrylate (MMA) polymerization using alkyl lithium initiators and the effect of chelation of lithium counterion on the kinetics of the anionic polymerization of MMA in THF at -20 °C.
- to study the effect of $LiClO_4$ as a ligand in the anionic polymerization of alkyl (meth)acrylate to obtain well-defined polymers with narrow molecular weight distribution in THF as well as in toluene-THF (9:1 v/v) mixed solvent and the influence of $LiClO_4$ on the kinetics of the anionic polymerization of MMA in THF at -30 to 0 °C.
- to perform kinetic and mechanistic investigations on metal-free anionic polymerization of MMA using tetraphenylphosphonium as counter cation in THF at ambient temperature.
- to synthesize and characterize new metal-free anionic initiators with tetrabutylammonium counterion and to study their ability for the controlled polymerization of acrylates and methacrylates at ambient temperature.

3.1 Purification of Solvents and Other Reagents

3.1.1 Purification of Nitrogen Gas

Commercial N_2 gas (INOX-1, IOC, Bombay) contains traces of moisture, H_2 and O_2. In order to remove these impurities, N_2 gas was first passed through a column (1m) containing activated A4 molecular sieves, a column (1m) containing active Cu deposited on kieselguhr kept at 200 °C and activated A5 molecular sieves. The molecular sieves and Cu columns were regularly activated. The copper column was activated by passing H_2 at 170 °C for 5-8 h. The water formed from the reaction of H_2 and CuO was removed under vacuum. The activation of copper column was completed when the Cu turn into maroon color. Molecular sieves column was activated under vacuum at 200 °C for several hours and cooled under N_2.

The purified N_2 gas was further bubbled through a solution of toluene containing living styryllithium anion. The red color of the oligo styryllithium anion in toluene serves as a indicator for the purity of N_2. The pure N_2 was connected to a manifold through a rubber tube from where the N_2 was taken into reaction flask or distillation unit through rota-flow/glass stop-cocks.

3.1.2 Solvents

THF (SD, Bombay or BASF AG, Germany) was purified by refluxing over deep purple colored sodium-benzophenone complex. The required amount of THF was distilled over sodium-benzophenone complex and collected into bulb 'A' of a distillation-unit (Fig. 3.1) under pure N_2 pressure using stainless steel capillary tube through a rubber septum (S). The traces of protic impurities present in THF was titrated using a solution of toluene containing living-oligostyryllithium anion. The orange solution of oligostyryllithium in toluene was added drop by drop under stirring into THF until the orange color of anion persisted. This ensures the removal of traces of moisture or other impurities present in THF. Just before polymerization, the pure THF was condensed under vacuum into the cylinder 'B' of the distillation-unit and transferred into a polymerization flask under pure N_2 pressure through capillary tubes via septum (S).

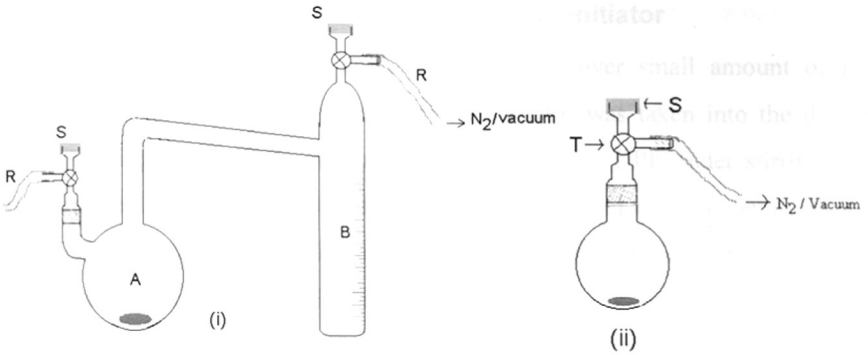

Fig. 3.1: Distillation apparatus (i) and batch polymerization reactor (ii) for anionic polymerization of alkyl(meth)acrylate; (S) rubber septum, (R) natural rubber tube for taking N_2/vacuum from manifold, and (T) three-way stop-cock.

Toluene, (SD, Bombay or BASF AG, Germany) was distilled in a similar way. For bulk consumption of solvents, especially for kinetic experiments (in flow-tube reactor), THF was first fractionated over a 1.5 m column, twice stirred over sodium/potassium alloy, degassed and distilled in high vacuum.

3.1.3 Monomers

All the monomers were obtained from either Aldrich, USA or E Merck, Bombay. Methyl methacrylate (MMA), Methyl acrylate (MA), n-Butyl acrylate (nBA) and tert-Butylacrylate (tBA), were all stirred over CaH_2 over night and distilled and stored under N_2 at 5 ^{o}C in refrigerator. The required amount of pre-purified monomer was taken into the bulb 'A' of the a distillation-unit (Fig. 3.1i) under N_2 using a syringe. Trialkylaluminum (TIBAL, Aldrich) neat or in hexane solution was added drop by drop to the monomer under N_2 until a persistent yellow green color formed. The formation of complex between trialkylaluminum and monomer carbonyl group indicates the monomer free of protic impurities[1]. Then the pure monomer was condensed using liquid nitrogen into cylinder 'B' of the distillation-unit. The monomer was then transferred into the polymerization flask containing initiator solution using a syringe or cannula.

For kinetics studies, MMA (Rohm GmbH, Germany) was fractionated from CaH_2 over a 1m column filled with sulzer packing at 45 mbar. After degassing, the distillate was stirred over CaH_2 and distilled in high vacuum before polymerization.

3.2 Synthesis of 1,1'-Diphenylhexyllithium Initiator

1,1'-Diphenyl ethylene (DPE) was distilled over small amount of n-BuLi (1.6M n-hexane solution). Required amount of DPE was taken into the distillation unit by syringe and n-BuLi was added drop by drop to DPE under stirring at room temperature. n-BuLi reacts with traces of impurities and residual benzophenone in DPE. After reacting with impurities, the excess of n-BuLi then adds to DPE and forms 1,1'-diphenylhexyllithium (DPHLi) anion. The red color of DPHLi was kept as an end point of impurity titration. The excess DPE was distilled over DPHLi under dynamic high vacuum at 120 °C.

The required amount of DPE in dry THF was added to equimolar amount of n-BuLi at -40 °C under dry N_2. The solution immediately turned into red indicating the formation of DPHLi. The reaction temperature was slowly brought to room temperature and stirred for 1 h and stored under N_2 in refrigerator.

3.2.1 Determination of Initiator Concentration

The concentration of initiators such as nBuLi, DPHLi, etc., was determined using Gilman's double titration method[2]. Definite amount of (1-2 ml) of the initiator solution was added to excess dry 1,4-dibromobutane (Aldrich, distilled over CaH_2) solution in 5 ml THF at 0 °C. The solution was stirred for few minutes, during which all the lithium in the initiator as RLi was completely converted into LiBr. Thereafter, a small amount of water (1 mL) and methanol (5 mL) was added to the solution in order to convert other lithium species (such as alkoxides, etc.,) into LiOH. The concentration of LiOH was determined by titration against standard solution of potassiumhydrogenphalate (PHP). This gives the concentration of lithium present as other than RLi form in the known amount of initiator solution.

The same amount of the initiator solution was hydrolysed in dry THF directly by slow addition of water. To this solution, 5 mL of methanol was added for dilution and the solution was titrated against standard acid (0.1N PHP) which gave the total amount of lithium in the known amount of initiator solution. The difference of the above two titration values gives the actual amount of RLi present in the initiator solution. The titrations were repeated twice and in case of slight deviation in the titration results (< 5 %), the average value was used as the initiator concentration.

The other initiators used in this study are benzyllithium (BzLi), potassium triphenyl methanide (TPMK), methyl-α-tetraphenylphosphonium isobutyrate ($MIBPPh_4$), ethyl-α-tetraphenylphosphonium isobutyrate ($EIBPPh_4$), tetraphenylphosphonium triphenylmethanide (TPPTPM), tetra-n-butylammonium diethylphenylmalonate (TBADEPM), tetra-n-butylammonium 9-ethylfluorenide (TBA9EFl), tetra-n-butylammonium fluorenide (TBAFl) and tetra-n-butylammonium 1,1-diphenylhexane. The synthesis of these initiators are described in the appropriate chapters.

3.3 General Procedure for Anionic Polymerization of Alkyl (meth)acrylate

Anionic polymerization of alkyl (meth)acrylate (MMA, tBA, nBA, MA etc.,) using DPHLi or BzLi in presence and absence of additives (TMEDA or $LiClO_4$) as well as using metal-free initiators were done in batch experiment by adding neat monomer or the solution of monomer into initiator solution at desired temperature. A typical experimental procedure in case of anionic polymerization of MMA using DPHLi as initiator is given below:

To a flame dried 250 mL single neck-round bottom flask fitted with a septum adapter with N_2/vacuum inlet (Fig. 3.1 ii), required amount of dry solvent (THF or toluene) was transferred by stainless steel capillary tube under N_2. The DPHLi solution was added drop by drop unit a persistent red-color of the initiator remained. Usually 0.2 mL to 0.5 mL of 0.08 M initiator solution was required for 100 mL of THF to completely quench all the impurities. Subsequently, the calculated amount of initiator was added through syringe and the temperature of the flask was brought to -78 °C using solid CO_2-acetone bath. The purified monomer (3-5 mL) was added to the initiator solution within 5-10 s through stainless steel capillary tube. Reaction was terminated after 15 minutes with degassed methanol.

The polymer solution (in THF or toluene) was concentrated and the polymer was precipitated by adding drop by drop into excess n-hexane or methanol (4 times of polymer solution). The polymer was filtered and dried under vacuum for 4 h at 80 °C. In some cases, especially in acrylate polymerization and in kinetic experiments, the polymer was recovered by removing solvent and the residue was dissolved in benzene and freeze dried.

3.4 General Procedure for Kinetics in Bench-top Stirred-tank Reactor

The kinetics of the anionic polymerization of MMA in low polar medium such as toluene:THF (9:1 v/v) using DPHLi/$LiClO_4$ initiating system and few metal-free anionic initiators were done in a bench-top stirred-tank reactor as shown below (Fig 3.2):

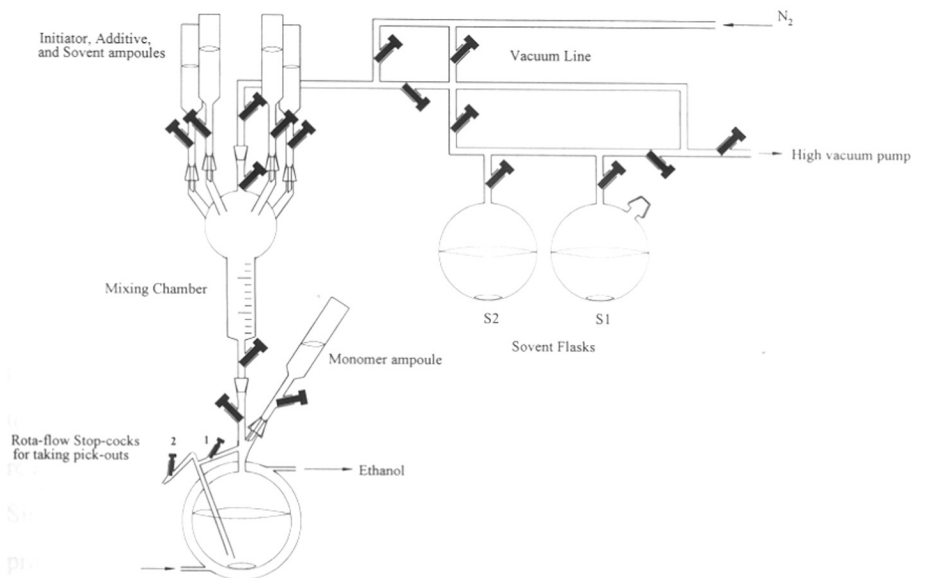

Fig. 3.2: High vacuum line and a bench-top stir-tank reactor

The solvents and monomers were distilled directly into the ampoule fitted with rota-flow stop cock in a vacuum-line from solvent reservior flasks, S1 and S2. Required molar solution of initiator, monomer and additive were prepared in side a glove-box and taken in ampoules under N_2. To the monomer solution, a small amount of n-octane (0.3 %, vol.) was added as an internal standard for the determination of monomer conversion by Gas Chromatography. A small amount of the monomer solution was taken first for the determination of total monomer concentration at zero time.

These ampoules were fixed on the top arms of the mixing chamber through glass joints as shown in Fig. 3.2. One of the mixing chamber arm is connected to the vacuum/N_2 line and the graduated burette of the mixing chamber is connected to the 250 mL stirred-tank glass jacketed-reactor through a rotor-flow stop cock with a glass

joing (B24). The monomer ampuole is directly connected to the stirred-tank glass reactor which has a provision to take samples under N_2 pressure through rota-flow stop cocks as shown in Fig. 3.2.

The reactor was first heated under dynamic high vacuum (10^{-4} mm) for 30 minutes. Then the system was allowed to cool under pure N_2. The evacuation and N_2 filling was repeated thrice. The required amount of additive ($LiClO_4$ solution) and solvent was added slowly under slight vacuum into the reactor with a help of graduated burette of the mixing chamber by opening the corresponding stop cocks. The initiator solution (eg. DPHLi or MFA initiators) was added drop by drop until the color of the initiator persisted and then calculated amount of initiator was added through the burette of the mixing chamber.

The reactor temperature was brought down to a desired polymerization temperature (-78 to 25 °C) with a cryostat using ethanol as a coolant. After attaining the desired temperature, the monomer ampoule was opened with a slight vacuum inside the reactor, so that all the monomer falls into the initiator solution within 2/3 s. Simultaneously a clock was started and the reactor was filled with positive N_2 pressure. The reaction was continued for several hours and the reaction solution (10 mL) was taken at different time intervals using rota-flow stop cocks (2 in Fig. 3.2) and terminated with degassed methanol (1-2 mL) containing small amount of diluted HCl acid.

A small amount of the reaction solution of each time intervals was analyzed by GC and the monomer concentration was measured in comparison with zero sample as below:

$$x_p = 1 - \left[\left(\frac{M_t}{I_t} \right) \Big/ \left(\frac{M_0}{I_0} \right) \right]$$

where x_p is the conversion at given time, t,

M_t and M_0 are the peak area of monomer at time, t and 0 repectively,

I_t and I_0 are the peak area of internal standard (n-octane) at time, t and 0 respectively.

The polymers were recovered by stripping off the solvent and the residue was dissolved in benzene, filtered and freeze dried.

3.5 General Procedure for Kinetics in Flow-tube Reactor

Kinetics of the anionic polymerization of MMA in THF in presence and absence of additives such as TMEDA, $LiClO_4$ were done in flow-tube reactor (Fig. 3.3). Flow-tube reactor consist of a motor, glass reagent-burettes, four-way mixing jet (Fig. 3.4) and capillary tubes (1mm diameter).

The pistons of the reagent-burettes are connected to the motor which enables to raise the piston either upward or downward with variable speed (12 position) using a control button. The top of the reagent burettes are connected to reagent reservoir flask containing monomer, initiator, terminating solutions and mixing jet-1 through a three way HPLC-valve with capillary tube (1mm diameter, HPLC tubes).

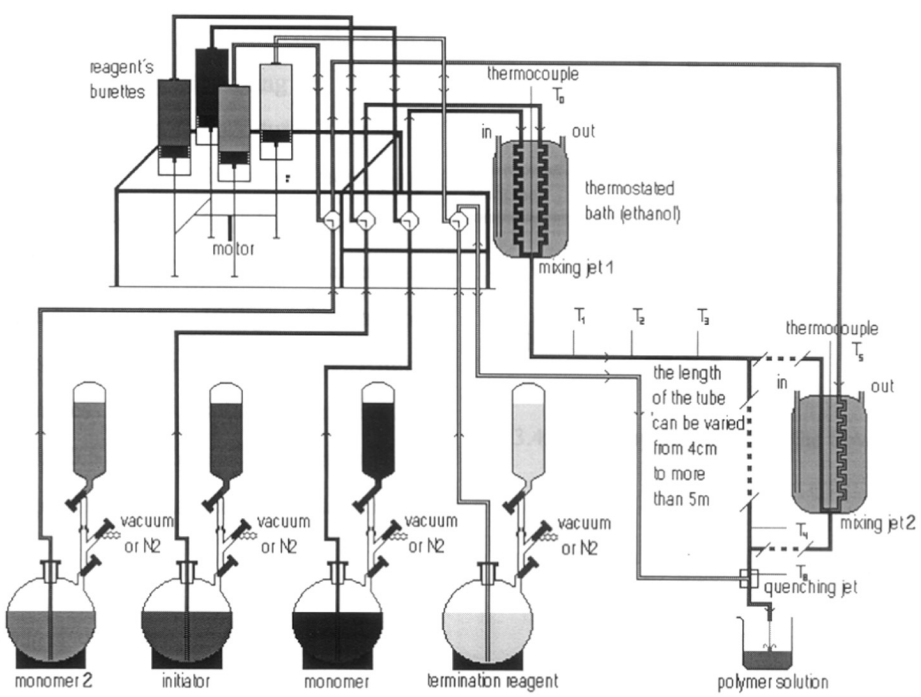

Fig. 3.3: Flow-tube reactor with motor driven piston and mixing jet

The mixing jet was kept inside the thermostat bath. A capillary tube of 5 m length was kept inside the thermostat bath so that the initiator and monomer solution gets cooled to desired bath-temperature before it reaches the mixing jet. The mixing jet has been specially designed with a small central cavity of few micro liter (volume). It has a tangential four way side-inlets with top and bottom outlets (Fig. 3.4). The capillary tubes of the monomer and initiator solution were splitted using a T-connector into two lines and connected to the tangential inlets of the mixing jet.

The monomer and initiator solution can be mixed efficiently in the mixing jet by operating the motor at a given speed and the polymerization solution will flow through the bottom outlet which is connected to a capillary flow-tube (1mm diameter) of desired length. The reaction proceeds inside the flow-tube upto the quenching jet (four way) and gets terminated with a flow of methanol containing small amount of acetic acid or dil HCl.

The mixing temperature (T_m) was measured using a thermocouple fixed at the top outlet of mixing jet (Fig 3.4). Similarly, the temperatures of reaction along the flow-tube at different points and at the point just before the quenching jet (T_q) were measured using thermocouples. Philips Thermocoax, type K (=NiCr/Ni = Chromel/Alumel) stainless steel insulated thermocouples with 0.5 mm o.d and 500 mm long with type K compensation cables were used.

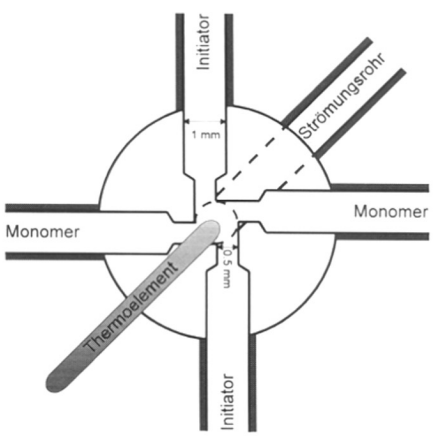

Fig. 3.4: Four-way mixing jet of the flow-tube reactor.

The analog signals of temperature were converted into digital and connected to a personal computer with a help of computer interface unit. Temperatures was measured on-line using a PC program (for thermovoltage to temperature conversion) (Fig. 3.5). The effective temperature, T_{eff} of the polymerization was determined using the equation[3]:

$$T_{eff} = T_m + f' \Delta T \tag{3.1}$$

where $f' = 0.55$ for conversion, $x_p \leq 0.7$ and $\Delta T = T_q - T_m = \Delta T_{trans} + \Delta T_{exo}$. Since ΔT_{exo} is proportional to conversion, x_p, the effective temperature (T_{eff}) of the each run in higher than T_m. Due to the fact that the polymerization is very fast, heat transfer (T_{rans}) through the walls of the tube is negligible. Thus, data points corresponding to T_{eff} were recalculated to T_m using the known activation energy, E_a = 24 kJ mol^{-1} for the MMA polymerization in THF with lithium as counterion[4] using the equation 3.2,

$$\ln k_{app}(T_m) = \ln k_{app}(T_{eff}) + \frac{E_a}{R} \cdot \left(\frac{1}{T_{eff}} - \frac{1}{T_m} \right) \tag{3.2}$$

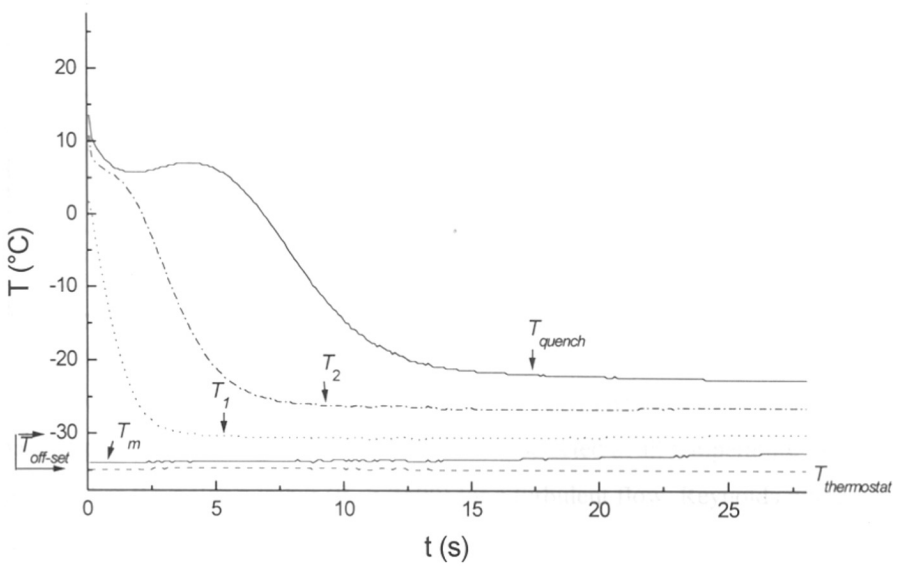

Fig. 3.5: Temperature versus flow-time plot of a MMA polymerization for the flow-tube lengh of 256 cm (1.76 s, residence time). T_1-temperature at 64 cm tube length, T_2-temperature at 128 cm tube length. The effective reaction temperature is, T_{eff} = -26.13 °C (at off-set termostat-temperature of -35 °C). Samples were taken in between 20 s to 30 s.

In order to compensate ΔT of the polymerization and to obtained a constant T_{eff} for all the experiments, an appropriate off set temperature was selected for T_m for each conversion. Using different piston-speed of the motor (12 levels) and with different length of the flow-tube (from 4 cm to more than 5 m), a large range of residence times, τ, is accessible ($5ms < \tau < 5s$).

The residence time, τ, is given by:

$$\tau = \frac{L \cdot \Omega}{Q} = \frac{V}{Q} \tag{3.3}$$

where L: length of the tube (cm)
Ω: cross-section of the tube (cm^2)
V: volume of the tube (cm^3)
Q: flow rate (cm^3/s)

Table 3.1: Reynolds number and residence time for various flow rate and flow-tube length

Piston speed No.*	Flow rate Q (cm^3/s)	Reynolds number at T °C			Residence Time at different flow-tube# length in seconds				
		-20°C	0 °C	20 °C	16 cm	128 cm	256 cm	384 cm	512cm
1	1.29	1919	2439	2992	0.0974	0.7789	1.5578	2.3367	3.1157
2	1.68	2500	3176	3897	0.0748	0.5981	1.1962	1.7943	2.3924
3	2.00	2976	3781	4639	0.0628	0.5024	1.0048	1.5072	2.0096
4	2.45	3645	4632	5683	0.0513	0.4101	0.8202	1.2304	1.6405
5	2.83	4211	5350	6565	0.0444	0.3551	0.7101	1.0652	1.4202
6	3.19	4746	6031	7400	0.0394	0.3150	0.6300	0.9450	1.2599
7	3.57	5312	6749	8281	0.0352	0.2815	0.5629	0.8444	1.1258
8	3.90	5803	7373	9047	0.0322	0.2576	0.5153	0.7729	1.0306
9	4.40	6547	8318	10207	0.0285	0.2284	0.4567	0.6851	0.9135
10	4.72	7023	8923	10949	0.0266	0.2129	0.4258	0.6386	0.8515
11	4.69	6978	8866	10880	0.0268	0.2142	0.4285	0.6457	0.8575
12	4.73	7038	8942	10972	0.0266	0.2124	0.4249	0.6373	0.8497

* Motor speed position number
# Cross-section of the flow-tube- 0.0079 cm^2.

It is necessary to maintain a turbulent flow in the tube. Hence, a right combination of piston-speed and the length of the flow tube was selected at all temperature in order to get a higher Reynolds number ($R_e > 2500$) for a turbulent flow. Reynolds number was calculated by the following equation:

$$R_e = \frac{\rho \cdot \vartheta \cdot d}{\eta} \geq 3000 \tag{3.4}$$

ρ : density of the fluid (kg/m^3)
ϑ : velocity of the fluid (m/s)

d : diameter of the tube (m)
η: viscosity of the fluid (Pa.s)

Since, a low solid content was maintained in the polymerization, R_e is calculated for pure solvent and considered for the polymerization. The residence time of the solvent and their R_e at different temperature are given in the Table 3.1.

Flow-rate of the solvent and the pressure of the reactor at each piston-speed position, at different temperature and at different flow-tube length was confirmed for its consistency. It was found that at higher piston speed position numbers at 10 and above did not give consistent flow rate and hence those higher flow rates were not used for polymerization.

In a typical experiments, the initiator and monomer solution at particular concentration, terminating agent are taken into the reagent burettes by actuating the pistons downwards. Once the reagent is filled in the burettes, the three way valve is turned to connect the burettes and the mixing jet so that the solutions can be transferred into the reaction tube through a thermostatic bath for both initiator and monomer solutions. By actuating the pistons upwards at certain speed, the initiator and monomer solution is pumped into the mixing jet and the solution gets mixed efficiently within < 5ms.

The reaction solution flows through the capillary tube. On the other side of the flow-tube, the polymerization solution is terminated in a quenching jet with methanol which comes directly from the burette. The polymer solution is collected in a bottle. The experiment was repeated with different flow rate or with different length of flow-tube in order to get conversions at various residence time. The polymer solution was analyzed by GC for monomer conversion and polymer was recovered by removing solvent under vacuum. The polymer was dissolved in benzene, filtered and freeze dried.

3.6 References

1. Allen, R. D.; McGrath, J. E. *Polym. Bull.* **1986**, 15, 127.
2. Gilman, H.; Haubein, A. H. *J. Am. Chem. Soc.*, **1944**, 66, 1515.
3. Lohr, G.; Schmitt, B. J.; Schulz, G. V. *Z. Phys. Chem. (Frankfurt am Main)*, **1972**, 78,177.
4. Jeuck, H.; Müller, A. H. E. *Makromol. Chem., Rapid Commun.* **1982**, 3, 121.

Chapter 4: N,N,N',N'-Tetramethylethylenediamine Ligiated Carbanionic Initiator for Methyl Methacrylate

4.1 Introduction

It is known from several kinetic and mechanistic studies that the nature of counter cations and their solvation exert great influence in determining both the efficiency and living nature of the anionic polymerization of methyl methacrylate (MMA)[1] . In non-polar solvents such as toluene, termination reactions complicate the kinetics and broaden molecular weight distribution (MWD)[2]. It was shown by Löhr and Schulz[3,4], and by Mita[5] that the anionic polymerization of MMA proceeds without any termination reaction in tetrahydrofuran (THF) at -78 °C using cesium as a counterion leading to polymers with narrow MWD. On the basis of kinetic investigations, it was suggested that the counterion is strongly co-ordinated with the carbonyl oxygen with partial enolate character and the strength of co-ordination with the α-carbon depends on the solvating power of the solvent and on temperature[1,6].

The kinetic investigation of MMA polymerization in THF and 1,2-dimethoxyethane (DME) using Na^+ and Cs^+ as counterions showed no dependence of the rate of polymerization on the nature of the counterion[7,8]. Johann and Müller[9] obtained significantly higher propagation rate constants using cryptated sodium as counterion in THF compared to sodium and cesium. This was explained by assuming that the active species exists as a contact ion pair. As the rate of polymerization of contact ion-pairs is supposed to decrease for smaller ionic radii, it was suggested that the smaller ionic radius of sodium, as compared to cesium is compensated by external solvation resulting in an increase of the interionic distance. Using lithium as counterion low propagation rate constants are observed compared to cesium, potassium, and sodium in THF[10,11].

The rate constant of propagation increases with increasing polarity of solvent. The cations are better solvated in polar solvents which increases the interionic distance in the ion pair. The propagation rate constants of ion-pairs are higher in DME than in THF for Na^+ and Cs^+ counterions. However, the propagation rate constants of ion-

pairs with lithium as counterion are smaller in DME than in THF[1,11]. The bidentate DME molecules solvate the lithium cation only peripherally. As a result of chelation, monomer insertion becomes sterically hindered by the DME molecule peripherally solvating the lithium cation.. Teyssié and coworker[12,13] demonstrated the polymerization of MMA in presence of crown ethers and obtained PMMA of narrow molecular weight distribution with good control of molecular weight. Electron-donating ligands are expected to interact with ion pairs and to decrease aggregation. In this connection, it is of interest to use other common chelating agents for lithium cation, such as N,N,N'-N'-tetramethylethylenediamine (TMEDA) in anionic polymerization of MMA in order to verify the above argument. In general, in several organic reactions it is evidenced that chelation of Li^+ with TMEDA increases the overall reaction rate[14,15].

In presence of chelating agents, organolithium compounds generally dissociate into smaller aggregates due to the co-ordination of lithium. The tendency of lithium enolates to form dimer and higher aggregates is much stronger than that of hydrocarbon-lithium compounds, e.g. polystyryl lithium. Tsvetanov et al[16] and Müller et al[17,18] showed the existence of associated ion pairs and their effect on rate constants of polymerization of MMA using Na^+ and Li^+ as counterions in THF. ^7Li and ^{13}C NMR measurements of Wang et al[19] in conjunction with VPO measurements of Lochmann et al[20] indicate that models of the chain end, e.g., methyl α-lithio-isobutyrate exist as tetramers at room temperature and as a mixture of dimer and tetramer at -78 °C. This is confirmed by recent MNDO and *ab initio* calculations[21]. Due to the steric hindrance of the polymer chains the existence of tetrameric aggregates of PMMALi is regarded as less probable. The propagating ion pairs in the anionic polymerization of MMA in THF are in equilibrium with dimeric THF solvated ion pairs.

Depending on the monomer studied either an increase or a decrease in reactivity was observed in presence of TMEDA[22-26]. Helary et al[25] observed that the co-ordination to lithium cation in the polymerization of styrene in cyclohexane results in a decrease or in an increase of the k_{app} depending on the active center concentration. This was explained on the basis that unimeric TMEDA co-ordinated species are formed from the dimeric aggregates. The polystyryl lithium anions chelated by TMEDA are less

reactive than the non-chelated unimers which are formed from the dissociation of non-chelated aggregates. Marchal et al[26] observed lower rate constants, $k_{\pm}$, for the polymerization of 2-vinylpyridine in presence of TMEDA and sparteine in toluene.

Matsuzaki et al[27] employed TMEDA in conjunction with nBuLi for MMA polymerization in toluene at 0 °C and obtained only a 4 % yield of PMMA. The objective of their work was only to investigate the effect of polar additives on the tacticity and yield of PMMA. The results are not surprising considering the fact that nBuLi reacts with carbonyl group of MMA. Under the conditions employed, reaction of nBuLi with toluene in the presence of TMEDA would lead to formation of only an insignificant amount of benzyllithium (BzLi).

Therefore, we undertook a study of the anionic polymerization of MMA using 1,1'-diphenylhexyllithium (DPHLi) and benzyllithium (BzLi) in THF using TMEDA as a ligand. The benzyl anion was chosen because, unlike the styryl anion, it lacks the methyl group on the carbon atom, making it a more suitable canditate for initiating MMA anionically. Moreover, this anion has been far less studied. Hatada et al[35] employed BzLi as an initiator for the anionic polymerization of MMA at -78 °C in THF with a view to study the effect of organolithium initiators on the tacticity of PMMA. High polydispersity of 1.84 was obtained. Yield data were not reported.

Recently, Marchal et al[26] showed the ability of various tertiary diamines to enhance the stability of active centers of MMA polymerization using monomer resumption experimental method. In order to evaluate the effect of chelation, kinetics of anionic polymerization of MMA were also performed using DPHLi as initiator in the presence of TMEDA in THF. This initiator was chosen in order to reduce the amount of side reactions resulting from the attack of the monomer carbonyl group[28]. Some control experiments in the absence of TMEDA and in presence of cyclic polyamine such as 1,4,8,11-tetramethyltetraazacyclotetradecane (TMTCT) were also performed in THF.

4.2 Experimental Section

4.2.1 Reagents

Methyl methacrylate (MMA, Röhm GmbH or Aldrich), tetrahydrofuran (THF, BASF AG or SD, Bombay) were purified as described in Chapter 2. Octane (internal

standard, Aldrich) was stirred over sodium/potassium alloy, degassed and distilled under high vacuum. n-BuLi (1.6 M in hexane, Aldrich) was used after determining its actual concentration by double titration. Diphenylethylene (DPE, Aldrich) was titrated with a small amount of n-BuLi and distilled under high vacuum. N,N,N',N'-tetramethylethylenediamine (TMEDA, Aldrich) was stirred over CaH_2, degassed and distilled under high vacuum. 1,4,8,11-tetramethyltetraazacyclo tetradecane (TMTCT, Fluka) was dried under dynamic high vacuum.

4.2.1.1 Preparation of Initiators (BzLi and DPHLi)

1,1'-Diphenylhexyllithium (DPHLi) was prepared as described in Chapter 2. Benzyllithium (BzLi) was prepared as follows:

Tribenzyltin chloride, used in the synthesis of benzyllithium, was prepared according to a previously reported procedure using tin powder and benzyl chloride in water[35]. After Soxhlet extraction with acetone to remove excess metallic tin from the crude tribenzyltin chloride, it was recrystallized from ethyl acetate (mp 140-143 °C) and used for initiator synthesis. Benzyllithium was then prepared by a metal displacement reaction using tribenzyltin chloride and lithium metal in THF at room temperature[36] for 12 h. The greenish brown colored benzyllithium in THF was used immediately for polymerization.

4.2.2 Batch Polymerization

Polymerization was carried out in a flame-dried 250 mL round bottom flask under a nitrogen atmosphere as described in Chapter 2. The solvent, initiator, TMEDA, and monomer were transferred using cannula and syringe techniques. Required amounts of THF and TMEDA were transferred into the flask, and the initiator solution was added drop by drop until a persistent red colour was observed. Usually, 0.2-0.4 mL of 0.08 M initiator solution was required for 100 mL of THF. After quenching the impurities, the required amount of initiator was added and the temperature of the flask was brought to desired temperature, -78 °C or -40 °C (with a dry ice-acetone or dry ice-acetonitrile bath). Freshly distilled MMA was then added to the initiator solution via conditioned cannula. Reaction was terminated after 15 min with distilled methanol, and a portion of the reaction mixture was precipitaed in excess (4 times of the concentrated polymer solution) methanol while the rest was

precipitated in n-hexane. The polymer samples were dried under vacuum at 80 °C for 4 h.

4.2.3 Kinetics Using Flow-tube Reactor

All experiments were carried out in a flow-tube reactor described in Chapter 3. Monomer and premixed initiator/TMEDA solution were pre-cooled and mixed efficiently within less than 1 ms in a mixing jet and allowed to pass through a capillary tube (1 mm inner diameter). The reaction mixture was terminated in a quenching jet at the end of capillary tube with methanol containing a small amount of acetic acid. The temperatures of the mixing jet (T_m) and quenching jet (T_q) were determined using thermocouples. The particular residence time (5ms $\leq \tau \leq$ 3s) of the polymerization solution was achieved by changing the flow rate ($\leq$ 6 ml/s) and tube length (4 cm $\leq l \leq$ 6 m). In all runs the flow rate was carefully chosen in order to maintain turbulent flow during the polymerization with a characteristic Reynolds number, Re >3000.

Experiments were carried out at mixing jet temperatures, T_m = -20 °C, -10 °C, 0 °C and 20 °C. The effective temperature (T_{eff}) of the each run is higher than T_m. The effective temperature of the each experiment was determined using the equations, $T_{eff} = T_m + 0.55\ \Delta T$ [29]. Since the polymerization is very fast, heat transfer through the walls of the tube is negligible, leading to a nearly adiabatic behavior. Thus, data points corresponding to T_{eff} were recalculated to T_m using the known activation energy, E_a = 24 kJ mol^{-1} for the MMA polymerization with lithium as counterion[10] and using the equation,

$$ln\,k_{app}(T_m) = ln\,k_{app}(T_{eff}) + \frac{E_a}{R}\cdot\left(\frac{1}{T_{eff}} - \frac{1}{T_m}\right)$$

In later experiments, an appropriate T_m was selected for each conversion in order to compensate ΔT of the polymerization and to obtain a constant T_{eff} for all experiments.

4.2.4 Polymer Characterization

Monomer conversion was determined with GC using n-octane as an internal standard. After evaporation of the solvent, the polymer was dissolved in benzene,

filtered and freeze-dried. Molecular weights and MWD were determined using GPC equipped with two UV detectors with variable wavelength, and an RI detector, and two 60 cm PSS SDV-gel columns: 1 x 5 μ/100 Å, 1 x 5μ/linear: 10^2-10^5 Å with THF as eluent at room temperature. The calibration was performed using monodisperse PMMA standards.

4.3 Results and discussion

4.3.1 Anionic Polymerization of MMA in Presence of TMEDA in THF

4.3.1.1 Benzyllithium (BzLi) as Initiator

Results of BzLi initiated MMA polymerization are summarized in Table 4.1. It is seen that at -78 °C BzLi alone is able to bring about controlled polymerization of MMA. The obtained PMMA possesses predicted number average molecular weight with narrow molecular weight distribution ($M_w/M_n < 1.13$).

Table 4.1: Influence of TMEDA on the BzLi-initiated Anionic Polymerization of -78 °C in THF.

S. No.	[BzLi] $\times 10^4$ mol	[MMA] mol	$\frac{[TMEDA]_0}{[BzLi]_0}$	Yield[a] %	$M_{n,calc}$ [b] 10^{-3}	$M_{n,SEC}$ [c] 10^{-3}	M_w/M_n	$M_{n,SEC}/M_{n,Calc.}$
1	1.40	0.0280	0	97	19.45	19.20	1.12	0.99
2	0.76	0.0280	0	100	36.80	40.40	1.13	1.10
3	1.40	0.0280	1	100	20.05	20.90	1.11	1.04
4	0.38	0.0541	3	98	173.70	174.40	1.11	1.00
5	0.69	0.0280	3	100	40.63	42.00	1.11	1.03
6[d]	3.39	0.0468	1	100	13.80	56.00	1.2	4.06
7[e]	1.97	0.0280	1	95	14.20	53.00	1.3	3.73
8[e]	3.94	0.0370	1	95	9.50	34.00	1.3	3.58
9[f]	3.88	0.0795	> 10	97	20.50	234.05	1.11	11.42
10[f]	3.88	0.0608	>10	100	15.68	124.02	1.21	7.91
11[g]	3.88	0.0936	>10	10	40.00	319.08	1.22	7.98

a) As precipitated from n-hexane, b) $M_{n,calc}$ = (moles of monomer/ moles of initiator) × (mol. wt. of monomer). c) M_n determined by size exclusion chromatography using standard PMMA calibration. d) BzLi synthesized by metalation of toluene at room temperature for 3 h. e) BzLi synthesized by metalation of toluene at 60 °C for 3 h. f) BzLi synthesized *insitu* by metalation of toluene in THF before polymerization at room temperature. g) n-BuLi was added to the THF solution containting TMEDA at RT and polymerization was performed at -78 °C.

These results are contrary to the earlier observations[35]. The difference in the results observed in this study and that reported by Hatada et al[35] seems to arise because of the abnormally high concentration of the monomer (10 wt %) used in the earlier study.

Thus, under appropriate conditions, BzLi can quantitatively initiate the anionic polymerization of MMA to yield monodisperse PMMA (Fig. 4.1) similar to DPHLi initiator.

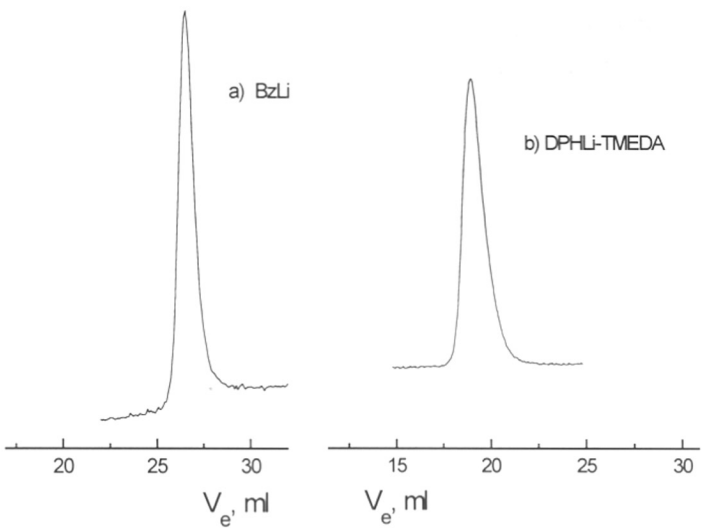

Fig. 4.1: SEC traces of PMMA prepared a) BzLi as initiator at -78 °C (run 1 in Table 4.1) and b) in presence of TMEDA using DPHLi at -40 °C (run 6 in Table 4.3).

It is interesting to note that (α-methylstyryl)lithium (α-MeStLi) under similar conditions does not initiate MMA polymerization in a controlled manner[36]. The subtle difference in reactivity between these two initiating systems is possibly due to the presence of one methyl group in α-MeStLi. It is also known that in the absence of any additive styryllithium is not a good initiator for MMA, due to its ability to attack the carbonyl group of MMA[37]. This is due to the higher reactivity of styryllithium and (α-methystyryl)lithium anions. Camparatively, benzyllithium is less active (absence of alkyl group with +I effect) and therefore carbonyl attack is minimized significantly.

Metalation of toluene using nBuLi and TMEDA at 60 °C was attempted. BzLi obtained by this method was used to polymerize MMA in THF at -78 °C. PMMA obtained using this initiator had broad MWD (runs 7 and 8 in Table 4.1). The molecular weight of the obtained PMMA is 5 times higher than the theoretical value calculated from the feed ratio of monomer to initiator concentration. The low initiator efficiency (20 %) suggest incomplete metalation reaction. Attempts were also made

to synthesis BzLi by *insitu* metalation of toluene using nBuLi in THF at room temperature for 15 min. The polymerization of MMA at -78 °C using the above initiator solution resulted in high molecular weight PMMA (runs 9-11 in Table 4.1).

The initiator efficiency was only 10 % indicating the formation of only small amount of BzLi. The excess nBuLi is probably destroyed by a side reaction with THF at room temperature. However, the obtained high molecular weight PMMA possesses narrow MWD. Polymerization of MMA at -40 °C using benzyllithium as initiator did not give controlled polymerization in both the presence and absence of TMEDA. Apparently, higher reactivity of the benzylic anion at -40 °C results in several side reactions which gave a broad MWD (M_w/M_n = 1.35).

4.3.1.2. 1,1'-diphenylhexyllithium (DPHLi) as Initiator

The polymerization of MMA using DPHLi initiator also gave good control of the molecular weight and MWD in the absence of TMEDA at -78 °C (Table 4.2). Increasing the reaction temperature to -40 °C and in the absence of TMEDA, molecular weight control is lost[38].

Table 4.2: Effect of TMEDA on the DPHLi-Initiated Anionic Polymerization in THF at -78°C

S. No.	[BzLi] $\times 10^4$ mol	[MMA] mol	$\frac{[TMEDA]_0}{[DPHLi]_0}$	Yield %[a]	$M_{n,calc}$ [b] 10^{-3}	$M_{n,SEC}$ [c] 10^{-3}	M_w/M_n	$M_{n,SEC}/M_{n,Calc.}$
1	0.886	0.0280	0	100	31.60	28.70	1.18	0.91
2	0.886	0.0280	4	100	31.60	30.90	1.18	0.98

a) As precipitated from n-hexane, b) Mn, calc = [M]/[I] × mol. wt. of monomer c) M_n determined by size exclusion chromatography using standard PMMA calibration.

In the absence of any additive at -40 °C, polymer yield was only ~ 70 % and the polydispersity of the resultant PMMA increased to 1.24 (Table 4.3). As much as 30 % polymer was isolated as methanol soluble oligomer possessing molecular weight less than Mn = 5000. This indicates that 30 % of the active species are deactivated due to the termination reaction occurring during the initial stages of the polymerization at -40 °C.

Table 4.3: Anionic Polymerization of MMA using TMEDA Chetated DPHLi-Initiator in THF at -40 °C

S. No.	[BzLi] $\times 10^4$ mol	[MMA] mol	$\frac{[TMEDA]_0}{[DPHLi]_0}$	Yield %[a]	$M_{n,calc}$ [b] 10^{-3}	$M_{n,SEC}$ [c] 10^{-3}	M_w/M_n	$M_{n,SEC}/M_{n,Calc.}$
1	1.47	0.0419	0	68	19.5	15.70	1.20	0.81
2	0.80	0.0280	0	68	23.8	36.60	1.22	1.54
3	0.88	0.0280	1	100	31.9	31.80	1.19	1.00
4	1.47	0.0367	3	100	25.0	25.65	1.16	1.03
5	1.54	0.0374	3	100	24.3	27.80	1.14	1.14
6	0.80	0.0280	4	100	35.0	36.20	1.21	1.03
7	0.80	0.0300	6	100	37.5	40.40	1.21	1.06

a) As precipitated from n-hexane, b) $M_{n,calc}$ = [M]/[I] × mol. wt. of monomer × yield factor. c) M_n determined by size exclusion chromatography using standard PMMA calibration.

The polymerization was then studied with various molar ratios of DPHLi:TMEDA. The presence of TMEDA in an equimolar amount with respect to the initiator DPHLi results in quantitative conversion with good control of molecular weight. The MWD of the resultant PMMA are narrow (M_w/M_n = 1.16-1.2) and free from oligomer contamination (Fig. 4.1b). Increasing the molar concentration of TMEDA does not significantly influence the molecular weight control or the MWD. Thus, chelation of the Li^+ cation is a convenient method to gain control of the anionic polymerization of MMA using DPHLi as initiator. Apparently, the termination reaction is suppressed by the chelating agent at -40 °C due to peripheral solvation. However, at -23 °C the control is lost (Table 4.4). Experiments done at -23 °C, in both the presence and absence of TMEDA, are characterized by broad MWDs and low conversions. The molar ratio of initiator to TMEDA does not seem to have any significant influence on the molecular weight and its distribution.

Table 4.4: Anionic Polymerization of MMA using DPHLi-Initiator in THF at -23 °C

S. No.	[BzLi] $\times 10^4$ mol	[MMA] mol	$\frac{[TMEDA]_0}{[DPHLi]_0}$	Yield %[a]	$M_{n,calc}$ [b] 10^{-3}	$M_{n,SEC}$ [c] 10^{-3}	M_w/M_n	$M_{n,SEC}/M_{n,Calc.}$
1	0.88	0.0280	0	68	32.0	38.70	1.44	1.21
2	0.88	0.0280	3	100	32.0	57.60	1.54	1.80

a) As precipitated from n-hexane, b) Mn, calc = [M]/[I] × mol. wt. of monomer c) M_n determined by size exclusion chromatography using standard PMMA calibration.

4.3.2 Effect of TMEDA on the Kinetics of the Anionic Polymerization of Methyl Methacrylate in THF.

The results of the kinetic experiments done in flow-tube reactor at -20, -10 and 0 °C are summarized in Tables 4.5 and 4.6. First, in a series of experiments the initiator concentration was varied at constant temperature, T_{eff} = -20 °C, and $[TMEDA]/[I]_0$ = 2. First-order time-conversion plots show a downward curvature irrespective of the concentration of initiator (Fig. 4.2). In general, the polymerization of MMA with Li^+ as counterion exhibits first-order kinetics under optimum condition provided the rate of initiation is faster than propagation ($k_i \geq k_p$).

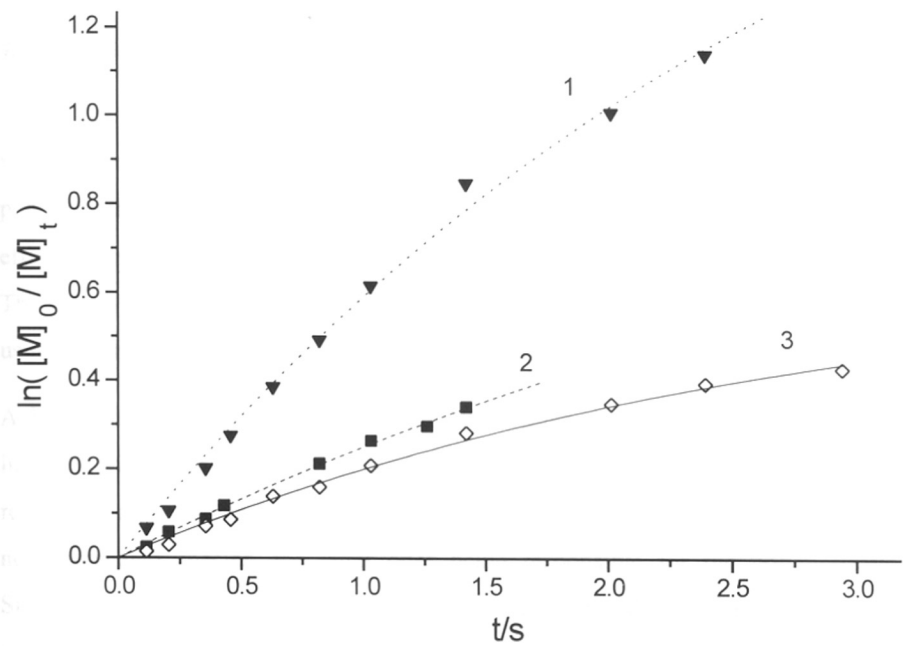

Fig.4.2: First-order time-conversion plots of the MMA polymerization in THF in presence of a 2-fold molar excess of TMEDA with respected to initiator concentration at -20 °C. $[M]_0$ = 0.23 mol/l, $[I]_0$ 1) $5.9 \cdot 10^{-3}$, 2) $1.4 \cdot 10^{-3}$ and 3) $0.8 \cdot 10^{-3}$ all in mol/l.

The non-linearity of the semilogarithamic time-conversion plots indicates that the apparent rate constant decreases during the polymerization due to the termination reaction competing with propagation. The rate expression for the polymerization with unimolecular termination is given by the equation 4.1:

$$ln \frac{[M]_0}{[M]_t} = \frac{k_{app}}{k_t} \cdot \left(1 - e^{-k_t \cdot t}\right) \qquad (4.1)$$

where the initial slope of the first-order time-conversion plot, $k_{app} = k_p \cdot [P^*]$ is the apparent rate constant, k_p and k_t are the rate constants of propagation and termination, respectively and $[P^*] = f \cdot [I]_0$ is the active center concentration.

4.3.2.1 Effect of Chelation on Reaction Order

The linearity of the plots of the number-average degree of polymerization, P_n, versus conversion, x_p, shows the absence of transfer reactions during the polymerization (Fig. 4.3). The deviation from the theoretical line shows the low efficiency of the DPHLi initiator in presence of TMEDA ($0.45 \leq f \leq 0.74$) at -20 °C. The values of k_{app} and k_t were determined by fitting to the experimental data points using equation 1 and a non-linear least-squares method (Table 4.5).

A bi-logarithamic plot of k_{app} versus active center concentration, $[P^*]$, results in linearity with a slope of 0.53 (Fig. 4.4). The fractional order of the reaction with respect to active center concentration indicates the co-existence of aggregated and non-aggregated species, the latter ones being responsible for the polymerization. Similar fractional reaction orders were obtained in the absence of additive in the anionic polymerization of MMA in THF[16-18].

Table 4.5: Kinetic results of MMA polymerization in presence of TMEDA as a chelating agent in THF using a flow-tube reactor , $[MMA]_0 = 0.23$ mol/l

Run	[DPHLi]$_0 \times 10^3$ mol/l	$\frac{[TMEDA]}{[DPHLi]_0}$	T_{eff} ° C	t_{max}[a], sec	$x_{p,max}$[b]	$P_{n,th}$[c]	$P_{n,SEC}$[d] at $x_{p,max}$	M_w/M_n at $x_{p,max}$	f[e]
1	5.9	2	-20	2.94	0.92	36.6	47.7	1.25	0.74
2	1.4	2	-20	1.42	0.40	161.0	272.0	1.29	0.58
3	0.8	2	-20	2.39	0.48	285.1	393.0	1.38	0.72
4	1.4	2	-10	1.03	0.34	161.0	248.8	1.28	0.63
5	1.9	2	0	2.01	0.58	118.6	116.9	1.46	0.71
6	1.4	0.3	-20.3	2.07	0.35	50.0	110.5	1.31[g]	0.48
7	1.4	0.7	-20.2	2.07	0.38	54.3	114.6	1.21[g]	0.51
8	1.4	1	-20.4	2.07	0.37	52.9	118.4	1.21	0.45
9	1.4	1.5	-19.9	2.07	0.37	52.9	119.3	1.16	0.45
10	1.4	3.5	-20.1	2.07	0.39	55.7	109.9	1.20	0.54
11	1.4	7	-20.4	2.07	0.37	52.9	109.8	1.22	0.49
12	1.4	0	-20.5	2.39	0.54	77.1	74.1	1.35	0.88
13	4.0	0	-19.2	2.39	0.74	37.0	47.4	1.25	0.80
14	1.4	0	-0.1	2.39	0.59	84.3	100.3	1.69	0.81
15	1.4	0	+19.2	2.39	0.55	78.6	93.5	1.95[g]	0.89
16	1.4	1.5[f]	-20	2.07	0.37	52.9	87.1	1.25	0.59

a) longest reaction time. b) conversion obtained at t_{max}. c) $P_{n,th} = ([M]_0 / [I]_0) \times x_{p,max}$. d) $P_{n,SEC} = (M_{n,SEC} - M_{initiator}) / M_{monomer}$. e) initiator efficiency, $f = P_{n,th} / P_{n,SEC}$ from the ratio of $[M]_0/[I]_0$ and slope of the plot of $P_{n,SEC}$ vs conversion. f) 1,4,8,11-tetramethyltetraazacyclotetradecan (TMTCT) was used. g) bimodal distribution

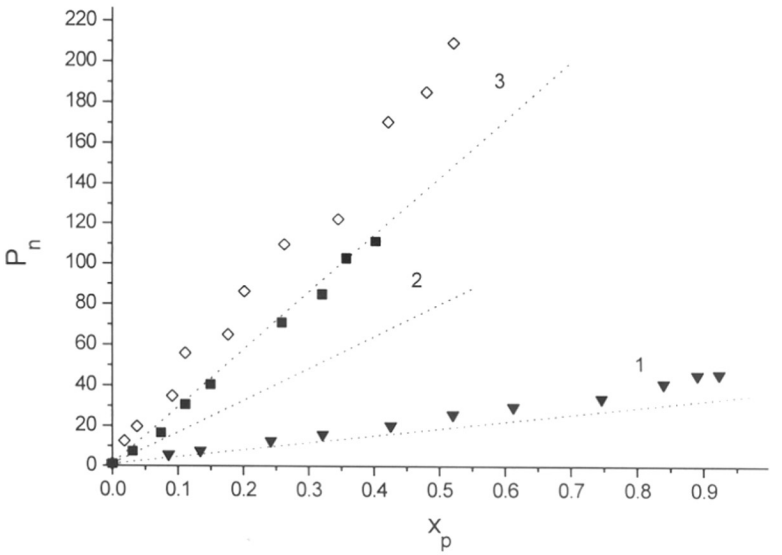

Fig. 4.3: Dependence of degree of polymerization, P_n with conversion, x_p of MMA polymerization using TMEDA chelated Li^+ counterion at -20 °C in THF. $[M]_0$=0.23 mol/l, $[I]_0$; 1) $5.9.10^{-3}$, 2) $1.4.10^{-3}$ and 3) $0.8.10^{-3}$ all in mol

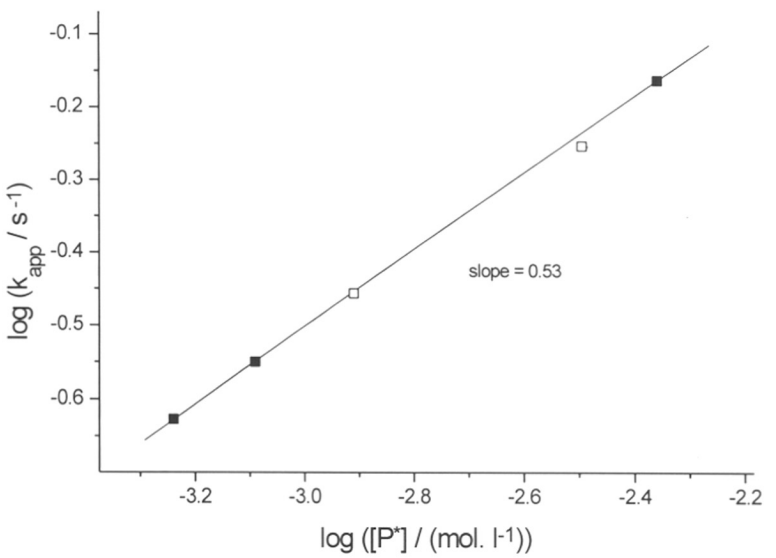

Fig. 4.4: Reaction order with respect to initiator concentration for the polymerization of MMA with TMEDA chelated Li^+ counterion in THF at -20 °C; (■) with TMEDA and (□) without TMEDA.

The existence of associated ion pairs in presence of TMEDA shows that the chelation of the Li cation in the anionic polymerization of MMA in THF does not effectively perturb the aggregation state of the enolate ion pair. Hence, the determined k_p values are only apparent because the effect of aggregation was not taken into account. The apparent propagation rate constant $\bar{k}_p$ is given by equation 4.2 assuming that the rate constant of propagation of the aggregates, $k_{ass} << k_p$ [6].

$$\bar{k}_p = \alpha \cdot k_{\pm} \tag{4.2}$$

where $\alpha = \frac{[P_{\pm}]}{[P^*]} = \left(2 \cdot K_a \cdot [P^*]\right)^{-1/2}$ is the fraction of unimers, and K_a is the equilibrium constant of aggregation. For $\alpha << 1$, this leads to equation 4.3.

$$\frac{k_{app}}{[P^*]^{1/2}} = \bar{k}_p \cdot [P^*]^{1/2} = \frac{k_{\pm}}{\sqrt{2 \cdot K_a}} \tag{4.3}$$

From this equation the ratio $\frac{k_{\pm}}{\sqrt{2 \cdot K_a}}$ can be determined. Since K_a = const. at a given temperature, this value should be constant. Table 4.2 shows that this is the case whereas $\bar{k}_p$ depends on $[P^*]$. As expected for a unimolecular termination, k_t does not significantly depend on $[P^*]$.

The obtained fractional reaction order of the reaction with respect to active center concentration indicates that the chelation with TMEDA only replaces the THF molecules in the dimeric enolate ion pair retaining a peripheral co-ordination with lithium (Scheme 4.1). The lithium enolates of tert-butylpropionate and tert-butyl isobutyrate are known to form dimeric aggregates with TMEDA and their crystal structure shows Li_2O_2 four-membered rings with one TMEDA per lithium cation[30]. MNDO calculations indicate the stability of a TMEDA co-ordinated dimer with methyl α-lithio isobutyrate[31].

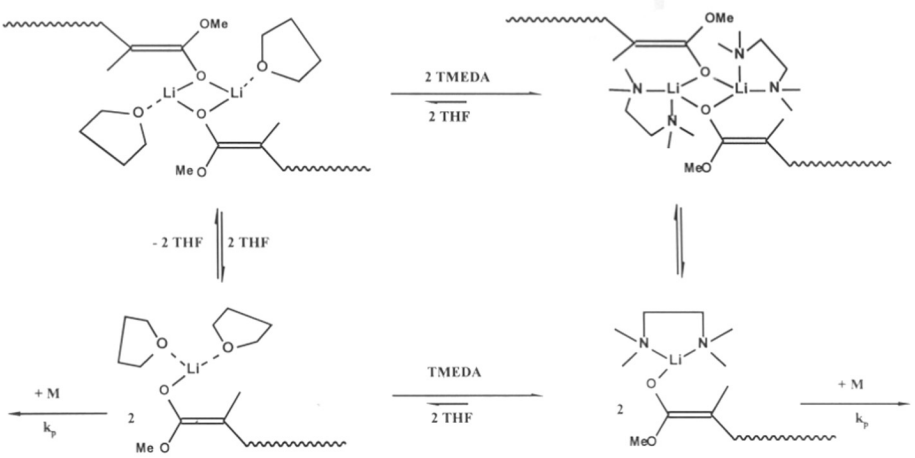

Scheme 4.1: Chelation and aggregation of PMMA-Li

4.3.2.2 Effect of TMEDA concentration on propagation rate constant.

Upon increasing the mole ratio of TMEDA to initial initiator concentration from 0 to 7, the apparent rate constant, k_{app} decreases (Table 4.6 and Fig 4.5). However, it is also observed that the initiator efficiency is significantly decreased in the presence of TMEDA even if the ratio r = $[TMEDA]/[I]_0 < 1$ (Table 4.5, Exp. 6, 7). The plots of the number average degree of polymerization, P_n, versus conversion in presence of various amounts of TMEDA show stronger deviations from the theoretical line than the control experiment carried out in the absence of TMEDA (Fig.4.6). This could have resulted from the enhanced nucleophilicity of the chelated DPHLi initiator leading to initiator destruction reaction either with THF molecules before mixing with monomer solution at room temperature or the carbonyl groups of monomer at -20 °C. The constant values of $\frac{k_{app}}{[P^*]^{1/2}} = \frac{k_{\pm}}{\sqrt{2 \cdot K_a}}$ in presence and in absence of TMEDA indicate that either the rate constants of polymerization, $k_{\pm}$, and the equilibrium constant of aggregation, K_a, are not affected by the addition of TMEDA at -20 °C or that the effects compensate (Table 4.6).

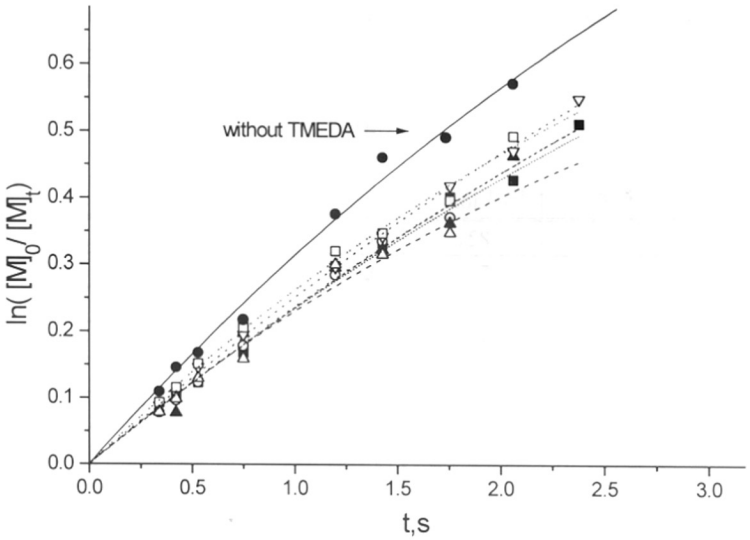

Fig.4.5: First-order time-conversion plots of MMA polymerization for various ratios r = $[TMEDA]_0/[DPHLi]_0$; r = (●), 0.3 (■), 0.7 (O), 1 (▲), 1.5 (▽), 3.5 (□), and 7 (Δ).

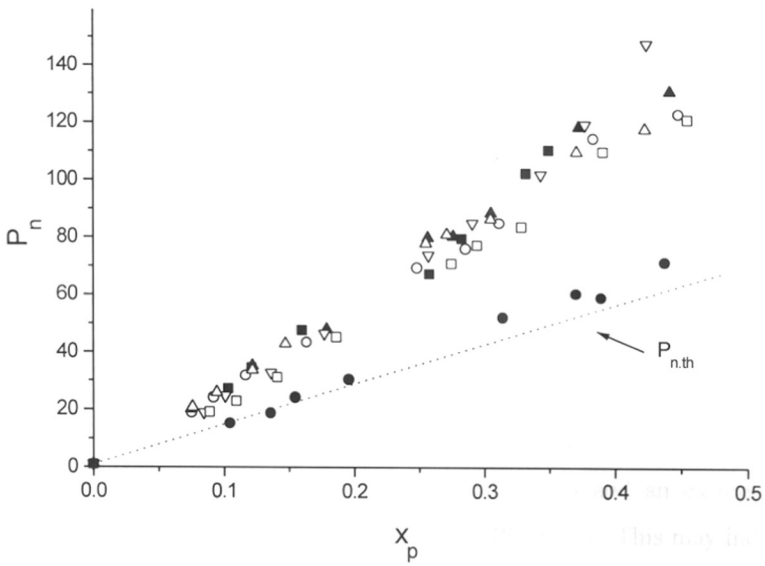

Fig. 4.6: Dependence of degree of polymerization, P_n, on conversion, x_p, of MMA polymerization in THF at various ratios r = (●), 0.3 (■), 0.7 (O), 1 (▲), 1.5 (▽), 3.5 (□), and 7 (Δ).

Table 4.6: Rate constants of propagation, k_p and termination, k_t, for the anionic polymerizsation of MMA using TMEDA chelated lithium as counterion in THF.

Run	$[P^*]^{a)} \times 10^3$ mol / l	T_{eff} °C	$\frac{[TMEDA]}{[P^*]}$	k_{app} s^{-1}	$\bar{k}_p = \frac{k_{app}}{[P^*]}$ $l \cdot mol^{-1}\ s^{-1}$	$\frac{k_{app}}{[P^*]^{1/2}} = \frac{k_t}{\sqrt{2 \cdot K_a}}$ (eq. 4.3)	k_t s^{-1}
1	4.360	-20	2.7	0.689	158	10.43	0.319
2	0.812	-20	3.4	0.282	347	9.89	0.243
3	0.576	-20	2.7	0.236	409	9.82	0.340
4	0.882	-10	3.2	0.393	445	13.22	0.453
5	1.35	0	2.8	0.861	638	23.44	1.210
6	0.714	-20.3	0.6	0.258	361	9.65	0.170
7	0.714	-20.2	1.4	0.256	358	9.57	0.160
8	0.630	-20.4	2.2	0.254	403	10.12	0.155
9	0.630	-19.9	3.3	0.269	426	10.69	0.140
10	0.756	-20.1	6.5	0.295	390	10.72	0.250
11	0.686	-20.4	14.3	0.266	388	10.16	0.290
12	1.230	-20.5	0	0.350	284	9.96	0.224
13	3.200	-19.2	0	0.560	175	9.90	-
14	1.130	-0.1	0	0.690	608	20.44	0.590
15	1.250	+19.2	0	0.923	740	26.16	0.930
16	0.826	-20.7	2.5[b)]	0.210	254	7.30	-

a) $[P^*] = f \cdot [I]_0$ where f is the initiator efficiency

b) 1,4,8,11-tetramethyltetraazacyclotetradecane (TMTCT) was used.

The values of k_t do not significantly depend on ratio r. The polymers obtained in presence of TMEDA possess narrow molecular weight distribution (M_w/M_n = 1.25) compared to the ones prepared in the absence (M_w/M_n = 1.35) at -20 °C (Fig. 4.7). A decrease of M_w/M_n versus conversion indicates a moderately slow exchange between aggregated and non-aggregated ion pairs[18]. When the ratio r = $[TMEDA]_0/[P]^*$ is less than unity, the obtained polymers have a bimodal MWD and an extremely high molecular weight polymer fraction is found in the GPC traces. This may indicate the existence of a slow equilibrium between the chelated aggregates and non-chelated enolate ion pairs at r < 1. A similar observation was reported for the polymerization of isoprene in presence of very small amounts of TMEDA with respect to $[P^*]$ in hexane[32]. Thus, an equimolar amount of TMEDA is necessary for the complete chelation of aggregated enolate and in order to obtain monodisperse PMMA.

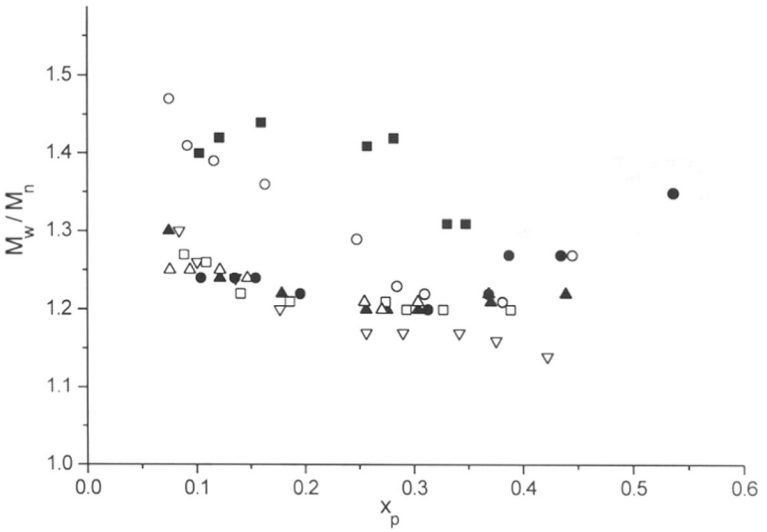

Fig. 4.7: Dependence of MWD on conversion in presence of various amount of TMEDA; r = (●), 0.3 (■), 0.7 (O), 1 (▲), 1.5 (▽), 3.5 (□), and 7 (Δ).

The first-order time conversion plot of the reaction in presence of a cyclic tertiary polyamine ('crown amine') such as 1,4,8,11-tetramethyltetraazacyclotetradecane (TMTCT) shows a lower k_p compared to the reaction in absence of any additive or in the presence of TMEDA. This is in contrast to the observed high rate constant in presence of cryptated sodium (Na^+, 222)[9], indicating that TMTCT does not form ligand-separated enolate ion pairs in THF. This confirms that the strong co-ordination between enolate anion and lithium in aggregates require powerful cation-binding agents such as cryptands to dissociate into unimeric species as shown by NMR measurements of Wang et al[13]. The initiator efficiency is high in presence of TMTCT (Table 4.6). The lower $k_{\pm}$ is attributed to the steric hindrance exerted by the cyclic polyamine. The linearity found in the first-order time conversion plot and the plot of P_n versus conversion indicate the absence of termination and transfer reactions in presence of TMTCT.

4.3.2.3 Evaluation of Arrhenius Parameters

The effect of temperature on the rate constants of propagation and termination is seen in Table 4.6 (runs 3, 4 and 5) and Fig. 4.8. Since the active center concentrations are not constant at different temperature due to aggregation, the determined rate constant, $\bar{k}_p$, and the Arrhenius parameters are only apparent. The

obtained apparent activation energy is E_a^{app}= 17.4 ± 2.2 kJ mol^{-1} and the frequency exponent, log A^{app} = 6.1 ± 0.4 (Fig. 8).

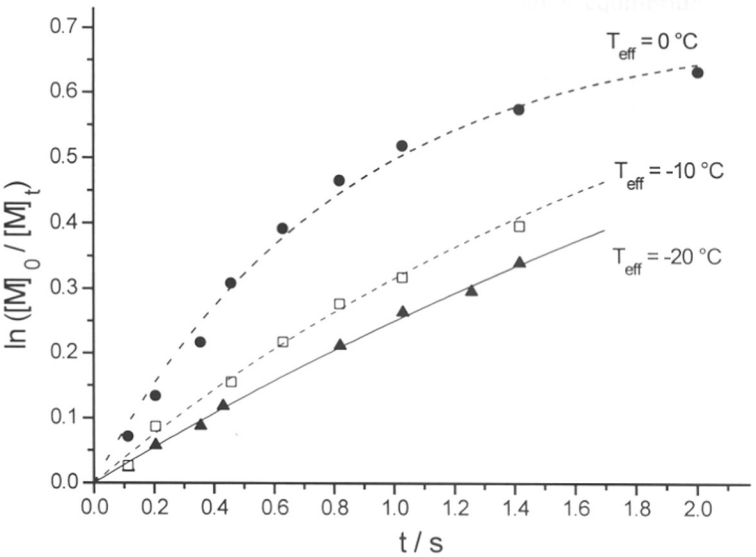

Fig. 4.8: First-order time-conversion plots at different temperature. $[M]_0$ = 0.23 mol/L, $[I]_0$ =1.4 10^{-3} mol/L; at 0 °C, $[I]_0$ = 1.9 10^{-3} mol/L

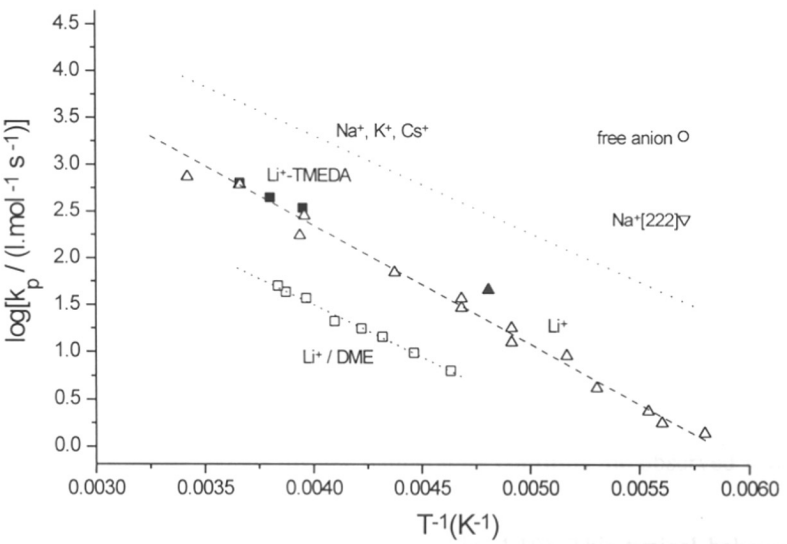

Fig. 4.9: Arrhenius plot of the propagation rate constants, kp in the anionic polymerization of MMA for TMEDA chelated Li^+ counterion (r < 3) in THF and the reported rate constanat for other conuterions and solvents (aggeration was not taken into account); (▲) $k_{\pm}$ rate constant at -65 °C.

These values are slightly lower than the reported ones for the Li counter ion in THF in the absence of additives (E_a^{app}= 24 kJ mol^{-1}, log A^{app} = 7.4). In order to compensate the effect of active centre concentration on the aggregation equilibrium, it is more useful to plot $\frac{k_{app}}{[P^*]^{1/2}} = \frac{k_{\pm}}{\sqrt{2 \cdot K_a}}$. The apparent activation energy of this plot (Fig. 4.10) is $E_{a,app} = E_{a,\pm} + \frac{1}{2} \Delta H_a$ and the apparent activation entropy contain the entropy of assoication. It has been previously observed that the rate constants of the polymerization of MMA with Li^+ as counterion in DME are lower than those obtained in THF.

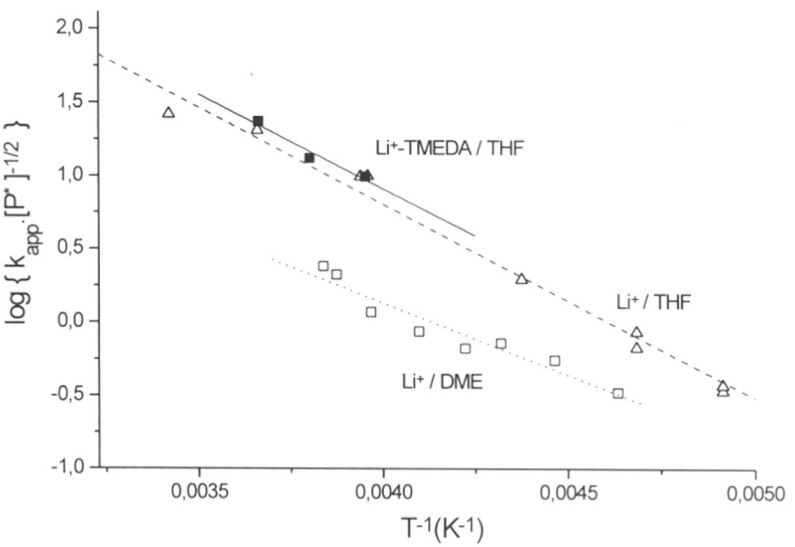

Fig. 4.10: The square root dependence of apparent rate constant, k_p on the active center concentration, $[P^*]$ in anionic polymerization of MMA for TMEDA chelated Li^+ counterion (r < 3) in THF and the reported rate contants in DME and THF solvent.

The plot of log $\frac{k_{\pm}}{\sqrt{2 \cdot K_a}}$ versus inverse temperature confirms the observed lower rate constants in DME with lithium as counterion (Fig. 4.10). This typical behavior was explained in terms of strong co-ordination of Li cation with the oxygen atoms of bidentate ligand DME. This peripheral solvation of the Li cation makes it more difficult for the incoming monomer to displace the DME molecules. The stronger bidentate ligand TMEDA chelates Li cation also peripherally (Scheme 4.1) and cannot

enhance the dissociation of the aggregated enolate ion pairs into unimeric species. The independence of rate constant from the TMEDA chelation would suggest that peripherally TMEDA-chelated enolate ion pairs are more reactive than in the case of DME-chelated ones (Fig. 4.10). The co-ordination of Li by the nitrogen atoms of TMEDA is stronger than that of the oxygen atoms of DME which may lead to a larger interionic distance in the contact ion pair. Our results suggest that the co-ordination of lithium cation in the polymerization of MMA in THF with excess TMEDA does not affect the rate of polymerization and forms only peripherally solvated ion pairs.

The presence of the competing termination reaction is evident as the polydispersity index increases gradually with conversion, x_p at higher polymerization temperatures. The control experiments carried out in the absence of TMEDA at temperatures -20, 0, and +19 °C showed a pronounced termination reaction. The activation energy for the termination reaction in presence of TMEDA is found to be $E_{a,t}$ = 46 ±7 kJ mol^{-1} and the frequency exponent, log A_t = 8.8 ± 1.4. These values are comparable to the reported ones for the MMA polymerization initiated with 9-methylfluorenylsodium in THF ($E_{a,t}$ = 48 kJ mol^{-1} and A_t = 10)[33]. They are higher than the values for Li/THF ($E_{a,t}$ = 22 ± 3 kJ mol-1 and log A_t = 4 ± 0.7). However, the effect of TMEDA on the rate constant of terminaton reaction is small within experimental error. The molecular weight distribution of the polymers obtained are broad and bimodal in absence of any additives at +19 °C (Table 4.5, run no. 14).

4.4 Conclusion

Anionic polymerization of MMA at -78 ^{0}C in THF using benzyllithium as initiator results to PMMA with predetermined molecular weight and narrow molecular weight distribution. At -40 ^{o}C, 1,1-diphenylhexyllithium (DPHLi) initiated MMA in THF produced PMMA contaminated with oligomers (15 %). Chelation of lithium cation in the anionic polymerization of MMA using TMEDA produces oligomer free PMMA with conrol on molecular weight and polydispersity values of less than 1.2.

The kinetic experiments carried out in flow-tube reactor at -20 ^{o}C, show that the reaction order with respect to active center concentration is 0.5 in the presence as well as in the absence of TMEDA. This indicates that the chelation of the lithium cation

does not effectively perturb the aggregation of the enolate ion pair. The rate constant of propagation via non-aggregated ion pair, $k_{\pm}$, and the equilibrium conastant of aggregation, K_a, are not significantly affected by TMEDA or the effects compensate. The rate constants of termination in absence and presence of TMEDA are comparable. Thus, to conclude that TMEDA is not superior to THF as a ligand for lithium ester enolates. In contrast, in presence of a cyclic tertiary polyamine ("crown amin") such as 1,4,8,11-tetramethyltetraazacyclotetradecan, a lower propagation rate constant and no termination are found at -20 °C.

4.5 References

1. Muller, A. H. E., *in Anionic Polymerization. Kinetics, Mechanisms and Synthesis;* J. E. McGrath, Ed., ACS Symp. Ser. No. 166, Washington **1981**, p. 441.
2. Wiles, D. M.; Bywater, S. *Polymer,* **1962**, 3, 175.
3. Löhr, G.; Schulz, G. V. *Makromol. Chem.* **1973**, 172, 137.
4. Löhr, G.; Schulz, G. V. Eur. *Polym. J.* **1974**, 10, 121.
5. Mita, I.; Watanabe, Y.; Akatsu, T.; Kambe, H. *Polym. J.* **1973**, 4, 271.
6. Müller, A. H. E. in: *Comprehensive Polymer Science*, Vol. 3; G. Allen, J.C. Bevington, Ed., Pergamon, Oxford **1988**, p. 387
7. Kraft, R.; Müller, A.H.E.; Warzelhan, V.; Hocker, H.; Schulz, G. V. *Macromolecules*, **1978**, 11, 1095.
8. Kraft, R.; Müller, A.H.E.; Höcker, H.; Schulz, G.V. *Makromol. Chem., Rapid Commun.* **1980**, 1, 363.
9. Johann, C.; Müller, A.H.E. *Makromol. Chem., Rapid Commun.* **1981**, 2, 687.
10. Jeuck, Müller, A.H.E. *Makromol. Chem., Rapid Commun.* **1982**, 3, 121.
11. Kilz. P: "Untersuchungen zur Kinetik der anionischen Polymerisation von Methylmethacrylat mit Lithium als Gegenion in Dimethoxyethan", *Diplomarbeit*, Mainz, **1982**
12. Varshney, S. K.; Jérôme, R.; Bayard, P.; Jacobs, C.; Fayt, R.; Teyssié, P. *Macronolecules,* **1992**, 25, 4457.
13. Wang, J. S.; Jérôme, R.; Warin, R.; Zhang, H.; Teyssié, P. *Macromolecules,* **1994**, 27, 3376.
14. Bernstein, M. P.; Romesberg, F.E.; Fuller, D.J.; Harrison, A.T.; Collum, D.B.; Liu, Q.; Williard, P.G. *J.Am.Chem.Soc.* **1992**, 114, 5100.
15. Seebach, D. *Angew. Chem.* **1988**,100, 1685.
16. Tsvetanov, C. B.; Müller, A.H.E.; Schulz, G.V. *Macromolecules*, **1985**, 18, 863.
17. Müller, A. H. E.; Lochmann, L.; Trekoval, J. *Makromol. Chem.* **1986**, 187, 1473.
18. Kunkel, D.; Müller, A.H.E.; Lochmann, L.; Janata, M. *Makromol. Chem., Macromol. Symp.* **1992**, 60, 315.
19. Wang, J.S.; Jérôme, R.; Warin, R.; Teyssié, P. *Macromolecules*, **1993**, 26, 1402.
20. Halaska, V.; Lochmann, L. *Collect. Czech. Chem. Commun.* **1973**, 38, 1780.
21. Weiss, H.;Yakimanski, A. V.; Müller, A.H.E. *J. Am. Chem. Soc.* **1996**, 118, 8897.

22. Davidjan, A.; Nikolaev, N.I.; Zgonnik, V.; Belenkii, B.; Nesterow, V.; Erussalimsky, B. *Makromol. Chem.* **1976**, 177, 2469-2479.
23. Adès, D.; Fontanille, M.; Léonard, J.; Thomas, M. *Eur. Polym. J.* **1983**, 19, 305.
24. Fontanille, M.; Helary, G.; Szwarc, M. *Macromolecules* **1988**, 21, 1532.
25. Helary, G.; Fontanille, M. *Eur. Polym. J.* **1978**,14, 345.
26. Marchal, J.; Gnanou, Y.; Fontanille, M. *Makromol. Chem., Macromol. Symp.* **1996**, 27, 107.
27. Matsuzaki, K.; Nishida, Y.; Kumahara, H.; Miyabashi, T.; Yasukawa, T. *Makromol. Chem.* **1973**, 167,139.
28. Wiles, D. M.; Bywater, S. *Trans. Faraday Soc.* **1965**, 61, 150.
29. Löhr,G.; Schmitt, B.J.; Schulz, G.V. *Z. Phys. Chem.* (Frankfurt am Main) **1972,** 78, 177.
30. Seebach, D.; Amstutz, R.; Laube, T.; Schweizer, W.B.; Dunitz, J.D. *J.Am.Chem.Soc.* **1985**, 107, 5403.
31. Yakimanski, A. V.; Müller, A.H.E. (to be published)
32. Davidjan, A.; Nikolaev, N.I.; Zgonnik, V.; Belenkii, B.; Nesterow, V.; Krasikow, V.; Erussalimsky, B. *Makromol. Chem.* **1978**,179, 2155-2160.
33. Warzelhan, V.; Höcker, H.; Schulz, G.V. *Makromol. Chem.* **1978**,179, 2221.
34. Lochmann, L.; Müller, A.H.E. *Makromol. Chem.* **1990**,191,1657.
35. Hatada, K.; Kitayama, T.; Ute, K. *Prog. Polym. Sci.* **1988**, 13, 189.
36. Varshney, S. K.; Jacobs, C.; Hautekeer, J. P.; Bayard, P.; Jerome, R.; Fayt, R.; Teyssie, Ph. *Macromolecules,* **1991**, 24, 4997
37. Jerome, R.; Forte, R.; Varshney, S. K.; Fayte, R.; Teyssie, Ph. In *Advances in Mechnical and Synthetic Aspects of Polymerization;* Fontanille, M.; Guyot, A., Eds.; NATO ASI Series C; Kluwer: Dordrecht, The Netherlands, 1987, Vol. 215, p 101.
38. Teyssie, Ph.; Fayt, R.; Hautekeer, J. P.; Jacobs, C.; Jerome, R.; Leemans, L.; Varshney, S. K. *Makromol. Chem., Macromol. Symp.* **1990**, 32, 61

Chapter 5: Living Anionic Polymerization of Alkyl (meth)acrylate Using Lithium Perchlorate Ligand

5.1 Introduction

Recent years have witnessed considerable efforts towards achieving 'living' polymerization of alkyl (meth)acrylate monomers[1,15,16-22]. The secondary side reactions in anionic polymerization of alkyl (meth) acrylates which involve the ester group of the monomer have prevented identification of optimum conditions for living polymerization[2,3]. Innumerable kinetic and mechanistic studies have contributed significantly to our understanding of this reaction, resulting in many strategies for enhancing the living character of methyl methacrylate (MMA) polymerization[1,4,5,16-22].

Kinetic experiments suggest that externally solvated contact ion-pairs are responsible for propagation. Tsvetanov et al[6] and Müller et al[7] showed the co-existence with associated ion pairs affects the rates of polymerization of MMA using Na^+ and Li^+ as counterion in THF. Kunkel et al[8] showed the strong influence of a dynamic equilibrium between aggregated and non-aggregated ion-pairs on the molecular weight distribution of the resulting polymers. The polymers with narrow molecular weight distribution is only obtained when the rate of interconversion of these aggregated living chain ends are faster than that of the monomer addition.

^7Li and ^{13}C NMR measurements of Wang et al[9] in conjunction with VPO measurements of Lochmann et al[10] indicate that models of the chain end, e.g methyl α-lithio isobutyrate exist as tetramers at room temperature and as a mixture of dimer and tetramer at -78 °C. This is also confirmed by recent MNDO and *ab initio* calculations[11]. Due to the steric hindrance of the polymer chains the existence of tetrameric aggregates of PMMALi is regarded as less probable. Thus, the propagating ion pairs in the anionic polymerization of MMA in THF are in equilibrium with dimeric THF solvated ion pairs.

Recently, several strategies have been developed and widely used for the controlled anionic polymerization of alkyl (meth)acrylates[12-16]. The addition of several

coordinating agents such as alkali alkoxides[17,18], alkali halide[19], alkali alkoxyalkoxide[18], and aluminum alkyl[22,23] in anionic polymerization of alkyl (meth)acrylate leads to better polymerization control and enables one to form a block copolymers with acrylates and hydrocarbon monomers such as styrene, butadiene, and isoprene[23,24].

Lochmann et al[25] demonstrated the stabilizing effect of lithium tert-butoxide in the anionic polymerization of MMA. Lochmann and Müller studied the effect of lithium tert-butoxide on the rate constants of the anionic polymerization of MMA[18,26] and tert-butylacrylate[8]. It was observed that the rate of termination via cyclization is decreased by two orders of magnitude in presence of lithium tert-butoxide and the rate of cyclization drops ten times more than that of propagation. However, the formation of mixed tetrameric aggregates with slow dynamics leads to a broadening of MWD of the resulting PMMA.

Teyssié and coworkers[25,27] showed the effect of LiCl on the polymerization of alkyl (meth)acrylate to yield well defined polymers with extremely narrow molecular weight distribution ($M_w/M_n > 1.05$) in THF at -78 °C. The beneficial effect of LiCl was attributed to the formation of μ- type complex with the ion pairs which results to a formation of mixed aggregates of similar reactivity[28]. It was shown that only LiCl had the most desirable effect in changing the course of anionic alkyl (meth)acrylate polymerization to yield extremely well defined polymers with narrow molecular weight distribution ($M_w/M_n \leq 1.05$)[19]. However, even LiCl requires a polar solvent (e.g. THF) and low temperatures (-78 °C) for producing PMMA's with narrow molecular weight distribution and high initiator efficiency. Other common-ion salt employed in anionic polymerization of MMA are LiF, LiBr, $Li(Ph_4B)$ and lithium acetate. These salts do not provide PMMA with narrow molecular weight distribution[19].

Kunkel et al[8] studied effect of LiCl on the kinetics of alkyl (meth)acrylate polymerization in THF and showed the formation of reactive 1:1 adduct and less reactive higher adducts of LiCl with enolate ion pairs. The dramatic effect of LiCl on the MWD of the polymers formed was explained on the basis of the higher

interconversion rate between free and LiCl complexed ion pair than that between free and associated ion pairs

The ion-pair association is known to be strongly influenced by the nature of cations[29,30]. The presence of organic and inorganic salts cabable of interacting with growing ion-pair have great influence on the course of anionic polymerization of alkyl (meth)acrylates[31]. This type of salt effect influencing the position of ionic dissociation equilibria of the anionic polymerization of alkyl (meth)acrylates mainly depends on the Lewis acidity and steric factor of the added salt[32]. Hence a better Lewis acid salt should have greater interaction with propagating ion-pairs. To verify this hypothesis, we examined the effect of $LiClO_4$ in various alkyl (meth)acrylate polymerizations.

5.2 Experimental Section

5.2.1 Reagents

Methyl methacrylate (MMA, Röhm GmbH or Aldrich) and tert-butylacrylate (tBA, Aldrich) was fractionated from CaH_2 over a 1 m column filled with Sulzer packing at 45 mbar. After degassing, the distillate was stirred over CaH_2 and distilled under high vacuum. For batch experimental work, MMA and tBA was purified as described in Chapter 2. Tetrahydrofuran (THF, BASF AG) and Toluene was fractionated over a 1.5 m column, stirred twice over sodium/potassium alloy, degassed and distilled under high vacuum. For batch experimental work, these solvents were purified as described in Chapter 2.

n-Octane (internal standard, Aldrich) was stirred over sodium/potassium alloy, degassed and distilled under high vacuum. n-BuLi (1.6 M in hexane, Aldrich) was used after determining its actual concentration by double titration. Diphenylethylene (DPE, Aldrich) was titrated with a small amount of n-BuLi and distilled under high vacuum. 1,1'-Diphenylhexyllithium (DPHLi) initiator was prepared by reacting a known amount of n-BuLi with a slight excess of DPE in THF at -40 °C. The concentration of DPHLi was determined by double titration (Chapter 2). Lithium perchlorate (anhydrous) ($LiClO_4$, Aldrich) was dried under dynamic high vacuum at 100 °C for 24 h.

5.2.2 Batch Polymerization of MMA and tBA

Batch polymerization was carried out in a flamed glass reactor under pure nitrogen atmosphere as described in Chapter 2. The solvent, initiator, $LiClO_4$ solution in THF, and the monomer were transferred by capillary technique or syringe. Required amount of solution of $LiClO_4$ in THF was added into the reactor containing 100 mL of THF. DPHLi solution was added drop by drop until persistent red color was observed. Subsequently the required amount of initiator was added and the temperature of the reactor was brought to -78 °C, or -40 °C. The purified neat MMA or tBA (60 % v/v) diluted with THF was added to the initiator solution. About 5-10s were usually required to add 5-10 mL of diluted monomer solution through stainless steel cannula. Reaction was terminated after 15 mins with degassed methanol. Poly (methyl methacrylate) (PMMA) was recovered by precipitation in n-hexane and dried under vacuum at 60 °C for 4 h. tBA conversion was determined gravimetrically after removing solvent by vacuum. The residue, poly (tert-butyl acrylate) (PtBA) was dissolved in benzene and freeze dried.

5.2.3 Kinetics of MMA Polymerization

The kinetic experiments were carried out in a specially designed flow-tube reactor as described in Chapter 2. Monomer and premixed initiator/$LiClO_4$ solution were pre-cooled and mixed efficiently within less than 1 ms in a mixing jet and allowed to pass through a capillary tube (1 mm inner diameter). The reaction mixture was terminated in a quenching jet at the end of capillary tube with methanol containing a small amount of acetic acid. The temperatures of the mixing jet (T_m) and quenching jet (T_q) were determined using thermocouples. The particular residence time ($5ms \leq \tau \leq 3s$) of the polymerization solution was achieved by changing the flow rate (≤ 6 ml/s) and tube length ($4\ cm \leq l \leq 6$ m). In all runs the flow rate was carefully chosen in order to maintain turbulent flow during the polymerization with a characteristic Reynolds number, $R_e > 3000$.

Experiments were carried out at mixing jet temperatures, T_m = -30 °C, -20 °C, -10 °C, and 0 °C. Since the polymerization is very fast, heat transfer through the walls of the tube is negligible, leading to a nearly adiabatic behavior. Thus, the effective temperature (T_{eff}) of the each run is higher than T_m. Hence, an appropriate, T_m was

selected for each conversion in order to compensate ΔT of the polymerization and to obtain a constant, T_{eff} for all experiments. The effective temperature of the each experiment was determined using the equation, $T_{eff} = T_m + 0.55\ \Delta T$ [33]. Monomer conversion was determined with GC using octane as an internal standard. After evaporation of the solvent, the polymer was dissolved in benzene, filtered and freeze-dried.

5.2.4 Characterization of PMMA and PtBA

Molecular weights and MWD were determined using GPC equipped with two UV detectors with variable wavelength, RI detector, and two 60 cm PSS SDV-gel columns: 1 x 5 μ/100 Å/60 cm, 1 x 5μ/linear: 10^2-10^5 Å or Waters GPC 150C equipped with two μ-ultrastyragel linear columns with THF as eluent at room temperature. The calibration was performed using monodisperse PMMA (Polymer Laboratory) standards.

The glass transition temperature (T_g) of the polymers was determined by differential scanning calorimeter (DSC) using Perkin-Elmer DSC 7 instrument, calibrated with indium and zinc. Tacticity of the polymers was determined by ^{1}H NMR using Bruker SE-200 MHz spectrometer.

5.3 Results and discussion

5.3.1 Polymerization of MMA in THF in Presence of $LiClO_4$

It is known that $LiClO_4$ co-ordinates with both THF as well as carbonyl group of esters[34,35]. The co-ordination behavior of $LiClO_4$ in presence of propagating enolate ion pair and their aggregates in THF is expected to be different. Table 5.1 shows the results of polymerization of MMA in presence of various amount of $LiClO_4$ with respect to DPHLi concentration at -78 °C in THF. The anionic polymerization of MMA in THF at -78 °C using DPHLi as an initiator in the absence of any additive proceeds very rapidly leading to 100 % conversion with good control on molecular weight and relatively narrow molecular weight distribution ($M_w/M_n \leq 1.18$). It was shown by Teyssie and coworkers[19,9] that lithium chloride in anionic polymerization of alkyl (meth)acrylates forms a μ -type complex with the growing ion-pair and shifts a relatively slow classical ion-pair association equilibrium involving different type of

reactive species towards a salt complexed single active species, thus improving the molecular weight distribution (MWD) of the resulting polymers.

Experiments done in the presence of varying quantities of $LiClO_4$ with respect to DPHLi initiator at -78 °C in THF shows specific salt effect of $LiClO_4$ in further narrowing the molecular weight distribution of PMMA. It can be seen from Table 5.1 that a presence of only 0.5 mol of $LiClO_4$ per mol of DPHLi improved the molecular weight distribution of PMMA from 1.18 to 1.14. Increasing the ratio to 5 causes further significant narrowing of MWD with M_w/M_n as low as 1.07. This indicates that $LiClO_4$ can perturb the dynamics of classical ion-pair equilibrium similar to LiCl[19,9].

Table 5.1: Anionic Polymerization of MMA in THF at -78 °C using (1,1-Diphenylhexyl) lithium Initiator in Presence of $LiClO_4$

Run	DPHLi 10^3 mol/L	$[M]_0$[a] mol/L	Mol.ratio of $[LiClO_4]$/ [DPHLi]	Yield[b] %	$M_{n,Calc}$ 10^{-3}	$M_{n,SEC}$[d] 10^{-3}	$M_{n,SEC}$ / $M_{n,Calc}$	M_w/M_n	f[c]
1A	1.10	0.28	0	>97	25.45	29.56	1.16	1.18	0.86
23	1.15	0.28	0.5	100	24.35	26.56	1.10	1.14	0.92
24	1.15	0.28	1	>98	24..35	25.90	1.06	1.11	0.94
25	1.15	0.28	5	100	24.35	26.89	1.10	1.07	0.90
1	1.15	0.28	10	100	24.35	27.80	1.14	1.08	0.88
2	1.27	0.20	10	> 97	16.26	18.33	1.13	1.07	0.89

a) Monomer was added with in 4-6 sec and polymerization was terminated after 10-15 min. b) Polymers were precipitated in n-hexane. c) Initiator efficiency = $M_{n\,calc}$ / $M_{n\,,SEC}$. d) Molecular weights were calculated on PMMA calibration.

The initiator efficiency, f, represented by the ratio of concentration of growing chains to that of initial initiator concentration is determined by the ratio of calculated number average molecular weight ($M_{n,cal}$) and the obtained M_n ($M_{n,SEC}$) using SEC. In the absence of $LiClO_4$, initiator efficiency is found to be low, 0.86. This indicates loss of initiators due to side reaction associated with ester group of monomer at the beginning of the reaction. The presence of $LiClO_4$ in THF solvent improves the initiator efficiency to a small extent.

However, upon increasing the temperature to -40 °C in the presence of LiCl ligand, it is reported that the control of both molecular weight and molecular weight distribution is lost[36]. In contrast, the beneficial effect of $LiClO_4$ as an additive can be seen even at -40 °C in THF using DPHLi as an initiator. The results are shown in Table 5.2.

In the absence of $LiClO_4$, PMMA obtained has a broad molecular weight distribution (M_w/M_n = 1.34) and also lower $M_{n,SEC}$ than the calculated $M_{n,cal}$. This indicates the absence of any control on the polymerization of MMA at -40 °C. This situation is dramatically improved by the addition of an equimolar amount of $LiClO_4$ with respect to DPHLi (Fig. 5.1 b, c). The resulting PMMA in THF at -40 °C exhibits a narrow molecular weight distribution (M_w/M_n = 1.1). The T_g's of the polymers synthesized in presence and in absence of $LiCLO_4$ are in accordance with their microstructure (120 °C < T_g <124 °C) (Table 5.2).

Table 5.2: Anionic Polymerization of MMA in THF at - 40 °C using DPHLi Initiator in presence of $LiClO_4$.

Run	DPHLi 10^3 mol/l	MMA[a] mol/l	Mol.ratio $\frac{[LiClO_4]}{[DPHLi]_0}$	Yield[b] %	$M_{n,cal}$ 10^{-3}	$M_{n,SEC}$ 10^{-3}	M_w/M_n	$M_{n,SEC}/M_{n,cal}$	f[c]	T_g[d]
1B	0.80	0.28	0	85	35.00	32.00	1.34	0.91	1.10	119.5
16	1.20	0.28	0.5	>96	23.33	26.98	1.13	1.16	0.86	109.0
17	1.20	0.374	1	100	31.16	32.07	1.10	1.03	0.97	122.3
18	1.20	0.374	2	>97	31.16	33.89	1.13	1.09	0.92	124..8
19	1.20	0.374	5	100	31.16	35.76	1.12	1.15	0.87	121.3
20	1.20	0.374	10	100	31.16	35.09	1.08	1.13	0.89	121.3

a) Monomer was added within 4-6 sec and polymerization was terminated after 10-15 mins. b) Polymers were precipitated in n-hexane. c) Initiator efficiency = $M_{n\,calc}$ / $M_{n\,,SEC}$. d) All the polymers have 70-74 % syndiotacticity as determined by ^1H NMR and Tg's were recorded at 10 °C/min.

Upon increasing the $LiClO_4$:DPHLi ratio to a value of 10, a better control on the polymerization is obtained resulting in an extremely narrow MWD, (M_w/M_n =1.08) (Fig. 5.1b). The $M_{n,SEC}$ of the resulting PMMA are close to the value of $M_{n,cal}$. It is evident that the presence of $LiClO_4$ provides living MMA polymerization at -40 °C in THF with complete conversion, predictable M_n, and high initiator efficiency (> 0.90).

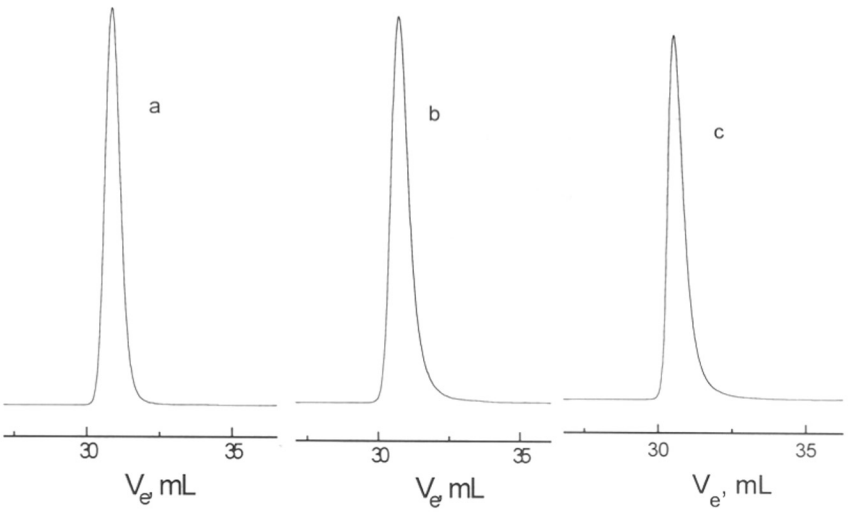

Fig. 5.1: SEC traces showing the effect of $LiClO_4$ addition on anionic polymerization of MMA in THF at -78 °C and -40 °C. a) PMMA prepared at -78 °C, $LiClO_4$/DPHLi = 10, $M_{n,SEC}$ = 27800, M_w/M_n = 1.08. b) PMMA prepared at -40 °C, $LiClO_4$/DPHLi = 1, $M_{n,SEC}$ = 32070, M_w/M_n= 1.10. c) PMMA prepared at -40 °C, $LiClO_4$/DPHLi = 10, $M_{n,SEC}$ = 35090, M_w/M_n = 1.08

5.3.2 Polymerization of tBA in THF in Presence of $LiClO_4$

The influence of $LiClO_4$ is also seen in the polymerization of tert-butyl acrylate in THF at -78 °C (Table 5.3). The obtained poly (tert-butyl acrylate) (PtBA) in the absence of $LiClO_4$ salt had a broad MWD (M_w/M_n = 2.1) with low initiator efficiency (0.56) compared to the one obtained in presence of $LiClO_4$ ($M_w/M_n \leq 1.18$, Table 5.3). This indicates that the majority of growing ester enolate ion-pairs get terminated in the absence of $LiClO_4$ possibly via a backbiting intramolecular reaction. This is consistent with the earlier results obtained by Teyssie and coworkers[31].

Table 5.3: Effect of $LiClO_4$ on Anionic Polymerization of tert-Butylacrylate in THF at -78 °C using DPHLi as an Initiator

Run	DPHLi $\times 10^3$ mol/L	tBA[a] mol/L	$\frac{[LiClO_4]}{[DPHLi]}$	Yield[b] %	$M_{n,calc}$[c] 10^{-3}	$M_{n,SEC}$[d] 10^{-3}	M_w/M_n	$M_{n,SEC}/M_{n,Calc.}$	Init. eff. f[e]
1	0.92	0.256	0	95	35.65	63.17	2.10	1.77	0.56
2	0.61	0.167	1	100	35.14	37.19	1.68	1.06	0.94
3	0.61	0.167	2	100	35.14	36.28	1.71	1.03	0.96
4	0.61	0.167	5	98	35.14	39.66	1.20	1.13	0.89
5	1.18	0.159	10	100	17.26	21.11	1.18	1.22	0.82
6	1.20	0.065	10	100	6.90	8.62	1.18	1.25	0.80
7	0.67	0.138	20	100	26.50	30.50	1.11	1.15	0.87
8	0.50	0.267	20	>95	68.40	71.53	1.08	1.04	0.96
9	0.40	0.178	20	>95	57.00	78.98	1.06	1.38	0.72

a) Diluted monomer (40% v/v) was added with in 5 sec and the polymerization was terminated after 10- 15 min. b) Polymer was recovered by removing solvent and dissolved in Benzene and freeze dried. c) $M_{n,Calc}$ = (moles of monomer / moles of initiator) (Mol.wt. of monomer). d) Molecular weights were calculated on PMMA calibration. e) Initiator efficiency = $M_{n,Calc}$ / $M_{n,SEC}$

SEC traces of the PtBA synthesized in the presence and absence of $LiClO_4$ is shown in Figure 5.2a. The molecular weight of PtBA were determined by SEC referenced to PMMA calibration standards. Hence, correlation of initiator efficiency calculated from $M_{n,cal}$/ $M_{n,SEC}$ should be considered approximate.

5.3.2.1 Monomer Resumption Experiment and Block Copolymer Formation

To provide confirmatory evidence for the enhanced livingness of tBA polymerization in presence of $LiClO_4$, monomer resumption experiment were performed. In a typical polymerization experiment, 3 mL of THF solution containing 1.34 g of tBA is added three times with an interval of 15 mins. Before adding the next monomer dose, small amount of sample was withdrawn for analysis. After 45 minutes, the reaction was terminated with methanol and PtBA was recovered by solvent evaporation. SEC analysis of the resulting PtBA is given in Table 5.4.

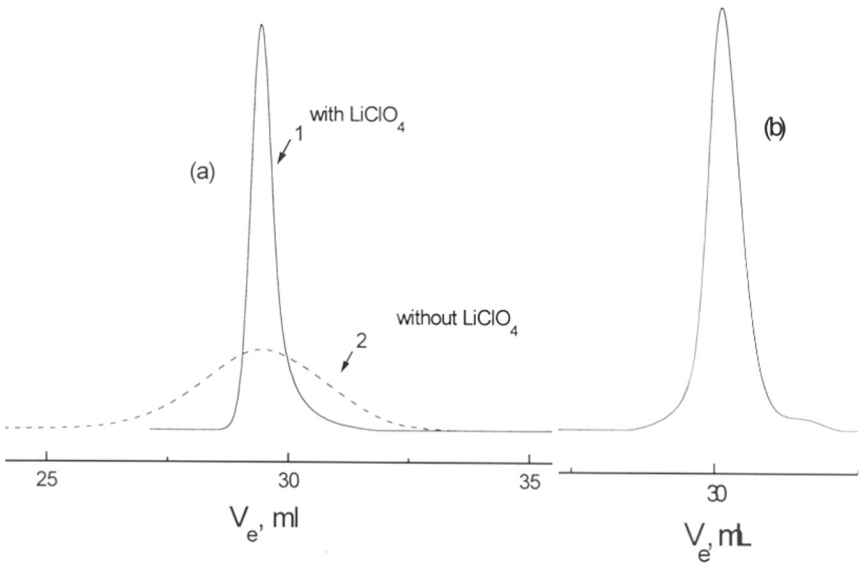

Fig. 5.2: Influence of $LiClO_4$ on the synthesis of PtBA in THF at -78 °C: (a) 1. in the presence of $LiClO_4$, $M_{n,SEC}$ = 78,980, M_w/M_n =1.06 (run No.9 in Table 5.3), and 2. in the absence of $LiClO_4$, $M_{n,SEC}$ = 63,170, M_w/M_n = 2.10 (run No.1 in Table 5.3),
(b) SEC trace of Poly(tert-butylacrylate-b-methyl methacrylate) diblock copolymer prepared in the presence of $LiClO_4$.

The enhanced livingness of the polymerization is clearly evident as the number average molecular weight increases for each dose of monomer addition. Upon complete conversion of 1st monomer dose, the obtained $M_{n,SEC}$ is 14270 g/mol which increases upon subsequent monomer does upto $M_{n,SEC}$ = 37,700 g/mol corresponding to the amount of fresh monomer fed. The polydispersity of the PtBA obtained remains narrow even after 3rd dose of tBA addition (M_w/M_n =1.17).

Table 5.4: Resumption Experiment on Anionic Polymerization tert.Butylacrylate using DPHLi - $LiClO_4$ Initiator[a] System in THF at -78 °C

No. of Dose	t.BA[b] grams	Time interval mins	Total conv. %	$M_{n,Calc.}$ g / mol	$M_{n,SEC}$[c)] g / mol	M_w/M_n
1	1.347	0[d]	100	10,362	14,270	1.24
2	1.347	15	>95	20,720	26,040	1.23
3	1.347	30	>95	31,080	37,700	1.17

a) initiator, DPHLi $1.3.10^{-4}$ moles were added to 100 mL of dry THF containing $1.3.10^{-3}$ moles of $LiClO_4$. b) diluted monomer (40 % v/v) was added with in 5 sec. c) molecular weights were calculated on PMMA calibration. d) polymerization of 1st dose only.

To further confirm the termination and transfer free nature of this process, formation of well defined block copolymer of tBA with MMA in presence of $LiClO_4$ was demonstrated. It is reported that the synthesis of PMMA-b-PtBA diblock copolymer in presence of 10 mole excess of LiCl resulted in a block copolymer contaminated with small amount of homo PMMA[26]. This was attributed to partial deactivation of PMMA anion upon addition of tBA solution. This type of deactivation was not observed while performing the reaction sequence in reverse, namely, initiating MMA with living PtBA anion. Hence we attempted to prepare PtBA-b-PMMA diblock copolymer starting with tBA in THF at -78° C. Specifically, 0.017 mol of tBA was first polymerized (DPHLi, 0.2×10^{-3} mol, $[LiClO_4]/[DPHLi] = 10$), after 15 mins, 0.028 mol of MMA was added with in 5 secs to the living PtBA solution. Reaction was terminated with methanol and block copolymer was recovered by solvent evaporation. The resulting P-tBA-b-PMMA diblock copolymer has a $M_{n,SEC} = 51940$ g/mol and an $M_w/M_n = 1.08$. The SEC trace of the final block copolymer (Fig. 5.2 b) shows that no residual homo PtBA present in the diblock copolymer

5.3.3 Polymerization of MMA in Presence of $LiClO_4$ in Toluene/THF (9:1, v/v) Mixed Solvent

The nature of solvent plays an important role in solvation of Li cation, thereby influencing the ion-pair association equilibrium of anionic polymerization of MMA. It is also known that solvent polarity largely affects the reactivity and identity of the propagating species[37]. It was shown that increasing the solvent polarity causes decrease in isotacticity and a narrowing of molecular weight distribution of PMMA[38].

The polymerization of MMA in toluene/THF (9:1, v/v) mixed solvent was carried out both in the presence and absence of $LiClO_4$ using DPHLi as initiator at different temperatures. The results are given in Table 5.5 and, Figure 5.3. In the absence of $LiClO_4$, the polymerization process is complex as evidenced by the formation of a gel phase. The soluble portion of PMMA shows that the $M_{n,SEC}$ is less than that of $M_{n,cal}$ with broad molecular weight distribution ($M_w/M_n = 2.8$).

Table 5.5: Polymerization of MMA in Toluene-THF (9:1 v/v) at -78 °C using DPHLi Initiator[a]

Run	DPHLi 10^3 mol/L	MMA mol/L	Mol.ratio $\frac{[LiClO_4]_o}{[DPHLi]_o}$	Yield[b] %	$M_{n,cal}$ [c] 10^{-3}	$M_{n,SEC}$ 10^{-3}	M_w/M_n	$M_{n,SEC}/M_{n,cal}$	Init. eff f[d]
12	0.345	0.28	0	85	68.98	43.24	2.86	0.63	1.60
13	0.345	0.28	1	65	52.75	71.94	1.10	1.36	0.73
14	0.345	0.28	2	64	51.94	63.67	1.07	1.22	0.82
15	0.345	0.28	5	66	53.56	60.00	1.08	1.12	0.89
4	1.75	0.20	10	80	9.14	10.11	1.05	1.10	0.90
7[e]	1.15	0.28	10	64	15.52	19.62	1.06	1.26	0.80
8	0.67	0.094	10	61	8.52	8.66	1.05	1.02	0.98
9[f]	0.67	0.28	10	61	25.49	27.07	1.09	1.06	0.94

a) Monomer was added neat with in 4-6 sec. Polymerization was terminated at 90-150 mins, before complete conversion. b) Polymers were precipitated in n-hexane. c) $M_{n,cal}$ was determined by (grams of MMA / moles of initiator) × conversion. d) Initiator efficiency = $M_{n,cal}/M_{n,SEC}$. e) 68 % syndiotacticity as determined by ^1H NMR and T_g is 110.6 °C. f) Experiment done at -40 °C.

The usefulness of $LiClO_4$ in improving the reaction, even in solvents of such low polarity, is clearly evident. The gel phase is totally absent during polymerization in presence of $LiClO_4$ in 9:1 v/v toluene:THF. It can be seen from Table 5.5 that addition of equimolar amount of $LiClO_4$ to DPHLi provides perfect control on polymerization resulting in a narrow MWD PMMA (M_w/M_n = 1.1).

Upon increasing the mole ratio of $LiClO_4$:DPHLi to a value higher than 5 does not appear to cause further improvement. In all cases the polymerization was terminated within 90-150 min. It was found that the conversion was not quantitative. Therefore, theoretical molecular weights were recalculated based on the conversion in each experiment assuming that the polymerization is a living process. The perfect control on MMA polymerization in the presence of $LiClO_4$ in a low polarity solvent can be seen even at -40 °C (Table 5.5, run 9).

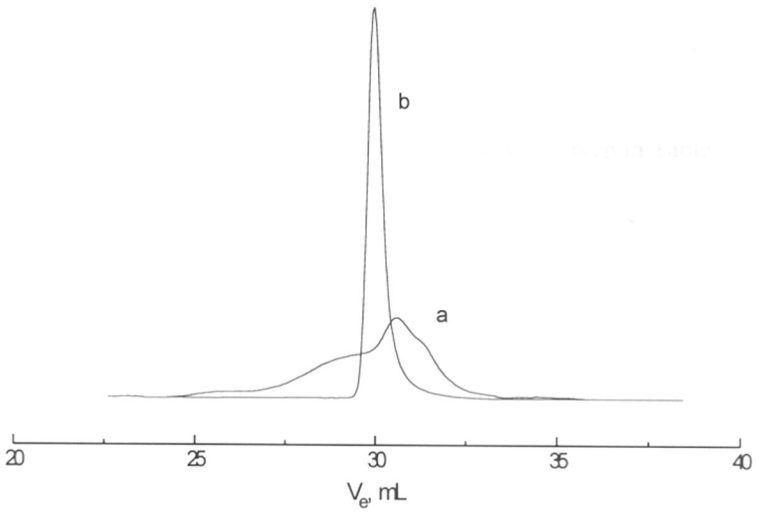

Fig. 5.3: SEC traces of PMMA synthesized in presence (b) and absence (a) of LiClO4 in Toluene/THF (9:1, v/v) mixed solvent at -78 °C (run No. 12 and 15 in Table 5.5).

5.3.3.1 Kinetics of MMA Polymerization in Toluene/THF (9:1, v/v) Solvent

To further confirm the termination and transfer free nature of this process, kinetic experiments were performed in toluene (90 mL) and THF (10 mL) mixture containing 0.0523×10^{-3} mol of DPHLi and 1×10^{-3} mol of $LiClO_4$ at -78 °C using a bench top stir-tank reactor as described in Chapter 2.

Table 5.6: Kinetics of MMA polymerization in presence of $LiClO_4$ in Toluene/THF (9:1, v/v) mixed solvent at -78 °C[a]

time, min.	conversion[b] %	$M_{n\ SEC}$	M_w/M_n
10	1.96	2,638	1.22
20	10.15	4,849	1.19
30	11.59	5,899	1.22
40	16.12	6,354	1.20
50	19.14	7,979	1.24
80	27.71	13,080	1.14
100	32.51	15,550	1.13
120	38,71	19,100	1.11

a) Polymerization was carried out in 100 mL toluene/THF (9:1, v/v) mixed solvent using $[DPHLi]_0 = 5.10^{-4}$ mol/L, $[MMA]_0 = 0.27$ mol/L, b) Monomer conversion was determined by GC using n-Octane as an internal standard and PMMA was recovered by removing solvent

Neat MMA (3 mL) was added within 3 sec using N_2 pressure. Samples were taken from the reaction mixture at definite intervals and terminated with degassed methanol. The monomer conversion was determined by GC. The number average molecular weight obtained by SEC of PMMA at different intervals are given in Table 5.6.

By following the disappearance of monomer concentration with respect to time, the rate of polymerization can be determined using the equation, $\ln ([M]_0/[M]_t) = k_{app} \cdot t$, assuming that the reaction follows first-order kinetics. The first -order time conversion plot is shown in Fig 5.4. The linearity of semilogarithmic conversion plot shows that the polymerization proceeds without any significant amount of termination reaction in the presence of excess $LiClO_4$ salt. The number average degree of polymerization, P_n determined by SEC is plotted against conversion in Fig 5.5. Any transfer reaction would lead to the decrease of P_n during the course of polymerization. The linear dependence of P_n with respect to conversion indicates absence of transfer reaction in this process.

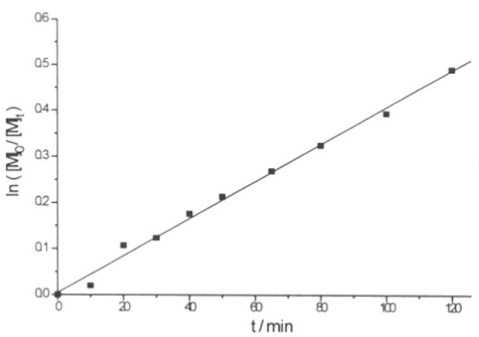

Fig.5.4: First-order time-conversion plot of MMA polymerization in Tolune/THF (9:1, v/v) mixed solvent in presence of $LiClO_4$ at -78 °C

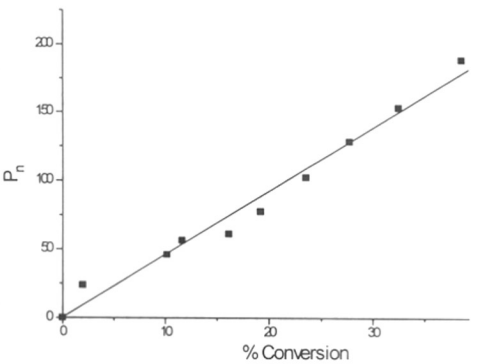

Fig.5.5: Linear dependency of degree of polymerization, P_n, vs conversion for the polymeri-zation of MMA in presence of $LiClO_4$ at -78 °C

It was reported[19] that under similar conditions, addition of LiCl does not provide adequate control of MMA polymerization. The solubility of LiCl is limited in a toluene/THF (9:1 v/v) mixed solvent. However, the PMMA produced using a homogeneous solution of LiCl-DPHLi (2.5×10^{-3} mol/L) had a bimodal distribution up to 50 % conversion (M_w/M_n = 2.35)[19]. The presence of $LiClO_4$ led to a unimodal symmetrical molecular weight distribution with a M_w/M_n = 1.22 right from the beginning of the polymerization. The relative solubilities of LiCl versus $LiClO_4$ in 9:1

v/v toluene: THF is not of major significance. The SEC traces of PMMA obtained in the presence of $LiClO_4$ at various intervals of time is given in Fig.5.6. It can be seen from the Table 5.6 and Fig. 5.6 that the molecular weight distribution remains narrow during the course of polymerization, and attains a value M_w/M_n = 1.11 at 38% conversion. These results demonstrate the remarkable ability and efficiency of $LiClO_4$ for the synthesis of well defined PMMA in solvents of low polarity.

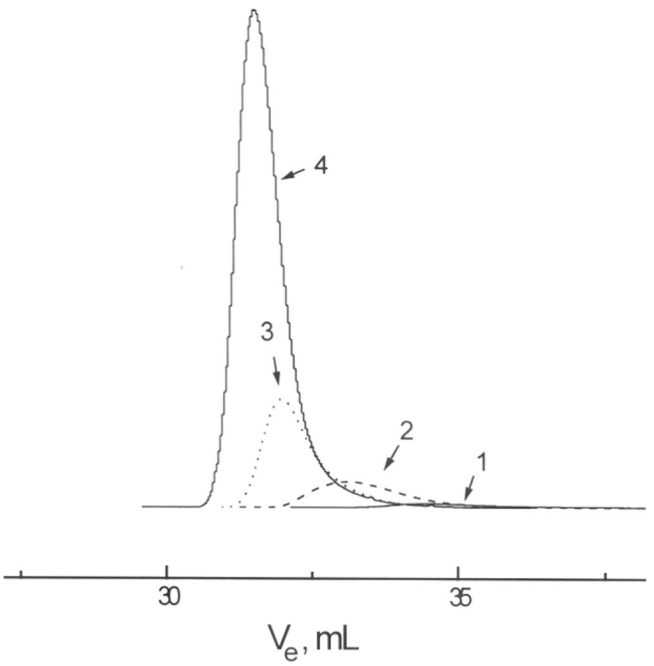

Fig. 5.6: SEC traces of PMMA samples at various time of polymerization in presence of $LiClO_4$ in Toluene/THF (9:1 v/v) at -78 °C; 1) after 10 mins 2) after 40 mins. 3) after 80 mins. and 4) after 120 mins.

5.3.4 Influence of Other Salts in MMA and tBA Polymerization in THF

It was found that the use of other salts such as $LiBF_4$ and $LiPF_5$ also improves the living character of anionic polymerization of MMA and tBA. The results are given in the following Table 5.7: This preliminary results also confirm the influence of some specific salts on the anionic polymerization of alkyl (meth)acrylates. Thus, it seems such a specific salt effect influencing the position of ion-pair association equilibrium mainly depends on the electronic and steric aspects of the added salt.

Table 5.7: Effect of $LiBF_4$ and $LiPF_5$ on Anionic Polymerization of MMA and tBA in THF at -78 °C using DPHLi as an Initiator

Run	Monomer	Salt	$\frac{[Salt]}{[DPHLi]}$	Temp. °C	Yield[b], %	$M_{n,SEC}$. 10^{-3}	M_w/M_n
1	MMA	$LiBF_4$	5	-40	>95	30.94	1.05
2	tBA	$LiBF_4$	10	-78	>95	37.95	1.08
3	MMA	$LiPF_5$	10	-40	100	37.17	1.17
4	tBA	$LiPF_5$	10	-78	92	40.20	1.20

a) Neat MMA and diluted tBA (40 % v/v in THF) was added with in 5 sec and the polymerization was terminated after 10-15 min. b) Polymer was recovered by removing solvent and dissolved in Benzene and freeze dried.

5.3.5 Kinetics of MMA Polymerization in Presence of $LiClO_4$ in THF Using Flow-tube Reactor

The polymerization of MMA using DPHLi as an initiator in the absence and in the presence of $LiClO_4$ was performed in a flow-tube reactor as described in Chapter 2. The results of the kinetic experiments performed at different temperatures, T_{eff}, and at different initial initiator concentrations, $[I]_0$, and different $LiClO_4$ concentrations, are summarized in Tables 5.8 and 5.9. The first-order time-conversion plot at different initiator concentration in presence of $LiClO_4$ is given in Fig. 5.7.

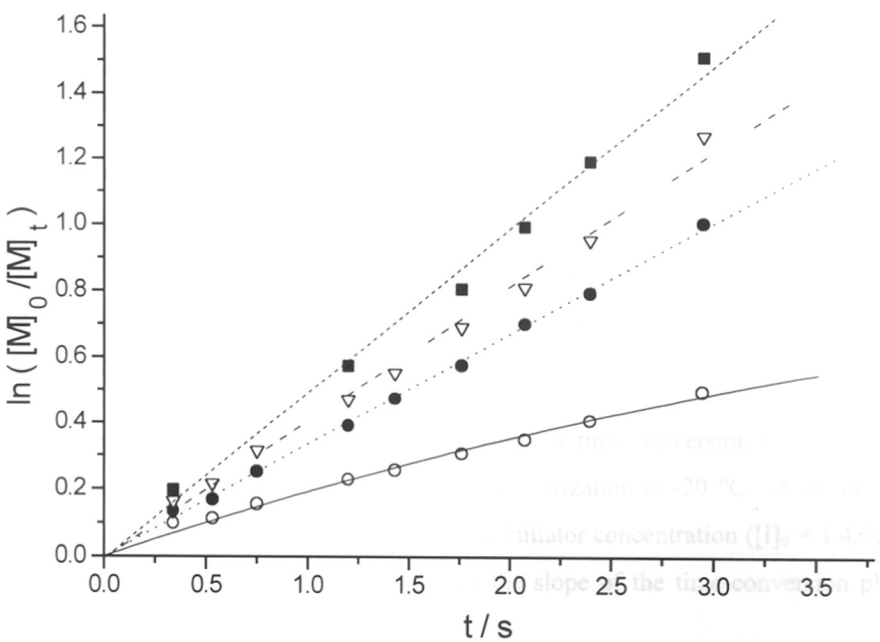

Fig. 5.7: First-order time-conversion plots of the MMA polymerization in THF in presence of $LiClO_4$ at -20 °C. $[M]_0$ = 0.2 mol/L, $[I]_0$ /(mol/L); (■) $9\cdot10^{-3}$, (▽) $6\cdot10^{-3}$, (●) $4\cdot10^{-3}$, and (O) $1.4\cdot10^{-3}$

Table 5.8: Kinetic results of the anionic polymerization of MMA with Li^+ counterion in the presence of $LiClO_4$ in THF, $[MMA]_0$ = 0.2 mol/L; variation of initiator, $LiClO_4$, and temperature.

Run	[DPHLi] $\times 10^3$, mol/L	$\frac{[LiClO_4]}{[DPHLi]_0}$	T_{eff} °C	t_{max} a), sec	$x_{p,max}$ b)	$P_{n,th}$ c) at $x_{p,max}$	$P_{n,GPC}$ d) at $x_{p,max}$	M_w/M_n at $x_{p,max}$	f e)
1	9.0	10	-18.8	2.94	0.78	19.9	16.4	1.11	0.94
2	6.0	10	-17.6	2.94	0.72	21.6	23.6	1.10	1.00
3	4.0	10	-19.1	2.39	0.55	27.5	28.0	1.08	1.00
4	4.0	5	-19.5	1.74	0.38	19.0	21.7	1.14	1.00
5	4.0	3	-19.4	2.39	0.60	30.0	46.9	1.20	0.78
6	4.0	1	-19.9	2.39	0.61	30.5	51.0	1.29	0.60
7	4.0	0.6	-19.8	2.39	0.63	31.5	48.7	1.30	0.61
8	4.0	0.3	-19.3	2.39	0.64	32.0	55.4	1.30	0.57
9	4.0	0	-19.2	2.39	0.74	37.0	47.4	1.25	0.80
10	1.4	0	-20.5	2.39	0.54	77.1	74.1	1.35	0.88
11	1.4	0	-0.1	2.39	0.59	84.3	100.3	1.69	0.81
12	1.4	0	+19.2	2.39	0.55	78.6	93.5	1.95 f)	0.89
13	1.4	10	-26.8	2.94	0.33	44.8	82.5	1.13	0.66
14	1.4	10	-19.6	2.94	0.39	53.0	73.8	1.12	0.72
15	1.4	10	-9.3	3.5	0.49	68.5	103.0	1.34	0.70
16	1.4	10	+0.7	2.94	0.46	63.3	99.0	1.40	0.67

a) longest reaction time. b) conversion obtained at t_{max}. c) $P_{n,th} = [M]_0 \times x_{p,max}/[I]_0$. d) $P_{n,SEC} = (M_{n,SEC}-M_{initiator})/M_{monomer}$. e) initiator efficiency, $f = P_{n,th}/P_{n,SEC}$ from the ratio of $[M]_0/[I]_0$ and slope of $P_{n,SEC}$ vs conversion plot.

The polymerization of MMA in the absence and also in the presence of $LiClO_4$ follows first-order kinetics with respect to monomer concentration at -20 °C. In the first series of experiments performed at -20 °C, only $[I]_0$ was varied from $1.4 \cdot 10^{-3}$ to $9 \cdot 10^{-3}$ mol/L in order to determine the reaction order. A ten-fold excess of $LiClO_4$ with respect to initial concentration was always maintained.

As seen from Fig.5.7, the linearity of semilogorithamic time-conversion plot indicates the absence of termination reactions during polymerization at -20 °C. A deviation from first-order linearity is also observed at low initiator concentration ($[I]_0 = 1.4.10^{-3}$ mol/L) indicating termination. This decreases the slope of the time-conversion plot during the polymerization.

The expression for the dependence of monomer concentration on time for a polymerization in presence of unimolecular termination is given by equation 5.1.

$$\ln \frac{[M]_0}{[M]_t} = \frac{k_{app}}{k_t} \cdot \left(1 - e^{-k_t \cdot t}\right) \tag{5.1}$$

where $k_{app} = k_p \cdot [P^*]$ is the apparent rate constant (i.e. the initial slope of first-order time-conversion plot), k_p and k_t are the rate constant of propagation and termination, respectively and $[P^*] = f \cdot [I]_0$ is the active center concentration. The values of k_{app} and k_t were determined by a fitting procedure using equation 1 (Table 5.9).

Table 5.9: Rate constants of propagation, k_p, and termination, k_t, for the anionic polymerization of MMA using Li^+ as counterion in the presence of $LiClO_4$.

Run	$10^3 \times [P^*]$[a] mol/L	T_{eff}, °C	$\frac{[LiClO_4]}{[P^*]}$	k_{app}, s^{-1}	$\bar{k}_p = \frac{k_{app}}{[P^*]}$ $l \cdot mol^{-1} s^{-1}$	$\frac{k_{app}}{[P^*]^{1/2}} = \frac{k_\pm}{\sqrt{2 \cdot K_a}}$	k_t, s^{-1}
1	8.73	-18.8	10.3	0.499	57.2	5.34	-
2	6.00	-17.6	10.0	0.412	68.7	5.32	-
3	4.00	-19.1	10.0	0.337	84.3	5.33	-
4	4.00	-19.5	5.0	0.298	74.5	4.71	-
5	3.12	-19.4	3.5	0.369	118.3	6.61	-
6	2.40	-19.9	1.5	0.370	154.2	7.55	-
7	2.44	-19.8	0.94	0.383	156.9	7.75	-
8	2.28	-19.3	0.51	0.408	178.9	8.54	-
9	3.20	-19.2	0	0.560	175.0	9.90	-
10	1.23	-20.5	0	0.350	284.0	9.96	0.224
11	1.13	-0.1	0	0.690	608.0	20.44	0.590
12	1.25	+19.2	0	0.923	740.0	26.16	0.930
13[b]	1.01	-26.8	15.2	0.140	151.0	4.58	-
14	0.98	-19.6	14.5	0.209	216.0	6.69	0.165
15	0.94	-9.3	15.2	0.276	285.0	8.71	0.241
16	0.89	0.7	15.6	0.392	437	13.04	0.490

a) $[P^*] = f \cdot [I]_0$. b) induction period (0.24 sec) was noticed

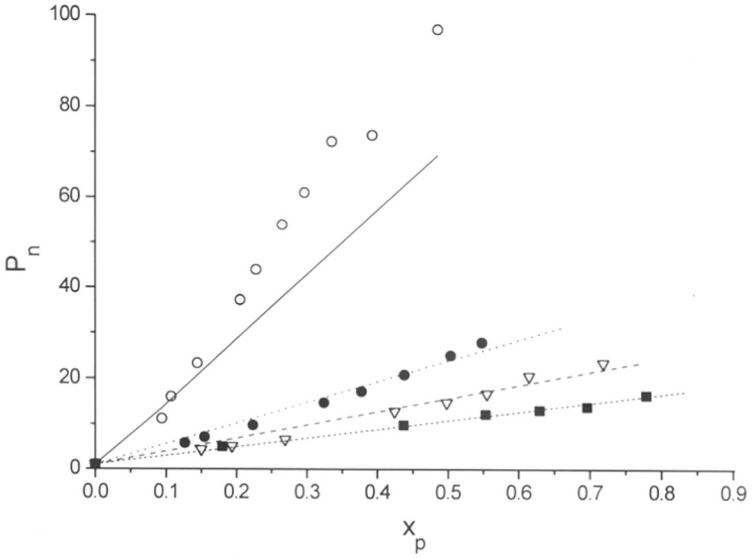

Fig. 5.8: Dependence of number-average degree of polymerization, Pn, versus xp at -20 °C with various initial concentration of DPHLi. All lines describe Pn,theor. $[M]_0$ = 0.2 mol/L, $[I]_0$/(mol/L); (■) $9 \cdot 10^{-3}$, (▽) $6 \cdot 10^{-3}$, (●) $4 \cdot 10^{-3}$, and (O) $1.4 \cdot 10^{-3}$

The linear dependence of the number-average degree of polymerization, P_n, on conversion, x_p, (Fig. 5.8), shows the absence of transfer reactions at -20 °C. However, at low concentration of initiator, $[I]_0 = 1.4 \cdot 10^{-3}$ mol/L, the obtained P_n deviates from the theoretical line indicating that the initiator efficiency decreases. The active center concentrations, [*P**], in Table 5.9 were determined using the initiator efficiencies calculated from the slope of the plot of P_n versus conversion.

5.3.5.1 Effect of $LiClO_4$ on the Reaction Order

Figure 5.9 shows a bi-logarithamic plot of k_{app} versus $[P^*]$ resulting in linearity with a slope of 0.5, similar to the plot in absence of $LiClO_4$. However, the rates are lower. The data point obtained at $[I]_0 = 1.4 \cdot 10^{-3}$ was not used due to low accuracy caused by termination and lower initiator efficiency. The fractional order of the reaction indicates that the propagating ion pairs exist in equilibrium with associated species. Fractional reaction orders were also obtained in the absence of any additive at lower temperatures (-65 °C)[8]. It was shown that in the presence of LiCl, aggregation of enolate ion pairs was decreased due to the formation of mixed aggregates.

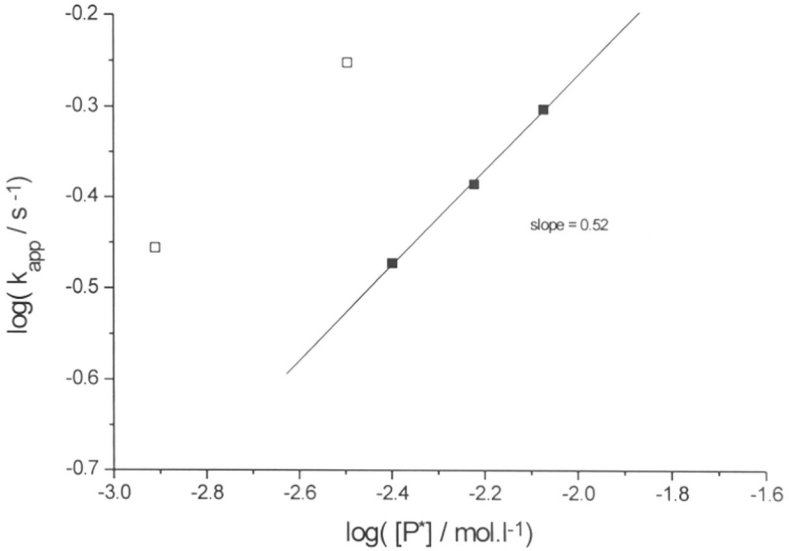

Fig. 5.9: Reaction order with respect to initiator concentration for the MMA polymerization in presence of $LiClO_4$ in THF at -20 °C; (■) with $LiClO_4$, (□) without $LiClO_4$.

The obtained fractional order indicates that $LiClO_4$ does not effectively perturb the aggregation of enolate ion pairs. The obtained lower rate constants, $\bar{k}_p$, in presence of $LiClO_4$ (Fig. 5.9) indicate the formation of less reactive mixed aggregates. The concentration dependence of the rate constants of polymerization, $\bar{k}_p$ (Table 5.9) shows that it must be regarded as an apparent constant. In fact, it is given by equation 5.2 assuming that the rate constant of propagation of aggregates, $k_p^{ass} \ll k_{\pm}$ [6,8].

$$k_p = \alpha k_{\pm} + \frac{1-\alpha}{2} k_p^{ass} \approx \alpha k_{\pm} \tag{5.2}$$

where $\alpha = \frac{[P_{\pm}]}{[P^*]} \approx \left(2 \cdot K_a \cdot [P^*]\right)^{-1/2}$ is the fraction of non-associated ion-pairs which depends on the initiator concentration and on the equilibrium constant of aggregation, K_a, and $k_{\pm}$ is the rate constants of ion-pairs. For $\alpha \ll 1$, $\left(2 \cdot K_a \cdot [P^*]\right)^{-1/2}$ this leads to equation 5.3.

$$\frac{k_{app}}{[P^*]^{1/2}} = \bar{k}_p \cdot [P^*]^{1/2} = \frac{k_{\pm}}{\sqrt{2 \cdot K_a}} \tag{5.3}$$

From this equation, the ratio $\frac{k_{\pm}}{\sqrt{2 \cdot K_a}}$ can be determined. At a given temperature, K_a = const. and this value should be a constant. Table 5.9 shows that this is the case whereas $\bar{k}_p$ depends on $[P^*]$.

The GPC traces of the polymers obtained at -20 °C show that they exhibit narrow molecular weight distributions ($M_w/M_n \leq 1.12$) which is better than the polymer obtained in the absence of ligand ($M_w/M_n = 1.25$). The similar results can be seen at the other temperatures (Table 5.8, runs 11 and 16). Fig. 5.10 shows the plot of polydispersity index, M_w/M_n, versus conversion, x_p, of the polymers obtained in presence of $LiClO_4$ at -20 °C. The MWD decreases with conversion indicating the existence of a moderately slow equilibrium between aggregated and non-aggregated ion pairs during polymerization

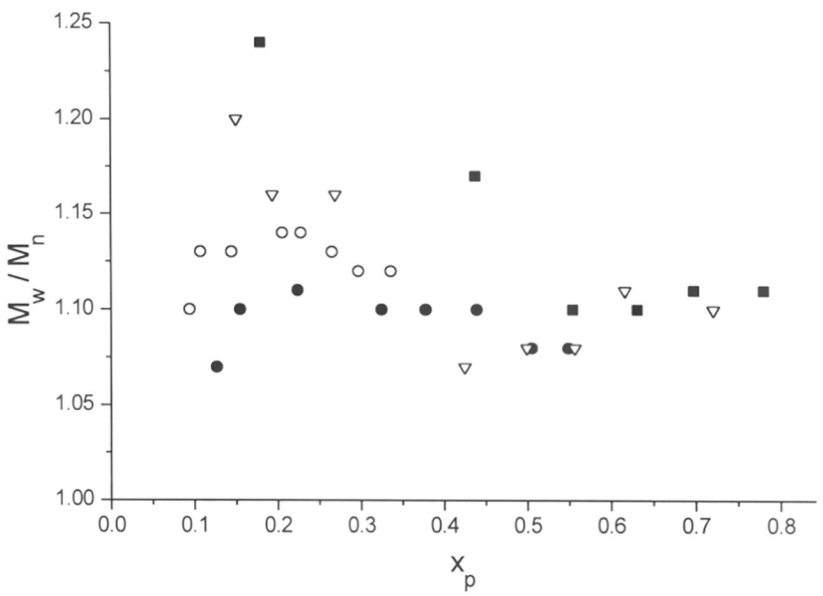

Fig. 5.10: Polydispersity index of the obtained PMMA with conversion at -20 °C at different initiator concentration. $[I]_0$/(mol/L); (■) $9 \cdot 10^{-3}$, (▽) $6 \cdot 10^{-3}$, (●) $4 \cdot 10^{-3}$, and (O) $1.4 \cdot 10^{-3}$

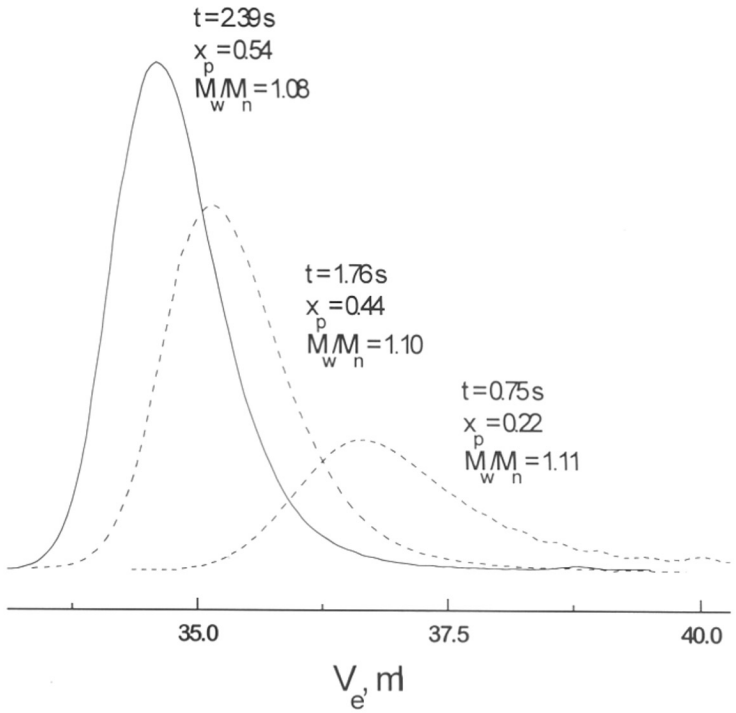

Fig. 5.11: SEC traces of PMMA at various time of polymerization in presence of $LiClO_4$ at -20 °C.(run no.3 in Table 5.8)

5.3.5.2 Influence of $LiClO_4$ Concentration on Propagation Rate Constant

In order to determine the effect of $LiClO_4$ concentration on the kinetics, experiments were performed at -20 °C at different ratios, $r = [LiClO_4]/[I]_0$, from 0 to 10. The linearity of the first-order time-conversion plots at different concentration of $LiClO_4$ shows the absence of termination reactions at higher initiator concentration, $[I]_0 = 4 \cdot 10^{-3}$ mol/L (Fig. 5.12). A linear dependence of P_n with conversion is again observed at different concentrations of $LiClO_4$ (Fig. 5.13). However, the initiator efficiency first decreases from 80 % to 60 % when $r \leq 3$ and improves to 100 % for $r \geq 5$. This may indicate the presence of unreactive mixed aggregates at low concentrations of $LiClO_4$ ($r \leq 3$).

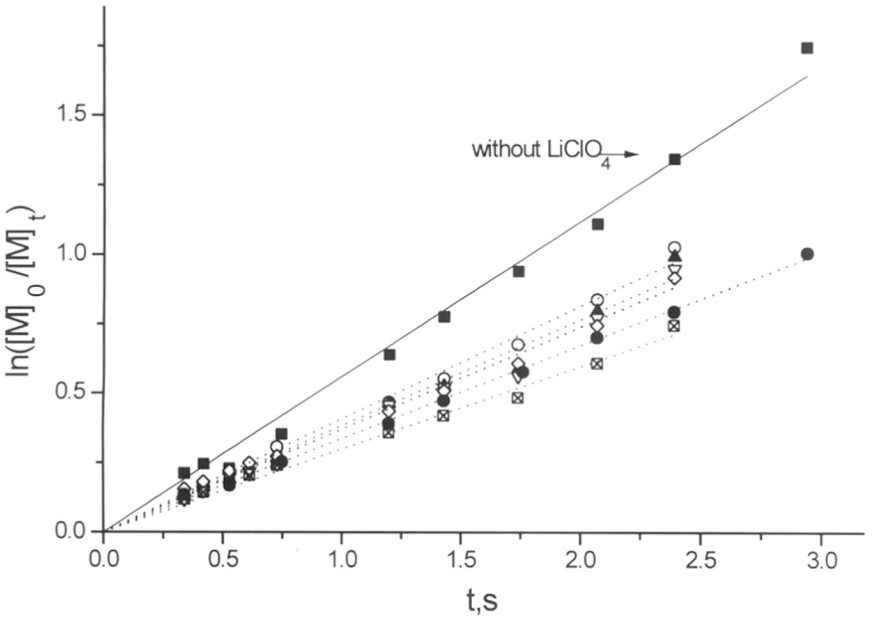

Fig. 5.12: First-order time-conversion plots of MMA polymerization in THF in presence of various concentration of $LiClO_4$ at -20 °C. r = $[LiClO_4]_0/[DPHLi]_0$; (■) r = 0, (O) r = 0.3, (▲) r = 0.6, (Δ) r= 1, (◇) r = 3, (⊠) r = 5, and (●) r = 10.

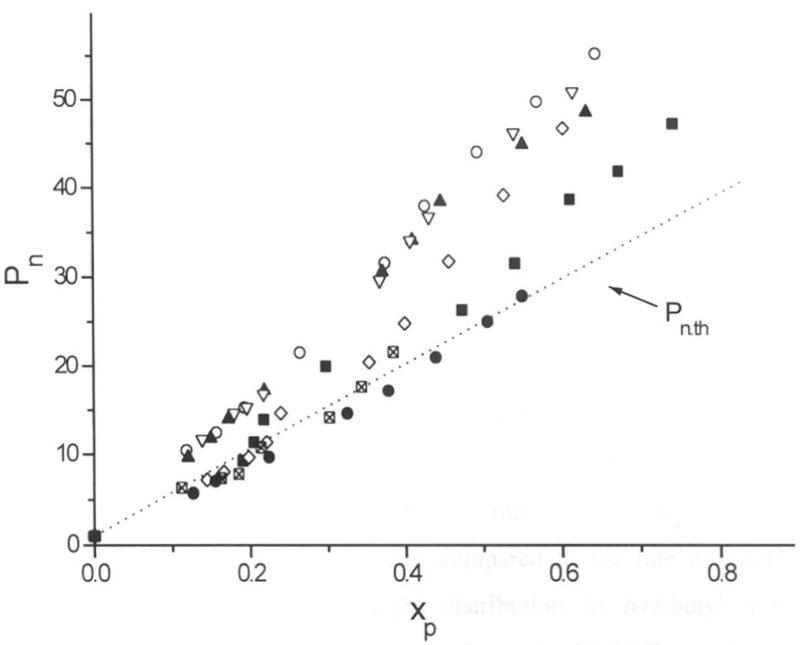

Fig. 5.13: Dependence of number-average degree of polymerization, P_n, on conversion. r = $[LiClO_4]_0/[DPHLi]_0$; (■) r = 0, (O) r = 0.3, (▲) r = 0.6, (Δ) r= 1, (◇) r = 3, (⊠) r = 5, and (●) r = 10.

The determined apparent rate constant, k_{app}, monotonously decreases with increasing ratio r (Table 5.9, Fig.5.14). The over all rate constant, $\bar{k}_p$, also decreases upon increasing the ratio, r from 0 to 10 and gradually reaches ca. 50 % of the initial value at $r = 10$ (Table 5.9).

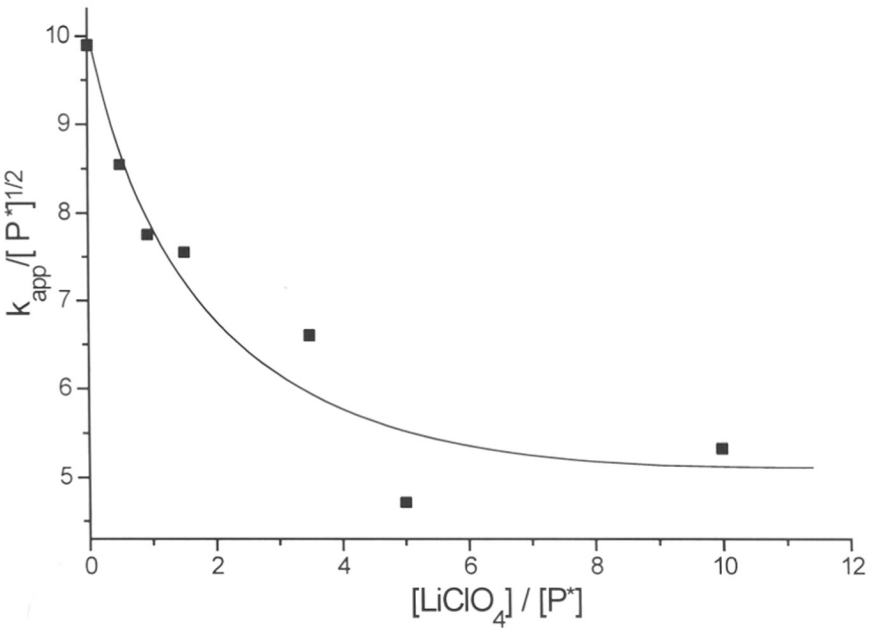

Fig. 5.14: Effect of $LiClO_4$ concentration on the rate constant, k_p, of MMA polymerization in THF at -20 °C.

Kunkel et al[8,39] observed similar effects for the polymerization of MMA and ter-butyl acrylate (tBuA) in presence of LiCl in THF at -65 °C. In presence of LiCl, a maximum in the plot of $\bar{k}_p$ versus r was observed at $r \approx 1$. This was attributed to the formation of reactive 1:1 adduct of LiCl with enolate ion pair leading to an overall increase of reaction rate. A similar maximum is not seen in the presence of $LiClO_4$ at -20 °C (Fig. 5.14). It was shown by Kunkel et al[8] that the slow rate of exchange between associated and non-associated species compared to the rate of monomer insertion results in broad molecular weight distribution in *tert*-butyl acrylate polymerization. In contrast to the de-aggregation observed with LiCl at -65 °C, the reaction order of 0.5 in case of $LiClO_4$ indicates that aggregates to be the predominant

species, possibly a mixed aggregates with $LiClO_4$ which may dissociate into 1:2 and 1:1 mixed complexes (Scheme 5.1).

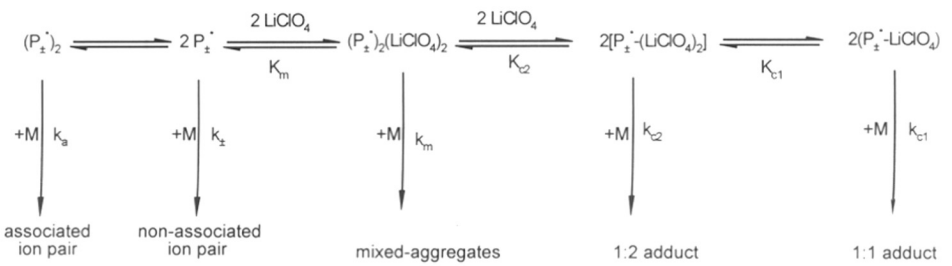

Scheme 5.1: Formation of adduct in the presence of $LiClO_4$ in the anionic polymerization of MMA in THF

In order to explain the lower M_w/M_n in presence of $LiClO_4$, we have to assume that the rate of de-aggregation of the mixed aggregate is higher than that of normal dimeric aggregates $(P_\pm^*)_2$. A plot of $\frac{k_{app}}{[P^*]^{-1/2}} = \frac{k_\pm}{\sqrt{2 \cdot K_a}}$ versus r which corrects the effect of concentration on the aggregation equilibrium also confirms the lower rates in presence of $LiClO_4$ at -20°C (Fig. 5.14). This indicates the co-ordination of $LiClO_4$ results either in the formation of less reactive mixed aggregates or in a lower K_a.

5.3.5.3 Evaluation of Arrhenius Parameters

The effect of temperature on the rate constant of polymerization and termination in presence of $LiClO_4$ was studied in the temperature range from -30 to 0 °C at lower $[I]_0 = 1.4 \cdot 10^{-3}$ mol/L. The first-order time conversion plots show a downward curvature for T ≥ - 20 °C (Fig.5.15). This indicates the presence of termination at lower $[I]_0$. An induction period was observed in presence of $LiClO_4$ at -30 °C. The Arrhenius plot obtained using the apparent propagation rate constant, $\bar{k}_p$, shows linearity with an activation energy, $E_a^{app} = 20 \pm 1.6$ kJ mol^{-1} and frequency exponent, $\log A^{app} = 6.5 \pm 0.2$ (Fig 5.16). The activation energy is slightly lower than that for Li^+/LiCl counterion in THF ($E_a^{app} = 25.3$ kJ mol^{-1} and $\log A^{app} = 7.4$)[40].

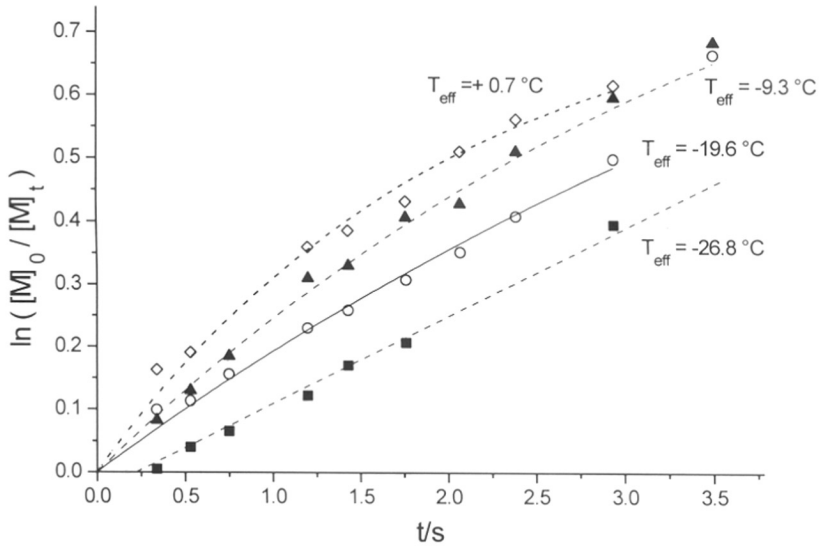

Fig. 5.15: First-order time-conversion plots at different temperatures. $[MMA]_0$ = 0.2 mol/L, $[I]_0 = 1.4 \cdot 10^{-3}$ mol/L.

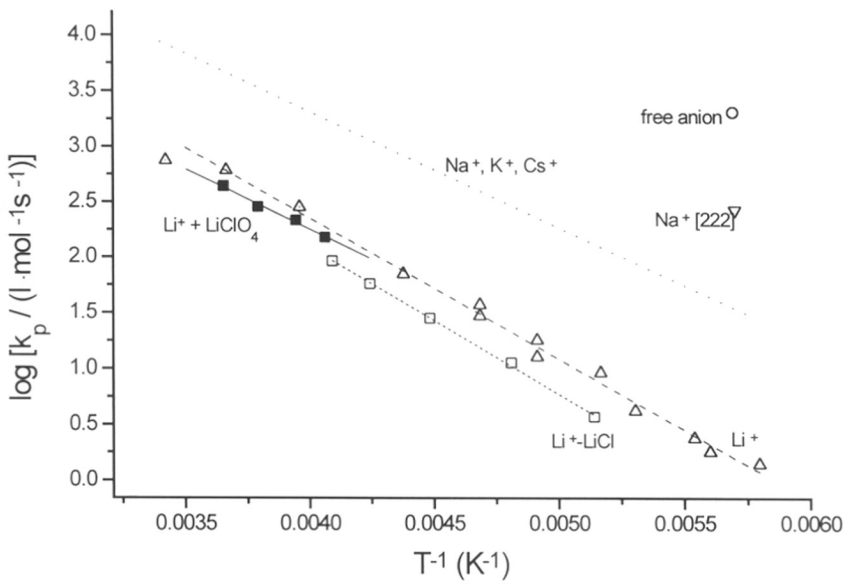

Fig. 5.16: Arrhenius plot of the propagation rate constants, kp in the anionic polymerization of MMA in THF for Li counterion with $LiClO_4$ ligand and the reported rate constants for other counterion and solvent (Aggregation was not taken into account).

It must be stressed that the activation parameters are only apparent ones since $\bar{k}_p$ depends on the fraction of non-associated ion-pairs, α (cf. eq.5.2), which is expected to depend on temperature. In order to compensate the effect of active center

concentration on the aggregation, it is more appropriate to plot $\log \frac{k_{app}}{[P^{\bullet}]^{-1/2}} = \log \frac{k_{\pm}}{\sqrt{2 \cdot K_a}}$ versus inverse temperature. The apparent activation energy of this plot (Fig. 5.17) is $E_a^{app} = E_{a,\pm} + \frac{1}{2} \Delta H_a$ and the apparent activation entropy contains the entropy of association.

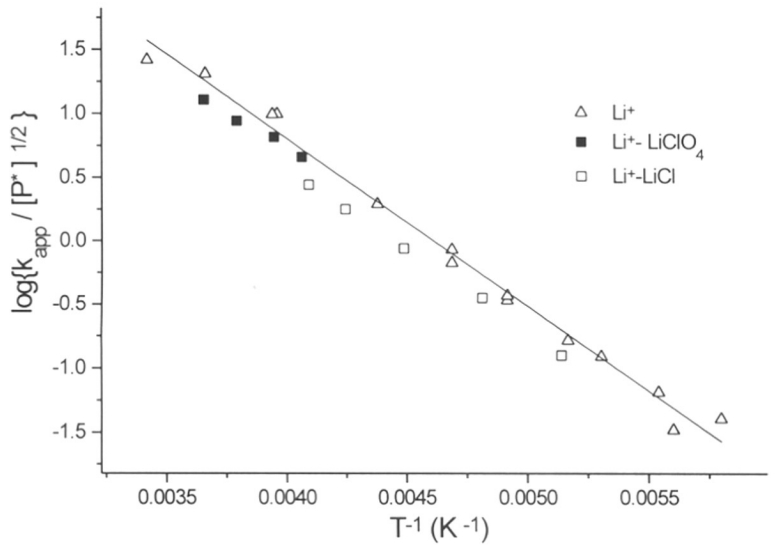

Fig. 5.17: The inverse square root dependence of rate constant, k_{app} at different temperatures in presence of $LiClO_4$ and also the reported rate constants for Li^+ and Li^+-LiCl in THF.

The plot of $\frac{k_{app}}{[P^{\bullet}]^{-1/2}} = \frac{k_{\pm}}{\sqrt{2 \cdot K_a}}$ versus inverse temperature results in a linearity and the ratio $\frac{k_{\pm}}{\sqrt{2 \cdot K_a}}$ is found to be independent in the presence of additive (Fig 5.17). This indicates the presence of additive such as $LiClO_4$, or LiCl either has no influence on the absolute rate constant, $k_{\pm}$ and K_a as the effects cancel. Thus, the decrease of $\bar{k}_p$ is presumably only due to the formation of less reactive mixed aggregates. The rate constant of termination, k_t, in the presence of $LiClO_4$ has an activation energy $E_{a,t}$ = 30.7 ± 6.4 kJ mol^{-1} and a frequency exponent, log A_t = 5.5 ± 1.3. These values are close to the activation energy for termination reaction in the absence of any additive,

$E_{a,t} = 22 \pm 3$ and $\log A_t = 4 \pm 1.7$ within experimental error (Fig 5.18) indicating that $LiClO_4$ is ineffective in suppressing termination reaction, similar to LiCl.

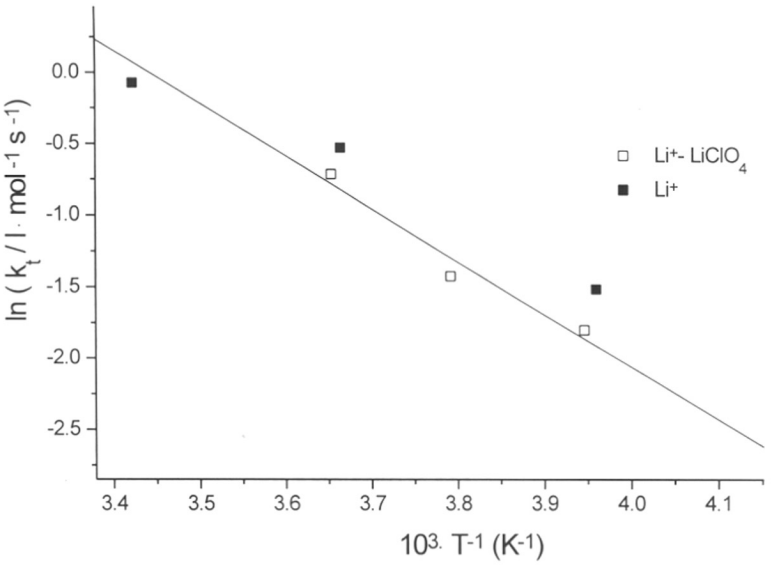

Fig. 5.18: Arrhenius plot of termination rate constant, k_t, of the anionic polymerization of MMA (□) in the presence and (■) the absence of $LiClO_4$.

5.4 Conclusion

Polymerization of MMA in presence of lithium perchlorate proceeds in a living manner at -40 °C in THF and -78 °C in toluene/THF (9:1 v/v) using 1,1'-diphenylhexyllithium as initiator. Similarly, the polymerizaion of tert-butylacrylate also preceeds in a living manner at -78 °C in THF. The ratio of $LiClO_4$ to initiator has a greater influence in determining the control of polymerization. The kinetic studies on MMA polymerization in presence and absence of $LiClO_4$ in a flow-tube reactor show a fractional reaction order indicating the existence of associated ion pairs in equilibrium with non-associated species. The obtained fractional reaction order indicates that $LiClO_4$ does not effectively perturb the aggregation of enolate ion pairs. However, the rate constant of propagation in presence of $LiClO_4$ is lower due to the formation of less reactive mixed aggregates. The determined rate constants of termination in presence and absence of $LiClO_4$ are comparable.

5.5 References

1. Müller, A.H.E. in: *Anionic Polymerization. Kinetics, Mechanisms and Synthesis*; McGrath, J.E., Ed., ACS Symp. Ser. No.166, Washington 1981, p. 441
2. Hatada, K.; Kitayama, T.; Fujikawa, K.; Ohta, K.; Yuki, H. *Polymer Bull.* (Berlin) **1978**, 1, 103
3. Löhr, G.; Schulz, G.V. *Eur. Polym. J.* **1974**, 10, 121
4. Löhr, G.; Schulz, G.V. *Makromol. Chem.* **1973**, 172, 137
5. Mita, I.; Watanabe, Y.; Akatsu, T.; Kambe, H. *Polym. J.* **1973**, 4, 271
6. Tsvetanov, C.B.; Müller, A.H.E.; Schulz, G.V. *Macromolecules* **1985**, 18, 863
7. Müller, A.H.E.;Lochmann, L.;Trekoval, J. *Makromol. Chem.* **1986**, 187, 1473
8. Kunkel, D.; Müller, A.H.E.; Lochmann, L.; Janata, M. Makromol. Chem., *Macromol. Symp.* **1992**, 60, 315
9. Wang, J.S.;Jérôme, R.;Warin, R.;Teyssié, P. *Macromolecules* **1993**, 26, 1402
10. Halaska, V.;Lochmann, L. *Collect. Czech. Chem. Commun.* **1973**, 38, 1780
11. Yakimanski, A.;Müller, A.H.E.;Weiss, H. in preparation
12. Gia, H.-B.; McGrath, J.E. in: *Recent Advances in Anionic Polymerization*; Hogen-Esch, T.; Smid, J., Ed., Elsevier , New York 1987, p. 173
13. Adachi, T.;Sugimoto, H.;Aida, T.;Inoue, S. *Macromolecules* **1993**, 26, 1238
14. Janata, M.;Lochmann, L.; Müller, A.H.E. *Makromol. Chem.* **1993**, 194, 625
15. Reetz, M. T.; Knauf, T.; Minet, U.; Bingel, C. *Angew. Chem.* **1988**, 100, 1422
16. Yasuda, H.;Yamamoto, H.;Yokota, K.;Miyake, S.;Nakamura, A. *J. Am. Chem. Soc.* **1992**, 114, 4908-4910
17. Lochmann, L.; Kolarik, J.; Doskocilova, D.; Vozka, S.; Trekoval, J. *J. Polym. Sci., Polym. Chem. Ed.* **1979**, 17, 1727
18. Lochmann, L.;Müller, A.H.E. Prepr., IUPAC Intl. Symp. on Macromol., Merseburg, Vol. 1 **1987**, 78
19. Varshney, S.K.; Hautekeer, J.P.; Fayt, R.; Jérôme, R.; Teyssié; P. *Macromolecules* **1990**, 23, 2618
20. Bidan,G.;Genies,M. *Tetrahedron Lett.* **1978**, 28, 2499
21. Kitayama, T.;Shinozaki, T.; Sakamoto, T.; Yamamoto, M.; Hatada, K. *Makromol. Chem., Supplement* **1989**, 15, 167
22. Haddleton,D.M.;Muir,A.V.G.;O'Donnell,J.P.;Richards,S.N.;Twose,D.L. *Macromol. Symp.* **1995**, 91, 91
23. Varshney, S.K.; Jacobs, C.; Hautekeer, J.P.; Bayard, P.; Jérôme, R.; Fayt, R.; Teyssié, P. *Macromolecules* **1991**, 24, 4997
24. Hautekeer, J.-P.; Varshney, S.K.; Fayt, R.; Jacobs, C.; Jérôme, R.; Teyssié, P. *Macromolecules* **1990**, 23, 3893
25. Lochmann, L.;Trekoval, J. Prepr., IUPAC Intl. Symp. on Macromol., Florence, Vol. 2, p. 1980, 1977
26. Lochmann, L.;Müller, A.H.E. *Makromol. Chem.* **1990**, 191, 1657
27. Teyssié, P.; Fayt, R.; Hautekeer, J.P.; Jacobs, C.; Jérôme, R.; Leemans, L.; Varshney, S.K. *Makromol. Chem., Macromol. Symp.* **1990**, 32, 61
28. Wang, J. S.; Jerome, R.; Teyssie, P.; *Macromolecules* **1994**, 27, 3376
29. Chang, C. J.; Kiesel, R. F.; Hogen-Esch, T. E. *J. Am. Chem. Soc.* **1973**, 95, 8446.
30. Boileau, S.; Hemery, P.; Kaempt, B.; Schue, F.; Viguier, M. *Polym. Lett.* **1974**, 12, 217.

31. Fayt, R.; Forte, R.; Jacobs, C.; Jerome, R.; Ouhadi, T.; Teyssie, Ph.; Varshney, S. K. *Macromolecules,* **1987**, 20, 1442.
32. Loupy, A.; Tchoubar, B. *'Salt effects in organic and organometallic chemistry'*, VCH Publishers, Inc., **1992**,Weinheim, Germany,.
33. Löhr, G.; Schmitt, B.J.; Schulz, G.V. Z. Phys. Chem. (Frankfurt am Main) 1972, 78, 177
34. Nichols, D.; Szwarc, M. *J. Phys. Chem.* **1967**, 71, 2727.
35. Murthy, A. S. N.; Bhardwaj, A. P. *J. Chem. Soc. Perkin. Trans.* **1984**, 2, 727.
36. Jerome, R.; Forte, R.; Varshney, S. K.; Fayt, R.; Teyssie, Ph. In *' Recent advances in mechanistic and synthetic aspects of polymerization';* Fontanille, M.; Guyot, A.; Eds.; NATO
37. Kraft, R.; Müller, A. H. E.; Hocker, H.; Schulz, G. V. *Makromol. Chem. Rapid Commun.* **1980**, 1, 363.
38. Glusker, D. L.; Galluccio, R. A.; Evans, R. H. *J. Am. Chem. Soc.* **1964**, 86, 187.
39. Kunkel, D.;Müller, A.H.E.;Janata, M.;Lochmann, L. *Polym. Prepr. (Am. Chem. Soc., Div. Polym. Chem.)* **1991**, 32(1), 301
40. Kunkel, D.: "*Einfluß von Lithiumchlorid auf die Kinetik der anionischen Homo- und Copolymerisation von Methacrylaten und Acrylaten mit Lithium als Gegenion in Tetrahydrofuran*", Dissertation, Mainz **1992.**

Chapter 6: Metal Free Anionic Polymerization of Methyl Methacrylate Using Tetraphenylphosphonium as Counterion

6.1 Introduction

In recent years considerable efforts have been made to polymerize alkyl (meth)acrylates at relatively high temperature keeping all the advantages of a living polymerization. The effect of cation in the anionic polymerization of methacrylates and other monomers is well-documented[1]. It was shown that both free anions and ion pairs contribute to propagation. The fraction as well as the propagation rate constants of ion pairs decrease with decreasing ionic radius indicating that these ion pairs are peripherally solvated contact ion pairs. The amount of termination as measured by the ratio of rate constants of termination and propagation, k_t/k_p increases from Li^+ to Cs^{+2}. Another problem is the tendency of ester enolates to aggregate to dimers or tetramers. In some cases the slow exchange between aggregated and non-aggregated ion-pairs causes a considerable broadening of the molecular weight distribution (MWD)[3].

Two routes have been followed in order to overcome termination and aggregation. Various σ-and μ-type ligands, such as crown ethers[4], cryptands[5], pyridine[6], alkali alkoxides[7,8], halides[9], and alkoxyalkoxides[10], as well as aluminum alkyls[11] have been used in order to stabilize the active centers. On the other hand, the chemical nature of the cation itself was varied by the use of metal-free initiator[12,13].

Using silyl ketene acetal, group transfer polymerization (GTP) provides an unique technique to prepare (meth)acrylates at ambient or even at higher temperatures without losing the living character[14]. However, GTP fails to polymerize non-polar monomers. Thus, the synthesis of corresponding block copolymers via sequential monomer addition is impossible. Moreover, polymerization of acrylates and methacrylates need vastly different solvent/catalyst systems, preventing the facile synthesis of acrylate-methacrylate block copolymers.

Reetz et al.[12,13] used tetrabutylammonium thiolate and malonate as initiators for the polymerization of n-butyl acrylate. Subsequently, Sivaram et al[15] have used functional metal-free initiators for the polymerization of acrylonitrile and alkyl acrylates. Although the preliminary results published by these authors were promising, the difficulties associated with the preparation of ammonium salts in a high levels of purity still exist[16]. Preliminary kinetic results showed that these polymerization have considerable induction periods, non-linear time-conversion plots, and broader MWD's than reported before[17]. Bidinger and Quirk et al[18] used Bu_4N^+ salt of 9-methylfluorenyl as an initiator for the polymerization of MMA in THF at ambient temperatures. At very low initiator concentration, they obtained PMMA of broad MWD (M_w/M_n = 2.16) in low yield (24 %). Recent studies of MMA polymerization using Bu_4N^+ salt of fluorenyl and 9-ethylfluorenyl as an initiators show that a large amount of initiator does not take part in the polymerization. Influence of non-metal cations especially tetrabutylammonium, Guanidium cations on the polymerization of MMA are dealt in detail in Chapter 7.

Recently, Zagala and Hogen-Esch[19] have reported the synthesis of PMMA with narrow molecular weight distribution at ambient temperatures in presence of tetraphenylphosphonium cation in THF. This chapter presents the results of a kinetic investigation on the anionic polymerization of MMA using tetraphenylphosphonium cation in THF at -20 °C, 0 °C and +20 °C.

6.2 Experimental Section

6.2.1 Materials

Methyl methacrylate (MMA) and n-butyl acrylate (nBA) obtained from Röhm GmbH, Germany, were first stirred over CaH_2 for 12 hours and then fractionated in presence of Irganox 1010 under reduced pressure over a 1m column filled with sulzer packing. The distillate was collected over fresh CaH_2 degassed and stirred for 12 hours at 0 °C and stored at -20 °C. This pre-purified MMA was redistilled just before polymerization. No impurities were detectable by GC. n-Octane was distilled over Na-K alloy and used as internal standard for GC. Fractionated THF was purified by refluxing over K metal and stored over fresh Na-K alloy in vacuum line.

6.2.2 Synthesis of Tetraphenylphosphonium Triphenylmethanide

Triphenylmethane (Aldrich) was dried under high vacuum for 2 days at RT. The precursor initiator triphenylmethylpotassium ($Ph_3C^-K^+$) was prepared under vacuum by the addition of THF solution of triphenylmethane to a flask contained potassium mirrors at room temperature. Immediate formation of red colored triphenylmethylpotasssium indicates the metalation reaction is fast. The reaction was kept stirring under vacuum for 6 h. The excess metal was filtered and the concentration of the resulting triphenylmethylpotassium solution was determined by double titration method. Tetraphenylphosphonium chloride (Ph_4PCl, Fluka) was dried under dynamic high vacuum at 90 °C for 15 hours.

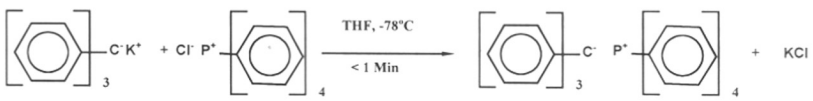

Scheme 6.1: Synthesis of $Ph_3C^-P^+PPh_4$ in THF at -78 °C

Tetraphenyl phosphonium triphenylmethanide ($Ph_3C^-P^+PPh_4$) was prepared *insitu* in THF at -78 °C by cation exchange reaction with slow addition of triphenylmethylpotassium in THF to the dry Ph_4PCl salt. The formation of $Ph_3C^-P^+PPh_4$ was characterized by UV (Fig 6.1a). The change of red color of the $Ph_3C^-K^+$ salt solution (λ_{max} = 502 nm) in to a deep maroon color (λ_{max} = 510 nm) confirms the formation of $Ph_3C^-P^+PPh_4$.

6.2.3 Synthesis of Alkyl α-tetraphenylphosphonium Isobutyrate

Methyl α-lithioisobutyrate (MiB-Li) and ethyl α-lithioisobutyrate (EiB-Li) were obtained from Dr. L. Lochmann (Prague). The metallated ester enolates were dissolved in THF and taken in ampoule A1 in an apparatus shown in Fig. 6.1a. This solution was slowly added at -78 °C or at room temperature to a flask containing dry tetraphenylphosphonium chloride (PPh_4Cl) (Fig.6.1).

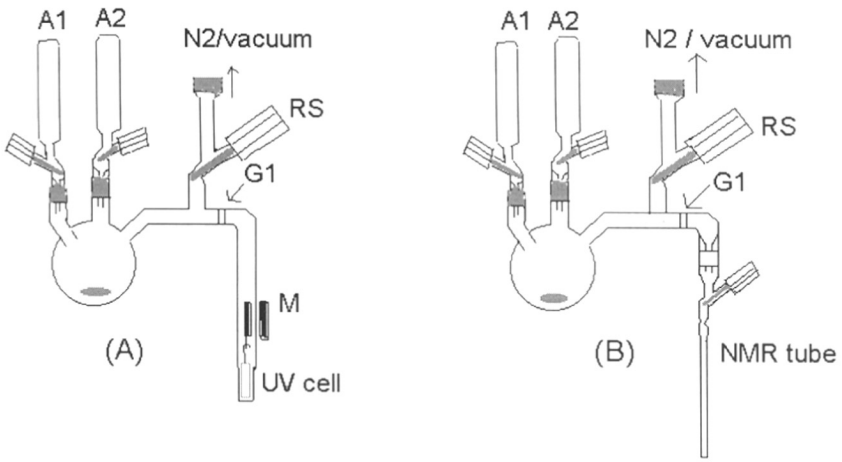

Fig. 6.1: Apparatus used for the UV and NMR analysis of initiator solution. A1, A2- ampoules THF (or THF-d_8) and precursor initiator, RS rota-flow stop-cocks, G1- coarse frit, M- magnet for holding the UV cell spacer.

The ampoule A2 contains THF for dilution of initiator solution for UV/NMR measurement. The initiator solution was filtered through a coarse frit in order to remove excess Ph_4PCl or KCl into the other side of the UV cell or the NMR tube (Fig. 6.1b). The formation of methyl α-tetraphenylphosphonium isobutyrate ($MIBPPh_4$) as well as ethyl α-tetraphenylphosphonium isobutyrate ($EIBPPH_4$) were characterized by the change of colorless solution of MIB-Li or EIM-Li into orange-red (λ_{max} = 415 nm) of the phosphonium salt and found to be stable (by UV and NMR) at room temperature for many hours.

For NMR studies, the same initiators were prepared in THF-d_8 before just prior to the NMR experiments. The NMR tubes were sealed under vacuum and cooled with a liquid nitrogen bath until the NMR experiment was performed. The $MIBPPh_4$ and $EIBPPh_4$ samples prepared from MIBLi or EIBLi contained an equivalent amount of dissolved LiCl as seen by ^{7}Li NMR.

6.2.4 Spectroscopic Measurements.

The ^{1}H, ^{13}C, ^{7}Li and ^{31}P NMR spectra were obtained in THF-d_8 with Bruker AC-200, AM-400, AM-360 or AMX-500 FT-NMR spectrometers, equipped with a Bruker variable temperature controller (B-VT2000). The ^{13}C spectral assignments

were carried out using DEPT experiments and single frequency decoupling (SFD). Chemical shifts were referenced to the high-field resonance of THF-d_8, of which the chemical shift was determined to be 25.2 ppm relative to Me_4Si. The ^{31}P NMR spectra were referenced to phosphoric acid.

The UV/VIS spectrum was obtained with a Shimadzu UV-240 spectrophotometer. Using a reference cell, the background correction for solvent absorption was carried out in each measurement. The measurement was performed in 1 cm quartz cells with 0.965 cm quartz spacer

6.2.5 Batch Polymerization of nBA and MMA

The anionic polymerization of nBA and MMA initiated by $Ph_3C^-P^+PPh_4$ as well as $MiBPPh_4$ was carried out in a flamed glass reactor under an argon atmosphere. To the brick red colored $Ph_3C^-P^+PPh_4$ or to the orange-red colored methyl α-tetraphenylphosphonium isobutyrate initiator solution, the desired amount of THF was transferred. The initiator solution was brought to the particular reaction temperature and then the required amount of nBA or MMA (50 % v/v THF solution) was added within 2-5 s with high pure N_2 pressure. After the monomer addition, the maroon color of the initiator solution turned in to orange-red in case of MMA and orange color in case of n-BA. The color of the polymerization solution remained unchanged while using $MIBPPh_4$ (orange-red) as initiator. Polymerization was continued for few minutes and terminated with methanol containing a small amount of dilute HCl.

6.2.6 Kinetic Experiments

All the experiments were carried out in a specially designed flow-tube reactor. Monomer and initiator solution were pre-cooled and mixed efficiently within less than 1 ms in a mixing jet and allowed to pass through a capillary tube (1mm inner diameter). The reaction mixture was terminated in a quenching jet at the end of the capillary tube with methanol containing a small amount of acetic acid. The temperatures of the mixing jet (T_m) and quenching jet (T_q) were determined using thermocouples. The particular residence time (5 ms $\leq \tau \leq$ 5s) of the polymerization solution was achieved by changing the flow rate the and capillary tube length (4 cm $\leq$ l $\leq$ 6 m). In all the runs the flow rate was carefully chosen in order to maintain

turbulent flow during the polymerization with a characteristic Reynolds number, R_e >3000 at polymerization temperature.

Experiments were carried out at mixing jet temperatures, T_m = -20 °C, -10 °C, 0 °C and 20 °C. Since the polymerization is very fast, heat transfer through the walls of the tube is negligible, leading to a nearly adiabatic behavior. The effective temperature of the each experiment was determined using the equations, $T_{eff} = T_m + 0.55\ \Delta T^{20}$. The effective temperature of the each run is higher than T_m. Thus, data points corresponding to T_{eff} were recalculated to T_m using the activation energy obtained without temperature correction and using the equation,

$$\ln k_{app}(T_m) = \ln k_{app}(T_{eff}) + \frac{E_a}{R} \cdot \left(\frac{1}{T_{eff}} - \frac{1}{T_m} \right),$$

$$k_{app} = \frac{\ln([M]_0 / [M]_t)}{t}$$

The maximum slope of the first-order time-conversion plot obtained from these conversions was taken as the apparent rate constant, k_{app} as shown in Table 6.4.

6.2.7 Characterization of Polymers

Monomer conversion was determined with GC using n-octane as an internal standard. PMMA was recovered by stripping off the solvent and the residue was dissolved in CH_2Cl_2. This was washed twice with little distilled water in order to remove tetraphenylphosphonium chloride, once with $NaHCO_3$ solution, and once with NaCl solution. The organic layer was dried over anhydrous $MgSO_4$ and filtered. After evaporation of the solvent, the polymer was dissolved in benzene and freeze-dried. Molecular weights and MWD were determined using GPC equipped with two UV detectors with variable wavelength, an RI detector, and two 60 cm PSS-SDV gel columns: 1 x 5 μ/100 Å, 1 x 5μ/linear: 10^2-10^5 Å with THF as eluent at room temperature. The calibration was performed using PMMA standards.

6.3 Results and discussion

6.3.1 Batch Polymerization of tBA and MMA Using $Ph_3C^-P^+PPh_4$ as Initiator

The results of the polymerization of nBA and MMA using $Ph_3C^-P^+PPh_4$ in THF are shown in the Table 6.1 and 6.2. PnBAs of broad molecular weight distribution (M_w/M_n >1.5) with 80-90 % yield were obtained. The molecular weight of PnBAs were determined using PMMA calibration and hence should be considered as apparent molecular weights. However, the obtained molecular weights of PnBA and PMMA were higher than the theoretically calculated ones from the feed ratio of monomer to initiator.

Table 6.1: Polymerization of n-butylacrylate using $Ph_3C^-Ph_4P^+$ as an initiator in THF.

Run	$[I]\times10^3$ mole/L	$[M]\times10^2$ mole/L	I, prepared at ^oC	Reaction at ^oC	$M_{n,Calc}$	$M_{n,SEC}$	M_w/M_n	Yield %	f
3	14.8	50.7	30	5-10	4400	6500	1.92	80	0.67
4	14.4	58.8	30	5-10	5300	8300	1.89	87	0.64
5	8.0	87.7	30	0	13,000	22,900	1.46	80	0.56
6	8.4	57.3	30	0	9700	16,500	1.66	80	0.58
7	6.8	55.3	30	0	11,600	27,000	1.66	85	0.43
8	12.3	51.0	-78	0	6200	9000	1.56	90	0.69
9	14.8	60.1	0	0	5200	5800	1.72	80	0.89
11[a)]	14.3	64.0	-78	0	5750	6500	1.67	90	0.88
12[a)]	14.5	59.0	-78	0	5200	7000	1.65	92	0.74

a) Experiments were done using Fluka Ph_4PCl.

In all cases, the SEC trace shows a significant tail in the low molecular weight region. As it can be seen from the table, the initiator efficiency were low which could be due to the presence of termination reaction leading to the formation of dead oligomers[21]. Quantitative yields were obtained in case of MMA polymerization and the PMMA posseses relatively narrow molecular weight distribution compared to PnBA (Table 6.2). The lower initiator efficiencies were attributed to the decomposition of initiator at 0°C.

Table 6.2: Polymerization of Methylmethacrylate using $Ph_3C^-P^+PPh_4$ as initiator[a] in THF at 0°C

Run	$[I]\times10^3$ mol/L	$[M]\times10^2$ mol/L	$M_{n,Calc}$	$M_{n,SEC}$	M_w/M_n	Yield %	f
2[b]	11.2	47.2	4200	6400	1.29	100	0.65
3[b]	7.3	51.8	7000	15,000	1.33	100	0.46

a) Initiator was prepared *in situ* at -78 °C. b) Fluka Ph_4PCl was used.

In order to avoid the decomposition of the initiator, experiments were done immediately after the initiator preparation (at -78 °C) by adding warm THF to the initiator solution (which brings to 0 °C within 5 minutes) and subsequently monomer solution was added rapidly within 2-3 sec using N_2 pressure in a bench top reactor set-up. The fast addition did not improve the results (Table 6.3).

Table 6.3: Polymerization of MMA using $Ph_3C^-P^+PPh_4$ with fast/slow addition of monomer at 0 °C in THF.

Run	$[I]\times10^3$ mol/L	[M] mol/L	$M_{n,calc}$	$M_{n,SEC}$	M_w/M_n	Mode of monomer addition[a]	Yield %
4	37.9	1.06	2790	7000	2.2	fast	>95
5[b]	26.9	1.27	4800	7000	1.4	slow	100
6	12.9	1.06	8250	16430	broad[c]	fast	100
7	12.9	1.06	8250	16440	broad	fast	>95
8	14.2	0.917	6400	11000	broad	fast	100
9	14.8	0.792	5400	12000	broad	fast	100
10	11.0	0.705	6400	3400	broad	fast	>80
11	107.0	0.40	400	890	1.15	slow	100
13	4.48	0.372	8300	8000	1.28	slow	100

a) fast monomer addition with in 2-3 sec. and slow monomer addition with in 15-30 sec. b) initiator was prepared and kept for 1 hr at -78 °C before monomer addition. c) broad MWD : 2.1-3.0

The influence of the mode of monomer addition (slow/fast) is seen on the MWD of the obtained PMMA. This could be due to the inhomogeneous mixing of initiator and monomer. In some cases, the obtained PMMA posseses comparatively narrow molecular weight distribution. As it can be seen in the Table 6.3, the rate of mixing plays a major role in the polymerization. The fast addition of monomer using N_2 pressure in a bench-top reactor did not give a homogeneous mixing whereas slow addition of monomer(diluted) gave better results. In one experiment (run no:5 in Table 6.3) initiator was aged for about an hour before polymerization in order to see the effect of initiator decomposition. It was seen that at -78 °C, initiator is very stable as

the obtained PMMA posseses moderately narrow MWD. It is also seen in a separate experiment that the stability of the initiator strongly depends on the concentration at 0 °C and at low concentration, of the order of 10^{-4} mol/L, the initiator is not stable.

6.3.2 Kinetic Investigation of MMA Polymerization Using Tetraphenylphosphonium as Counterion in THF

The first kinetic experiment of MMA polymerization using $Ph_3C^-P^+PPh_4$ was done in a stirred-tank reactor[22]. It was found that quantitative conversion was obtained within 3 sec. Later, kinetic experiments were done using a flow tube reactor described in Chapter 3. The results of kinetic experiments of the anionic polymerization of MMA using $Ph_3C^-P^+PPh_4$ as initiator at different temperatures, and at different initial initiator concentrations, $[I]_0$ are summarized in Table 6.4.

Table 6.4: Kinetic results of MMA polymerization initiated by tetraphenyl phosphonium salts in THF using a flow-tube reactor, $[MMA]_0 = 0.2$ mol/L

Run	$[I]_0$ $\times 10^{-3}$ mol/L	T_{eff} °C	t_{max} [a] sec	$x_{p,max}$ [b]	$P_{n,SEC}$ at $x_{p,max}$ [c]	M_w/M_n at $x_{p,max}$	f [d]	$[P^*]$ [e] $\times 10^{-3}$ mol/L	k_{app} s^{-1}	$\bar{k}_p$ l mol^{-1} s^{-1}
Initiator $Ph_3C^-P^+PPh_4$										
1	9.95	0	1.40	1	24.4	1.04	0.90	8.96	2.31	258
2	5.30	0	1.85	1	43.4	1.04	0.96	5.09	1.55	305
3	2.37	0	1.98	0.78	76.5	1.07	0.75	1.78	0.654	368
4	1.42	0	2.40	0.80	168.0	1.06	0.76	1.08	0.541	501
5	5.20	-20	2.90	1	32.6	1.08	1	5.20	0.769	148
6	5.20	+20	1.00	1	37.6	1.05	0.93	4.84	3.744	773
Initiator $MIBPPh_4$										
7	5.10	+20	3.42	0.19	36.5	2.1	-	-	0.059	-

a) longest reaction time. b) conversion obtained at t_{max}. c) $P_{n,SEC} = (M_{n,SEC} - M_{init})/M_{mon}$. d) initiator efficiency, $f = P_{n,th}/P_{n,SEC}$ from the ratio of $[M]_0/[I]_0$ and slope of the plot of $P_{n,SEC}$ vs conversion. e) $[P^*] = f \cdot [I]_0$ where f is the initiator efficiency.

6.3.2.1 Determination of Reaction Order

A series of experiments was performed at 0 °C with a variation of initiator concentration from $[I]_0 = 1.42 \cdot 10^{-3}$ to $9.95 \cdot 10^{-3}$ mol/L. The semilogarithamic time conversion plots show an upward curvature with a small induction period (0.05 to 0.2s, depending on the initiator concentrations, Fig. 6.2). The induction period indicate a slow initiation step compared to propagation or a change in the structure of

the active chain end. The reaction half-lives are 0.3 to 1s. As seen from Fig. 6.2, the linearity of the semilogarithamic time-conversion plots at higher conversion indicates the absence of termination reactions during polymerization at 0 °C. The maximum slope of the first-order time-conversion plot was taken as the apparent rate constant, k_{app}.

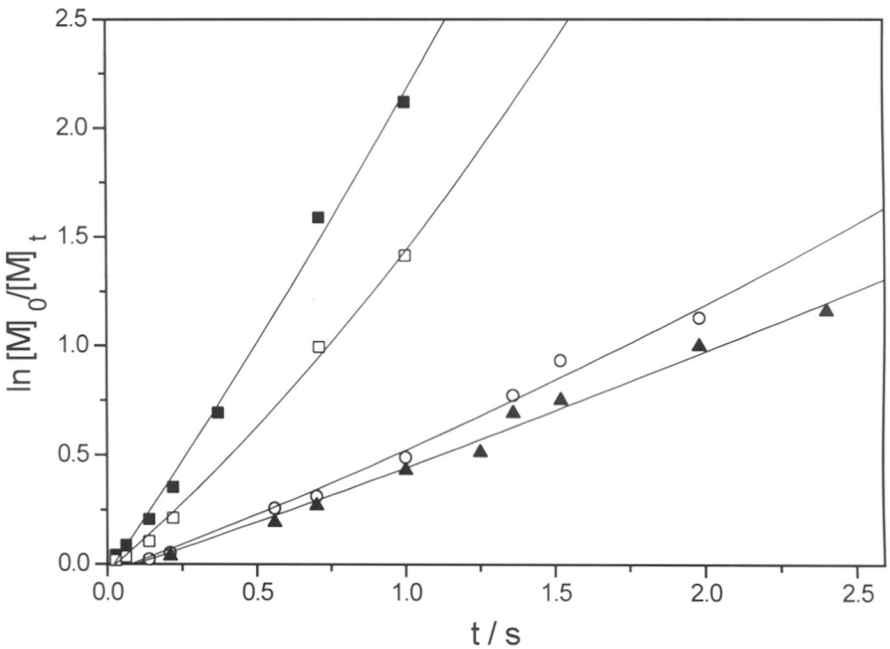

Fig. 6.2: First-order time-conversion plots of the anionic polymerization of MMA using $Ph_3C^-P^+Ph_4$ counterion at various initiator concentrations in THF at 0 °C. $[M]_0$ = 0.2 mol/L, $[I]_0$; (■) $9.95 \cdot 10^{-3}$, (□) $5.3 \cdot 10^{-3}$, (O) $2.37 \cdot 10^{-3}$, and (▲) $1.42 \cdot 10^{-3}$ all in mol/L.

The obtained polymers exhibit narrow molecular weight distribution indicating that the observed induction period is not due to slow initiation ($M_w/M_n \leq 1.1$) (Table 6.4). The linearity of the plot of the number-average degree of polymerization, P_n, versus conversion, x_p, does not give any indication of slow initiation and transfer reactions during the polymerization (Fig. 6.3).

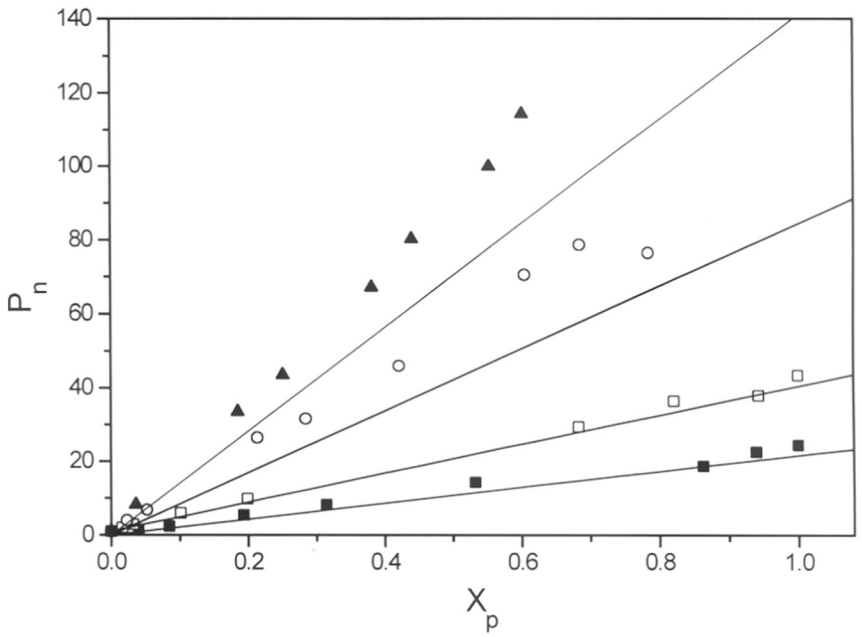

Fig. 6.3: Dependence of number-average degree of polymerization, P_n, on conversion, x_p, at 0 °C for the anionic polymerization of MMA in THF using PPh_4 as counterion. $[M]_0 = 0.2$ mol/L, $[I]_0$; (■) $9.95 \cdot 10^{-3}$, (□) $5.3 \cdot 10^{-3}$, (O) $2.37 \cdot 10^{-3}$, and (▲) $1.42 \cdot 10^{-3}$ all in mol/L.

However, at low concentration of initiator, $[I]_0 \leq 2.3 \cdot 10^{-3}$ mol/L, $P_{n,SEC}$ deviates from the theoretical line indicating a decrease of initiator efficiency, f, from unity to 0.75. This may be due to slow decomposition of initiator between the experiments. The active center concentration, $[P^*] = f \cdot [I]_0$, was determined using the initiator efficiencies, f, calculated from the slope of the plot of P_n versus conversion and the ratios of initial monomer to initiator concentration.

The SEC eluograms of PMMA obtained at various times during the polymerization is given in Figure 6.4. A gradual increase of number average molecular weight during the polymerization and a narrow molecular weight distribution of the obtained polymers at various conversion show that the polymerization is living. No oligomers are detected at higher conversion as can be seen from the eluograms (Fig. 6.4).

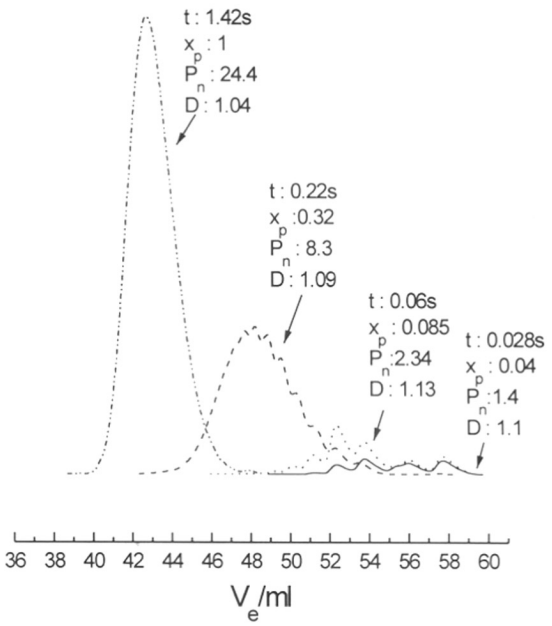

Fig. 6.4: SEC eluograms at different times during the polymerization of MMA using PPh_4 counterion in THF. $[M]_0$ = 0.2 mol/L, $[I]_0$ = $9.95 \cdot 10^{-3}$ mol/L (run No. 4 in Table 6.4).

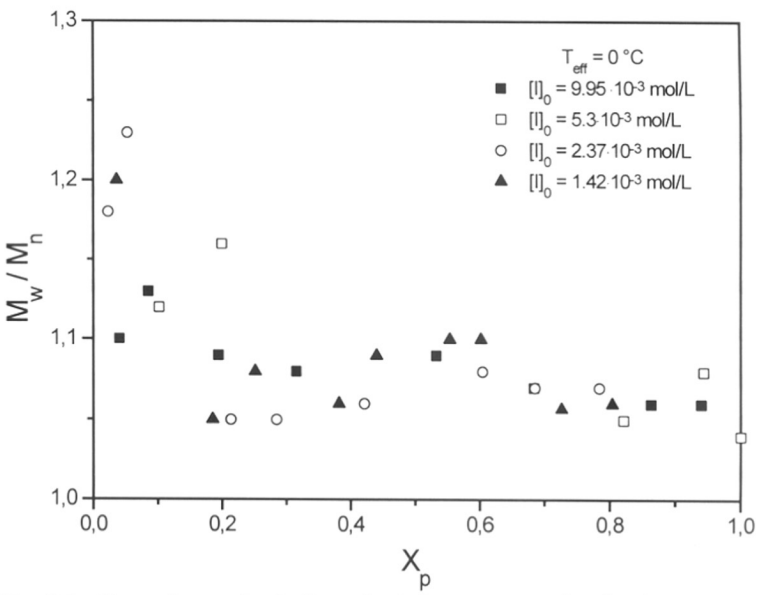

Fig. 6.5: Dependence of polydispersity index on conversion for the anionic polymerization of MMA using PPh_4 as counterion in THF at 0 °C.

The polydispersity index decreases with conversion in all experiments indicating an existence of a slow equilibrium between dormant and active species or species of

different activity (Fig. 6.5)[23]. A bi-logarithamic plot of k_{app} versus active center concentration, $[P^*]$, results in linearity with a slope of 0.71 (Fig. 6.6).

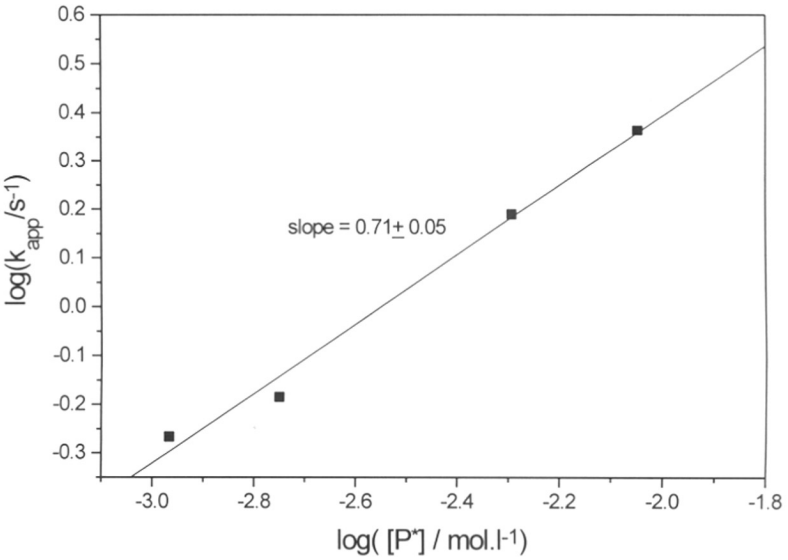

Fig. 6.6: Bi-logarithamic plot of active center concentration, $[P^*]$, versus apparent rate constant, k_{app}.

The fractional order of the reaction with respect to active center concentration indicates that the active species may be involved in dynamic equilibrium with different kinds of reactive species. Similar fractional reaction orders were observed in anionic polymerization of MMA and non-polar monomers using alkalimetal counterions. They can be attributed to the formation of aggregated ion pairs or to dissociation into free ions. Aggregation is very unlikely for these bulky counterions. Thus, the concentration dependence of the rate constants of polymerization is attributed to the co-existence of ion pairs and free ions propagating with different rate constants, $k_{\pm}$ and k_{-} respectively (Fig. 6.7). For the equilibrium between free ions and ion pairs, the overall rate constant k_p for the polymerization is given by the equation 6.1,

$$k_p = \alpha \cdot k_- + (1-\alpha) \cdot k_\pm = k_\pm + (k_- - k_\pm) \cdot \alpha \qquad (6.1)$$

where $\alpha = \left(\frac{K_D}{[P^*]}\right)^{1/2}$ is the degree of dissociation and K_D is the dissociation constant. The rate constant for the polymerization via ion-pairs, $k_{\pm}$ = 135 ± 4 l mol^{-1} s^{-1} is determined as the intercept of Fig. 6.7. From the slope, the product $(k_{-} - k_{\pm}) K_D^{1/2}$ = 11.3 ± 1.94 is obtained.

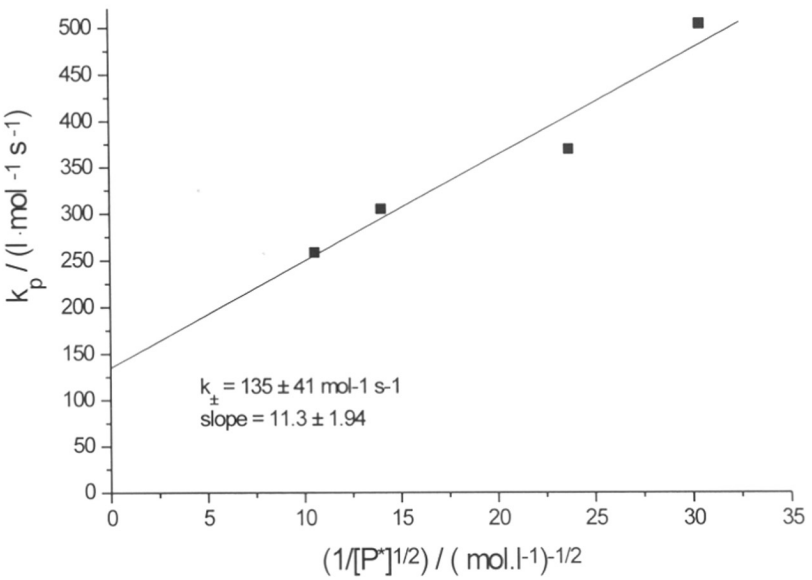

Fig. 6.7: Dependence of the rate constants of polymerization on the concentration of active centers at 0 °C. The rate constant of ion pair, $k_{\pm}$ = 153 ± 4 l mol^{-1} s^{-1}.

6.3.2.2 Evaluation of Arrhenius Parameters and Comparison of Propagation Rate Constant, k_p with Metal Cations

Experiments carried out at -20 °C and +20 °C also show a slight upward curvature in the first-order time conversion plot indicating the absence of termination reactions (Fig. 6.8). A considerable induction period is noticed at -20 °C (≈ 0.3s) if we assume the plot to be linear. A linear dependence of P_n versus conversion is again observed with $f \approx 1$ (Fig 6.9).

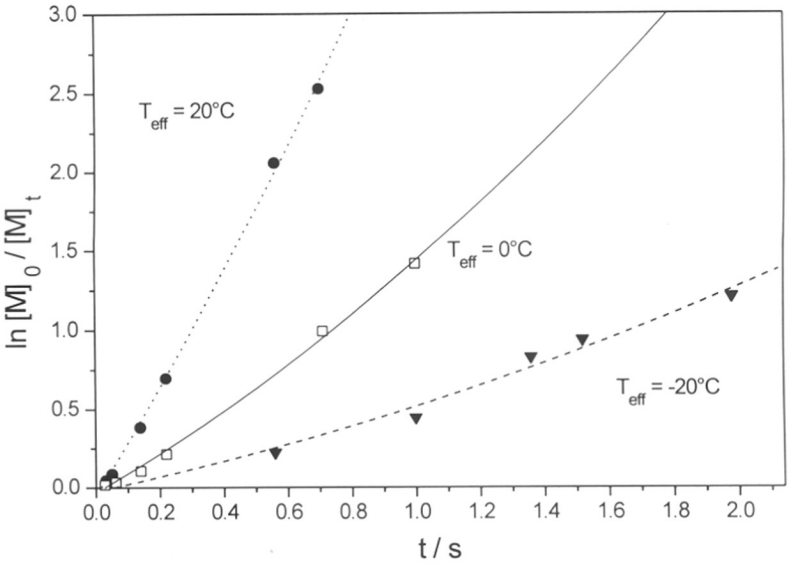

Fig. 6.8: First-order time-conversion plots at -20 °C, 0 °C and +20 °C for the anionic polymerization of MMA in THF using PPh_4 as counterion. $[M]_0 = 0.2$ mol/L, $[I]_0 = 5.2.10^{-3}$ mol/L.

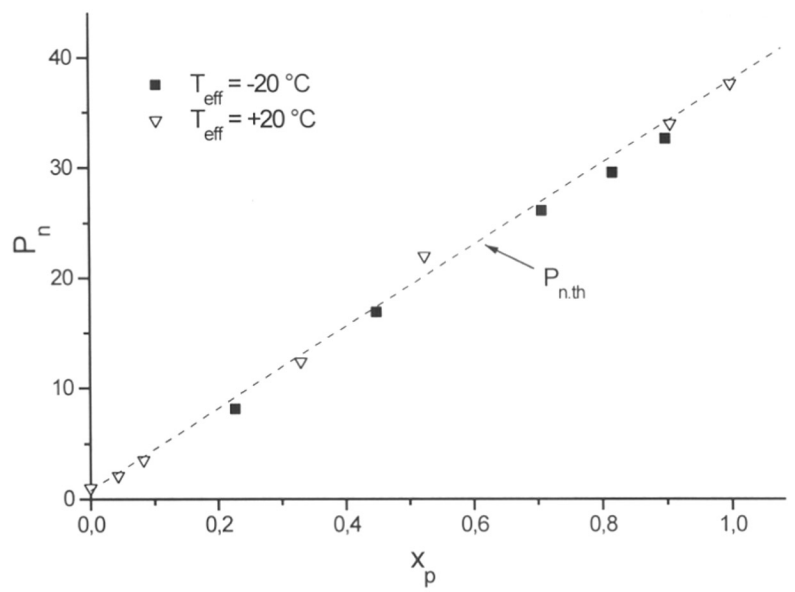

Fig. 6.9: Linear dependence of P_n versus x_p at different temperature using PPh_4 as a counterion (run no: 5,6 in Table 6.4).

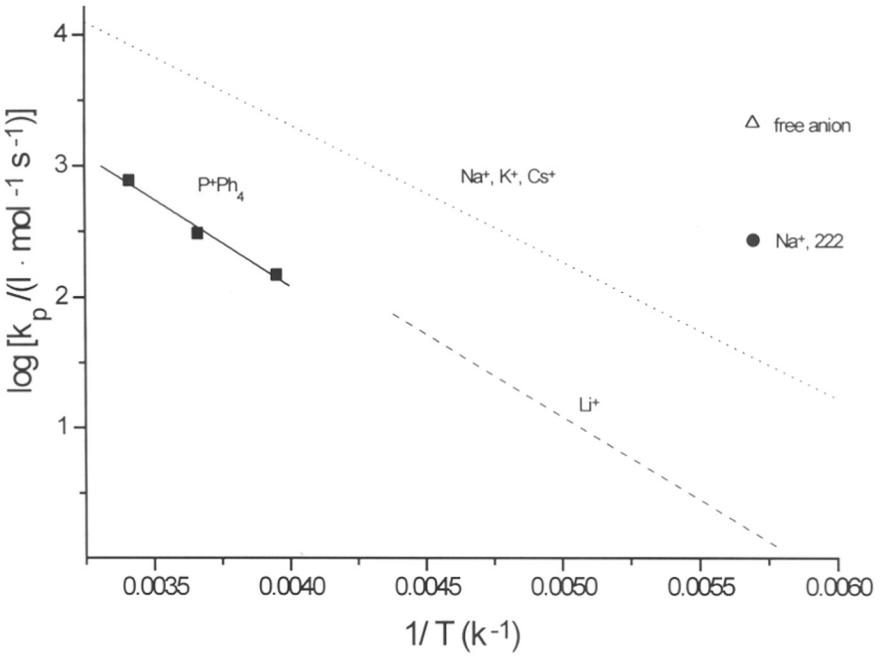

Fig. 6.10: Arrhenius plot of the overall propagation rate constants, k_p, in the anionic polymerization of MMA for PPh_4 counterion in THF and the reported rate constants of ion pairs for other counterions.

The effect of temperature on the rate constants of propagation is seen in Table 6.4 (runs, 2, 5, and 6). The Arrhenius plot obtained using the apparent values of k_p at different temperatures results in linearity with an activation energy, E_a = 25 ± 2 kJ mol^{-1} and the frequency exponent, log A = 7.4 ± 0.5 (Fig. 6.10). Surprisingly, the rate constants and activation parameters are comparable to the ones reported for Li^+ counterion in THF[24] (E_a = 24 kJ mol^{-1} and log A = 7.4).

Quantum mechanical calculations[25] indicate that the interionic distance, a, for the enolate anion with PPh_4 counterion is 4.1Å which is in-between that with cryptated sodium (Na^+, 222), a = 6.1Å, and with Cs^+ counterion (a = 3.3 Å). However, the obtained rate constants with PPh_4 counterion are one to two orders of magnitude lower than expected for such a bulky cation, especially when we use $k_{\pm}$ instead of k_p for the comparison (Fig. 6.10). This indicates that only a fraction of active species takes part in the polymerization. The high initiator efficiencies and the narrow MWD

The model compound of the growing PMMA chain end, i.e., Methyl tetraphenylphosphonium isobutyrate ($MIBPPh_4$) was prepared and used as an initiator for the polymerization of MMA in THF. The orange-red color of the $MIBPPh_4$ solution has a UV/VIS absorption with a maximum at λ_{max} = 415 nm and the color is similar to that of growing PMMA chain end with PPh_4 counterion indicating that the structure of the model compound may resemble that of the active chain end.

6.3.2.3 Phosphorous Ylide Intermediates As a Dormant Species

The detailed NMR and UV studies (see below, section 6.3.4) of model compound, $MIBPPh_4$, revealed the existence of a phosphorous ylide as the major (dormant) species in equilibrium with (active) phosphonium enolate ion pair and the latter is responsible for the polymerization (Scheme 6.2).

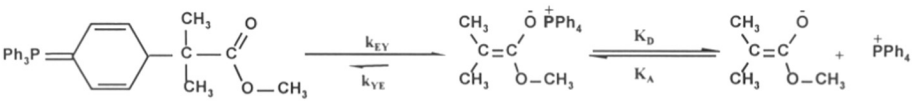

Scheme 6.2: Dynamic equilibrium between ylide and phosphonium enolate

As a consequence of the existence of a large fraction of dormant species we must correct equation 6.1 for the reactions of enolate ion pairs and anions,

$$\alpha_E = \frac{[P_\pm] + [P_-]}{[P^*]}$$

leading to

$$\bar{k}_p = \alpha_E k_\pm + \alpha_E (k_- - k_\pm) \cdot \alpha \qquad (6.3)$$

with $\alpha \approx \left(\frac{K_D}{\alpha_E [P^*]} \right)^{1/2}$. Thus, we obtained for the slope of the plot of $\bar{k}_p$ versus [P*]:

$$\text{slope} = (k_- - k_\pm) \cdot \sqrt{\alpha_E} K_D \qquad (6.4)$$

The dissociation constant can be estimated using the Fuoss equation[26]:

$$\text{slope} = \left(k_{-} - k_{\pm}\right) \cdot \sqrt{\alpha_{E}}\, K_{D} \tag{6.4}$$

The dissociation constant can be estimated using the Fuoss equation[26]:

$$K_{D} = \frac{3000}{4\pi N_{A} a^{3}} \exp\left(\frac{e_{0}^{2}}{a\, DkT}\right) \approx 10^{-7}\, l \cdot mol^{-1} \tag{6.5}$$

with dielectric constant, D = 8.24, temperature, T= 272 K, and the interionic distance obtained from quantum-mechanical calculations[25], a = 4.1 Å. A rough estimate of $k_{\pm} \approx$ 104 $l\,mol^{-1}\,s^{-1}$ (in between Cs^{+} and the extrapolated value for Na^{+},222) leads to a fraction of enolate, $\alpha_{E} \approx 10^{-2}$. From eq. 6.4, with a slope of 11.3 and $K_{D} \approx 10^{-7}$ $l\ mol^{-1}$ we obtain $k_{-} \approx 6.10^{5}$ $l\ mol^{-1}\,s^{-1}$ which is in the order of magnitude of the value extrapolated for the anion from Fig. 6.10 assuming similar activation energies for all counterions and the free anion.

6.3.3 Batch and Kinetic Experiments of MMA Polymerization Using Model phosphonium Ester Enolate ($MIBPPh_4$) as Initiator

The results of the batch experiments carried out using $MIBPPh_4$ as initiator at -78 °C and 0 °C are shown in Table 6.5. The polymers obtained exhibit a broad molecular weight distribution compared to the ones prepared using trityl tetraphenylphosphonium initiator. The initiator efficiencies are 50 % at 0 °C and only 20 % at -78 °C. It was also noticed at -78 °C that the red color of the living polymerization solution did not disappear upon addition of methanol indicating a very slow isomerization of dormant ylide species to ion pairs at that temperature.

Table 6.5: Polymerization of MMA in a batch reactor using Methyl α-tetraphenylphosphonium isobutyrate ($MiBPPh_4$)as an initiator in THF. Conversions are > 95 % in all cases.

Run	$[I] \times 10^{3}$ mol/L	[M] mol/L	Temp. T/ °C	$P_{n.th}$	$P_{n,SEC}$	M_w/M_n	f
2	1.30	0.48	0	370	722	1.77	0.51
3	1.53	0.42	-78	275	1118	1.22	0.24
4	0.97	0.33	0	344	620	2.10	0.55
5	1.50	0.31	-78	206	941	1.20	0.21

A kinetic experiment of MMA polymerization performed at +20 °C using $MiBPPh_4$ as an initiator in the flow-tube reactor (Fig. 6.11) shows a large induction period (0.5 s)

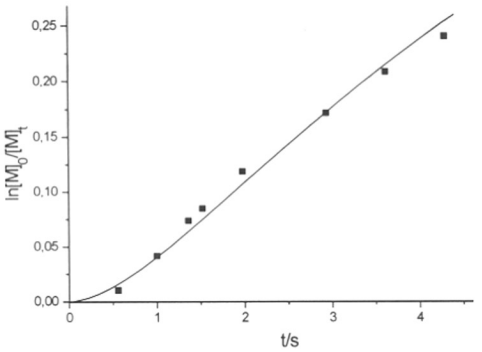

Fig. 6.11:First-order time-conversion plot for the anionic polymerization of MMA using $MiBPPh_4$ as an initiator in THF at +20 °C.

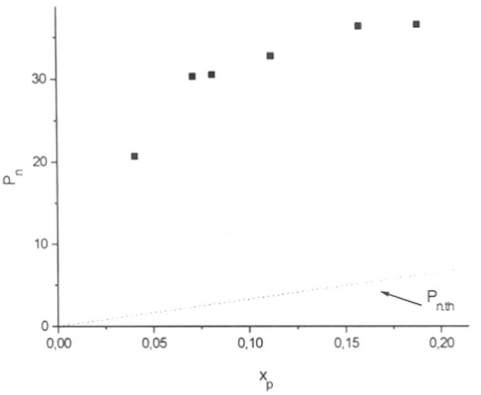

Fig.6.12:Dependence of number-average degree of polymerization, P_n, on conversion, x_p, using $MiBPPh_4$ as an initiator in THF at +20 °C

A plot of the number-average degree of polymerization, P_n, versus conversion (Fig. 6.12) shows a strong downward curvature indicating slow initiation. The initiator efficiency, as determined from the last point of that plot, is low (f = 20 %). These results may be explained by a slower isomerization of ylides to ion pairs in the initiator as compared to the living polymers. This is confirmed by NOE kinetic experiments in the following discussion of NMR results.

6.3.4 Spectroscopic Studies on Phosphonium Enolates of Methyl and Ethyl isobutyrate

As seen from the kinetic studies the anionic polymerization of (meth)acrylates in THF at ambient temperatures initiated by tetraphenylphosphonium (PPh_4) salt of the triphenylmethyl anion proceed rapidly to yield polymers with narrow molecular weight distribution. These polymerizations are quite fast having half-lives of 0.3-0.5 seconds for MMA at 0° C. However, they are still ca.1-2 orders of magnitude slower than expected for such a large counterion. Upon monomer addition the deep maroon color of the $Ph_3C^-P^+PPh_4$ initiator solution instantly changes into brick red which was ascribed to the formation of the phosphonium enolate. This color disappears upon addition of methanol containing acetic acid. This brick red color is very unusual for ester enolates which normally are colorless or faint yellow[27-29]. Several groups have studied enolates and related compounds in the presence of various organic and

studied enolates and related compounds in the presence of various organic and inorganic counterions[27-35] which are models of the active center in these polymerizations, but tetraphenylphosphonium enolates have not been investigated.

Scheme 6.3: Canonical forms of ester enolates

Alkali metallated salts of methyl and ethyl isobutyrate are known to be represented by two major canonical forms exhibiting anion and enolate structure[31,34,36] (Scheme 6.3). Their contributions were shown to depend on the nature of the cation. Thus NMR and IR spectroscopic measurements on alkali enolates are consistent with an increase in electron density on α-carbon with increasing cation size[30,31,37]. For a better understanding of MMA polymerization with PPh_4 counterion, detailed ^1H,^{13}C, ^{31}P NMR of the PPh_4 enolates of methyl (MIB) and ethyl isobutyrate (EIB) were studied.

6.3.4.1 UV/VIS absorption of Tetraphenylphosphonium Salts of Methyl Isobutyrate (MIB)

The synthesis of $MIBPPh_4$ (**4**) was performed *in situ* by cation metathesis of MIBLi or MIBNa or MIBK (**1**) with Ph_4PCl (**3**) in THF-d_8 at -78° C (Scheme 6.4). The cation exchange was very rapid as shown by an instantaneous formation of a brick red solution upon addition of the colorless metal enolate solution in THF-d_8 to dry Ph_4PCl.

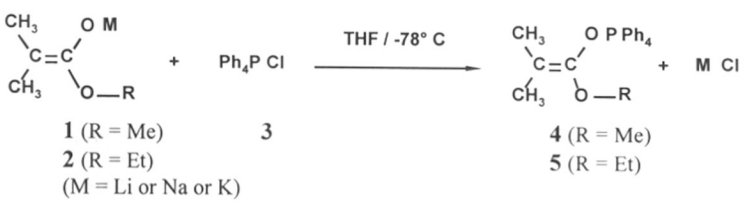

Scheme 6.4: Synthesis of tetraphenylphosphonium ester enolates

The color of the $MIBPPh_4$ solution was similar to that of the growing PMMA chain end indicating that the structure of the model compound may resemble that of the active chain end. The solution showed a striking UV/VIS absorption with a maximum

at λ_{max} = 415 nm, the intensity of which did not change even after 5 hours indicating considerable stability of this species. This is in strong contrast to the absorption of PMMA-Li and MIBLi ($\lambda_{max} \approx 335$ nm).

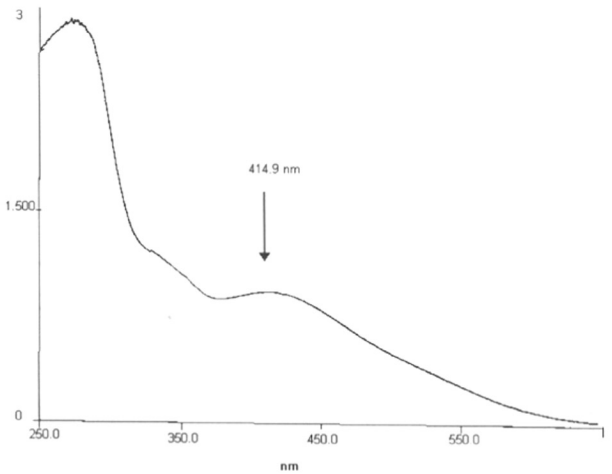

Fig. 6.13: UV/VIS absorption spectrum of **4** showing λ_{max} at ~ 415 nm

6.3.4.2 NMR studies of Tetraphenylphosphonium Salts of Methyl Isobutyrate (MIB) and Ethyl Isobutyrate (EIB) in THF-d_8

NMR Spectra: The ^{1}H and ^{13}C-NMR spectra of $MIBPPh_4$ and $EIBPPh_4$ (**1**, **2**) salts obtained in THF-d_8 at several temperatures are shown in Figures 6.14 - 6.17, and Tables 6.6 - 6.10 along with literature data for MIBLi and related compounds. The spectra obtained for MIBLi are similar to those reported in the literature[31,34]. The ^{1}H NMR spectrum of the reaction product of **4** and **5** shows signals belonging to two components with a ratio of ca. 10/1. However, in some cases the minor component is hidden in the baseline and hardly detected due to line broadening. The chemical shifts of the minor component are consistent with our expectations for an phosphonium enolate, **4** (Fig 6.14, Table 6.6).

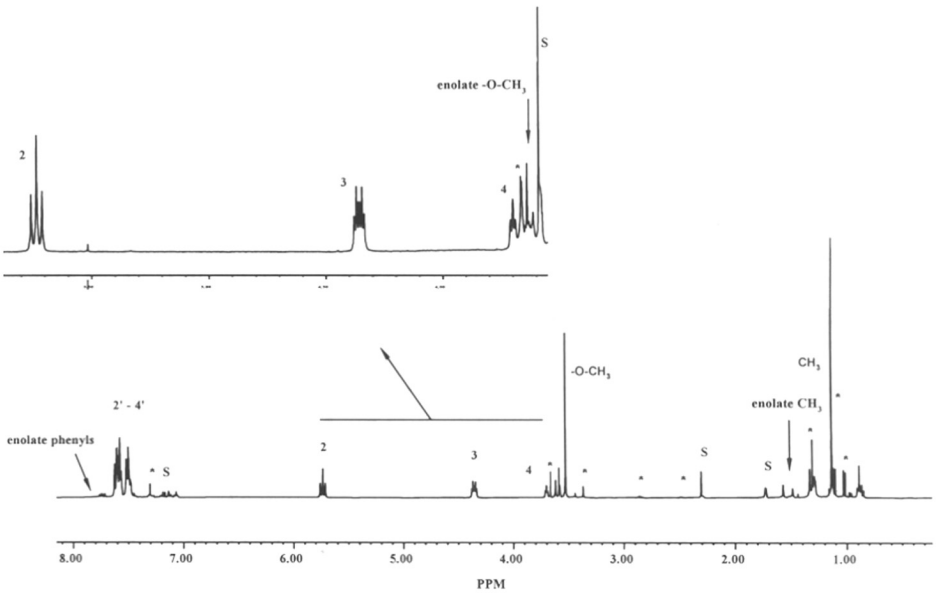

Fig. 6.14: ^{1}H NMR of $MIBPPh_4$ in THF-d_8 at room temperature showing clearly the spliting of protons of one phenyl ring.

Evidence for phosphorous ylide intermediates with phosphonium enolate:

The signal of the geminal methyl protons of the phosphonium enolate, **4**, at 1.5 ppm is broad. The ^{1}H spectrum also shows two sets of phenyl signal. The small and broad signal for the phenyl protons of phosphonium enolate resonate at 7.8-7.9 ppm downfield from other predominant phenyl signals at 7.5-7.6 ppm. It is also seen in the ^{1}H spectrum that there are additional methyl and methoxy signals having chemical shifts similar to that of the parent ester.

Table 6.6: ^{1}H NMR chemical shifts of lithium and PPh_4 enolates of methyl isobutyrate (MIB), and ethyl isobutyrate (EIB) and related compounds in THF-d_8

	T/ °C	-CH_3	-O-R	H-2	H-3	H-4	H-2'-H-4'
Parent MIB (sp^3)	20	1.11 *(d)*	3.59	-	-	-	-
MTS (sp^2)	20	1.54, 1.49	3.44	-	-	-	-
MIBLi (tetramer)	20	1.50	3.43	-	-	-	-
MIBPPh_4(**6**) (enolate, **4**)[1)]	20	1.15 (1.58)	3.55 (3.65)	5.72*(t)* -	4.35*(m)* -	3.7*(t)* -	7.4-7.6*(m)* (7.8-7.9)
	-40	1.15 (1.50)	3.52 (3.60)	5.72 -	4.35 -	3.75 -	7.4-7.6*(m)* (7.85-7.92)
EIBPPh_4(**7**) (enolate, **5**)[1)]	20	1.12 (1.5)	3.9 (4.1)*(q)*, 1.18(1.08)*(t)*	5.72*(t)* -	4.33*(m)* -	3.75*(t)* -	7.0-7.9*(m)* (7.8- 7.9)

1) broad small signals; *d)* doublet, *t)* triplet, *q)* quatruplet, *m)* multiplet

The predominant compound exhibits narrow lines for all protons. Integration reveals the presence of one PPh_4 per MIB group. Remarkably the five protons of one phenyl ring are shifted upfield by 2-4 ppm (5.72, 4.35, and 3.7 ppm) from the other three phenyls at 7.4-7.6 ppm. The integration ratio of 2:2:1 of these five protons and the ABCX like spin pattern (A,B,C = ^{1}H, and X = ^{31}P), indicates a symmetry plane through C-1 to C-4 and that the MIB group is attached at the para position of the ring.

Assignment is obvious from 2D ^{1}H,^{1}H-COSY and homodecoupling experiments, which connect protons H-2, H-3 (5.72, 4.35 ppm) and H-3, H-4 (4.35, 3.7 ppm) (Fig.16.15). Since the proton coupling constants (^{3}J(H-2,H-3) = 9.44 Hz, ^{3}J(H-3, H-4) = 4.1 Hz) indicates higher bond order between C-2 and C-3 in comparison to C-3, C-4, one can conclude that the substituted ring exhibits 1,4-cyclohexadiene structure. Further confirmation is drawn from ^{1}H, ^{31}P coupling constants (^{3}J (H-2,P) = 10.3 Hz, ^{4}J (H-3, P) = 4.1 Hz, ^{5}J (H-4, P) = 1.0 Hz) showing decreased size of coupling with increased number of intervening bonds (Table 6.7).

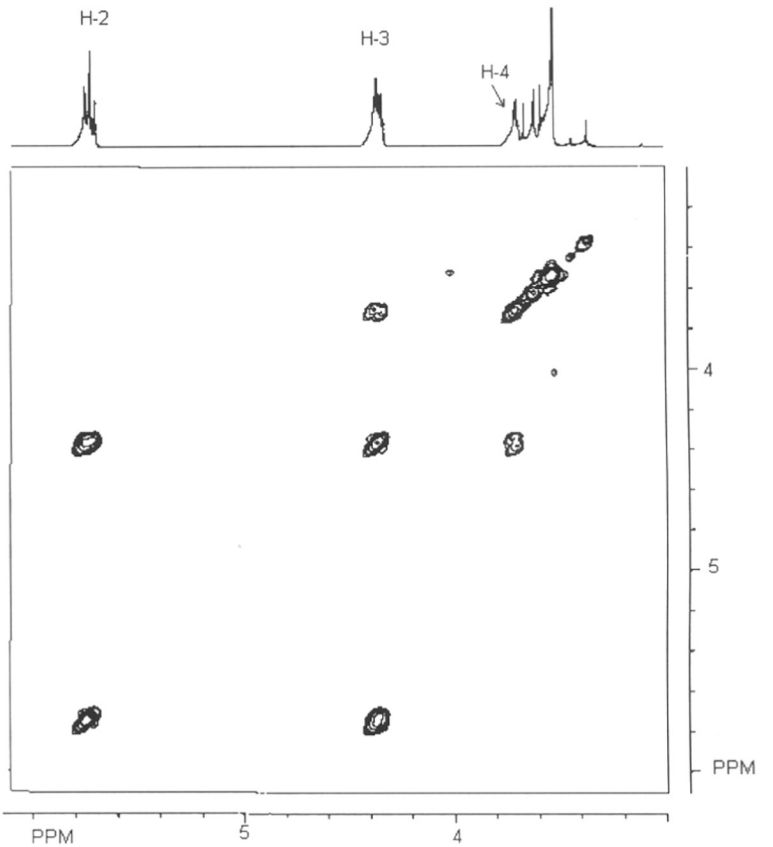

Fig. 16.15: 2D ^{1}H, ^{1}H- COSY spectrum of **4** showing a long-range coupling of the cyclohexadienyl ring proton

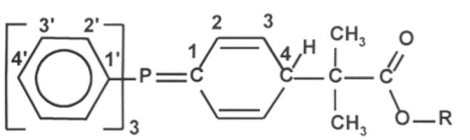

6 (R = Me), **7** (R = Et)

The MIB group of the predominant compound exhibits one narrow signal for both methyl groups indicating the loss of the enolate character due to bonding with one phenyl ring. Thus, ^{1}H NMR findings are consistent with an ylide structure, **6**. The formation of ylide **6** is consistent with the observed UV/VIS absorption at λ_{max} = 415 nm.

Table 6.7: ^{1}H-^{1}H and ^{1}H-^{13}P coupling constants for the cyclohexadiene ring of **6**.

Protons position No.	^{1}H NMR shift in δ	Type of multiplicity	Nature of coupling	Coupling constant in Hz
H-2	5.72	triplet	^{3}J(H2-H3) ^{3}J(H2-P)	9.4 10.3
H-3	4.35	multiplet	^{5}J(H3-P) ^{3}J(H 3-H4) ^{3}J(H3-H2)	≈ 4.1 4.1 9.4
H-4	3.7	triplet	^{3}J(H4-H3) ^{5}J(H4-P)	4.1 1.2

Unlike **6**, most of the signals corresponding to enolate **4** are broad indicating that there is a dynamic equilibrium with a different state of phosphonium enolate. It is also evident from the ^{1}H NMR that the phosphonium enolate very slowly decomposes at room temperature by proton abstraction resulting in parent ester (MIB) which further undergoes Claisen condensation with the enolate ion. At room temperature the intensity of these side product signals increases slowly with time (after a few days).

^{13}C and ^{31}P-NMR Spectra: The ^{13}C spectra are shown in Fig 6.16 and Tables 6.8-6.9. The spectra of **4/6** does not clearly show the signals corresponding to the phosphonium enolate (except for two small signals for geminal methyl groups of **4**) due to its low concentration. The ^{13}C spectrum of ylide **6** shows signals of the MIB group at 21.4 ppm (CH_3), 50.7 ppm (C_α), 50.9 ppm (-OCH_3), and 178.2 ppm (C=O), which can be compared to the corresponding carbon shifts in the related parent MIB and MIBLi (Table 6.8).

For $MIBPPh_4$ and $EIBPPh_4$, the appearance of one methyl carbon signal (21.2 ppm) and carbonyl shift at 178.2 ppm reveals the similarity to the parent MIB and loss of the enolate character. The remaining α-carbon is now found at 50.7 ppm in **6** (Fig 6.16) and at 50.4 ppm in **7**, resonating upfield from the MIBLi enolate tetramer (72.04 ppm) and downfield from the carbon in the parent MIB (36.3 ppm). The upfield shift relative to MIBLi would imply a substantial increase of charge density or a rehybridization from sp^2 to sp^3. The downfield shift relative to MIB is explained by substitution of the α-carbon in the parent MIB. Furthermore, the related silyl enolate,

1-methoxy-1-(trimethylsiloxy)-2-methyl-1-propene (MTS) exhibits an α-carbon shift at 92 ppm, downfield from differently aggregated or cryptated metal enolates (60-75 ppm, Table 6.8).

Table 6.8: ^{13}C chemical shifts of lithium and phosphonium enolates and related compounds in THF-d_8.

	T/ °C	C=O	C_α	$-CH_3$	$-OCH_3$/ $-OCH_2-CH_3$
Parent MIB (sp^3)	20	178.8	36.35	21.14	53.26
MTS (sp^2)	20	152.67	92.37	18.2, 19.04	58.47
Methyl Pivalate	20	180.19	41.1	29.41	53.5
MIBLi (**1**) tetramer	20	160.97	72.04	17.47, 18.29	56.41
MIB (Li,211)[a] cryptated unimer	-30	159.4	59.9	19.9, 18.6	50.9
$MIBPPh_4$ (**6**)	20 -40	178.2 178.12	50.7 51.14	21.4 21.14	50.9 50.66
$EIBPPh_4$ (**7**)	20	177.7	50.4	21.35	59.69, 14.6

a) data taken from Ref.34

The geminal methyl groups of $MIBPPh_4$ are now equivalent, as they are for $EIBPPh_4$. However, the cryptated MIB,(Li, 211) salt shows non-equivalent methyl groups and an upfield α-carbon shift compared to MIBLi. This again is consistent with the ylide structure **6** for $MIBPPh_4$.

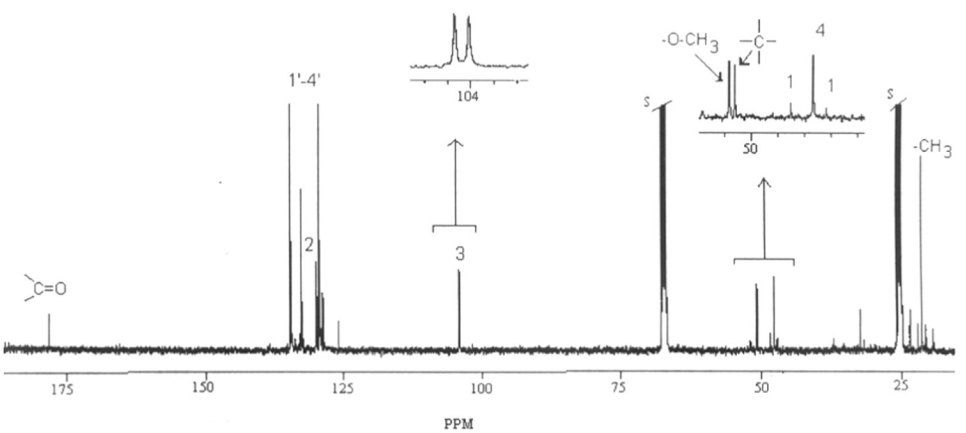

Fig. 6.16: ^{13}C NMR of tetraphenylphosphonium salt of methyl isobutyrate, an ylide **6**, at room temperature ($MIBPPh_4$).

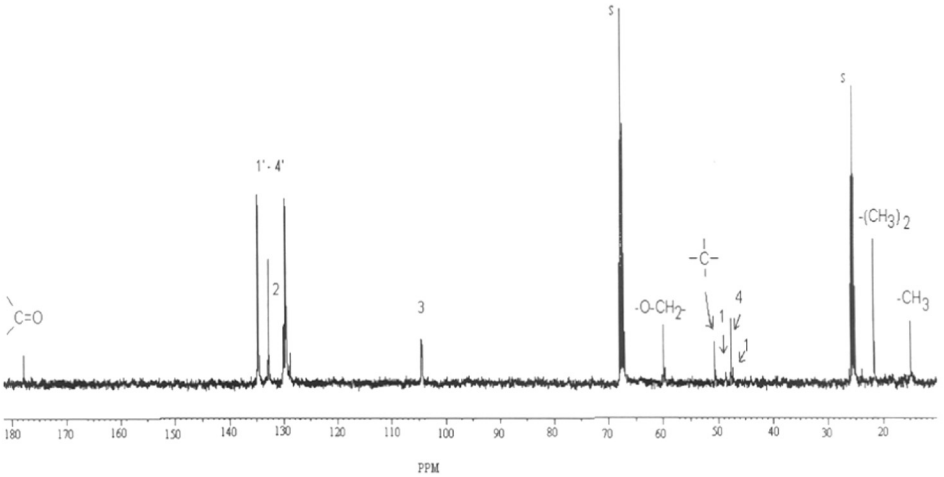

Fig. 6.17: ^{13}C NMR of tetraphenylphosphonium salt of ethyl isobutyrate, an ylide 7, at room temperature ($EIBPPh_4$).

Table 6.9: ^{13}C NMR chemical shifts and ^{13}C-^{31}P coupling constants of **6**, **7** and related compounds[a] in THF-d_8

	T °C	C-1	C-2	C-3	C-4	C-1'	C-2'	C-3'	C-4'
$MIBPPh_4$ (**6**)	+20	48.6 (134.5)	130.01 (12.5)	104.23 (15.1)	47.8	128.7 (86.8)	134.63 (9.3)	129.7 (11.6)	132 (3)
	-40[b]	48.5	130.03	103.45	47.61	128.8	134.56	129.75	132.8
$EIBPPh_4$ (**7**)	+20	48.4 (135.6)	129.94 (13.6)	104.33 (15.9)	47.49	128.6 (87.9)	134.55 (8.9)	129.4 (11.2)	132.6 (2)
8 [c]	+22	-4.1 (51.9)				132.3 (83.6)	133.1 (9.8)	128.6 (11.6)	131.1 (2.4)
9 [d]	+22	53.3 (128.7)	131.1 (14.0)	142.1 (14.8)		126.3 (88.8)	134.7 (10.7)	129.5 (11.8)	133.1 (3.0)
10 [d]	+22	78.3 (113.1)	117.2 (15.7)	114.6 (18.0)		126.6 (89.6)	134.0 (10.0)	129.2 (12.1)	132.9 (2.9)
13 [e]		78.1	127.9	91.7	30.8				
Ph_4PCl [f]	+22					117.1 (89.2)	134.1 (10.2)	130.7 (12.8)	135.7 (3.0)
Ph_3P [g]	+22					137.2 (11.9)	133.6 (19.5)	128.4 (6.8)	128.6

a) The numbers in parentheses are the ^{13}C-^{31}P coupling constants (in Hz) obtained from the ^{13}C NMR spectra. b) Coupling constants are similar to those obtained at +20 °C. c) taken from ref. 38. d) from ref.42. e) from ref. 44. f) ref. 19b. g) from ref.39.

The geminal methyl groups of $MIBPPh_4$ are now equivalent, as they are for $EIBPPh_4$. However, the cryptated MIB, (Li, 211) salt shows non-equivalent methyl groups and an upfield α-carbon shift compared to MIBLi. This again is consistent with the ylide structure **6** for $MIBPPh_4$.

Inspecting the phenyl carbon region, one can see a set of signals corresponding to shifts and couplings observed in the precursor PPh_4 cation (Fig. 6. 16 and Table 6.9). Additional signals are found at 130 ppm (J(C, P) = 12.5 Hz), 104.3 ppm (J(C, P) = 15.1 Hz), 48.6 ppm (J(C, P) = 134.5 Hz) and 47.8 ppm, which can be assigned to different ring carbons C-2, C-3, C-1 and C-4 respectively. These assignments were confirmed using single frequency decoupling (SFD) technique. On decoupling frequency of the H-4 proton resonance at 3.7 δ, the 13C spectrum showed only one carbon signal at C-4 at 47.8 ppm which indicates that the proton at 3.7δ corresponds to the carbon C-4. For other carbons due to the C-H coupling, multiplet were seen except for the quarternary carbons. Similarly on decoupling the H-3 resonance at 4.3 δ identified the a doublet carbon at 104.15/1-4.31 ppm (C-3).

The remarkable upfield shift for C-1, C-2 (80 ppm) and C-4 (24 ppm) in addition to the carbon-phosphorousous coupling of 134 Hz clearly points to a phosphorous ylide group with the ylide carbon involved in a 1,4-cyclohexadiene ring.

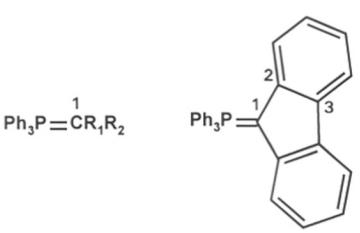

8 (R_1, R_2 = H)
11 (R_1 = H, R_2 = Ph)
12 (R_1, R_2 = Ph)

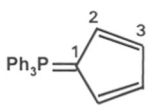

9

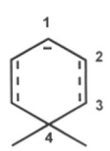

10

13

Table 6.10 : ^{31}P NMR chemical shifts of **6** and related compounds

Compound	δ (ppm)	Reference
Ph_3P	-5.0	*19b*
Ph_4PCl	25.3	*19b*
4 (enolate)	28.4	a
6	13.9	a
8	19.6	*40*
10	12.9	*40*
11	7.0	*40*
12	6.6	*41*

a) Spectra taken at 400 MHz in in THF-d_8

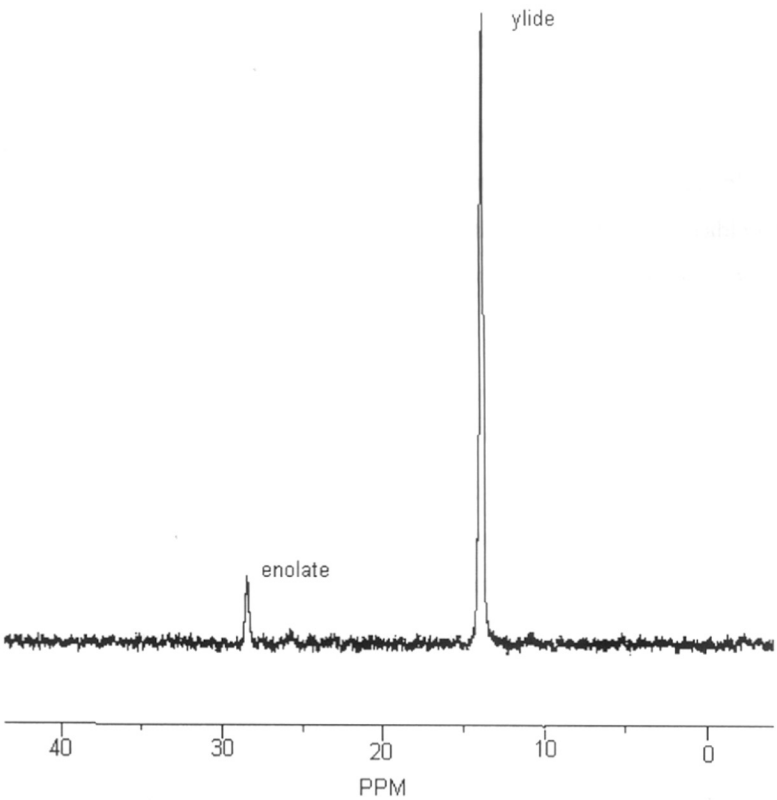

Fig. 6.18: ^{31}P-NMR of tetraphenylphosphonium salt of methyl isobutyrate at room temperature showing the presence of **6** (13.9 ppm) and **4** (23.4 ppm).

Furthermore, the ^{31}P NMR (Table 6.10, Fig. 6.18) shows two signals resonating at 13.9 ppm and 28.4 ppm respectively with ratio of 10/1 which is assigned to **6** and **4**.

The strong coupling of phosphorousous α-carbon (C-1) is also clearly seen from the ^{31}P NMR. The ylide structure **6** is also supported by ^{13}C and ^{31}P chemical shifts and ^{13}C-^{31}P coupling constants [38,39] of other ylides **8** - **10** (Table 6.9). Thus, the ^{13}C chemical shifts of C-1 are arranged as **8** > **6** > **9** > **10** in order of decreasing field whereas the ^{31}P chemical shifts [40,41] are arranged in opposite order (Table 6.10) **10** > **6** > **8** indicating a correlation with electron density. Thus the greater deshielding of C-1 in **10** compared to **9** is reported to be due to a greater delocalization of negative charge in **10** [42,43] and this is consistent the upfield shifts of C-2 and C-3 in **10** compared to the corresponding carbons in **9**.

The ^{13}C NMR assignments of carbons 1-3 in **6** and **7** are consistent with those of the anion of 3,3-dimethyl-1,4-cyclohexadiene[44] (**13**) where C-1 is shifted downfield with respect to the corresponding C-1 in ylides **6** and **7** while C-2 and C-3 are upfield compared to the corresponding carbons in **6** and **7**, respectively. The ^{13}C -^{31}P coupling constants again confirm the viability of ylide structures **6** and **7**. Thus coupling of ^{31}P with the C-1 is strong in **6** (135.8 Hz) as it is in other ylides **8** - **10** (Table 6.9, Fig. 6.18). Coupling with C-2 and C-3 is weaker (8.8 - 11.3.Hz) and weakest with C-4 (2.4 -3.0 Hz).

6.3.4.3 NOE Experiments: Evidence for the Existence of a Dynamic Equilibrium Between the Ionic and Covalent Structures of $MIBPPh_4$

In order to confirm structure **6** and to find evidence for the existence of an equilibrium between the ylide and enolate structures, NOE experiments were performed. Positive NOE signals were only detected at low temperatures while at room temperature mainly strong negative signals due to saturation transfer were observed.

At room temperature, irradiation of H-2 at 5.7 ppm gives a weak negative signal at H-3, strong negative signals of phenyls of **6** at 7.6 ppm and weak negative signals at the phenyls of **4** at 7.8 ppm (Fig. 6.19a). Upon irradiation of H-4 at 3.7 ppm, there is a strong negative signals at 7.6 ppm of the phenyls of **6** with small negative signals at the phenyls of **4** at 7.9 ppm (Fig. 6.19b).

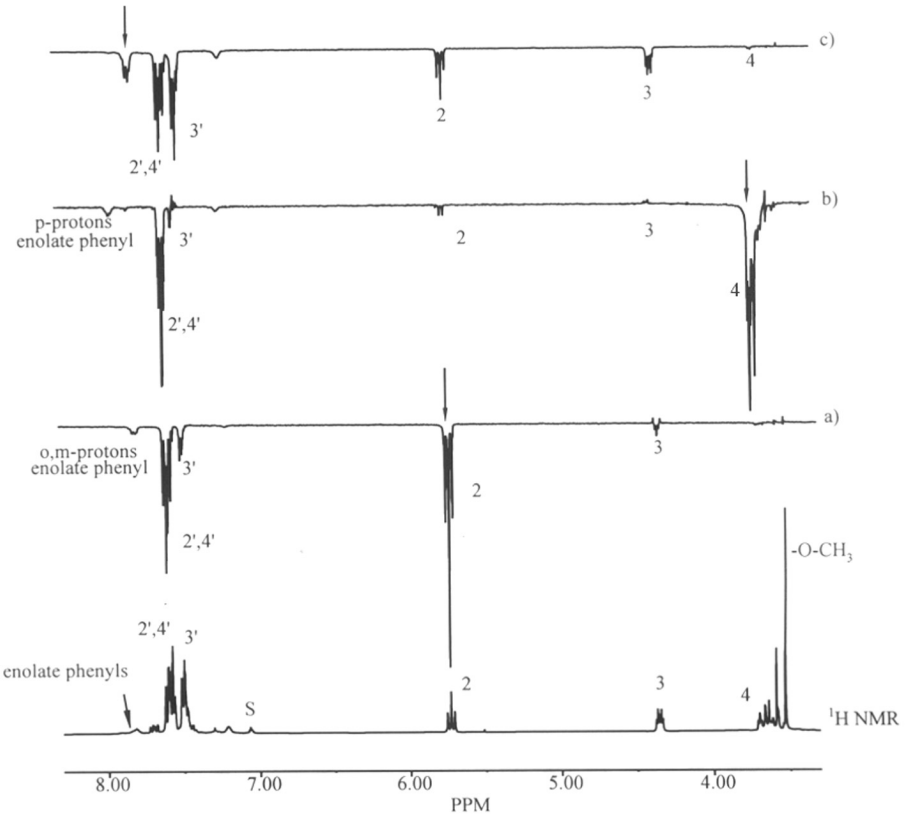

Fig. 6.19: Aromatic region of the NOE difference spectrum (400 MHz) of $MIBPPh_4$ (**6**) in THF-d_8 at 20 °C. a) NOE difference spectrum resuting from irradiation of the H-2 resonance. b) irradiation of the H-4 resonance. NOE signal at H-3 with strong saturation transferred signal at other phenyls including the enolate phenyls. c) Saturation-transferred signals of H-3 and H-4 and other phenyls on irradiation of o,m-proton resonances of phosphonium enolate phenyl of **4**

These strong negative enhancements cannot be attributed to NOE effects and to spatial proximity considering the internuclear distances. It could arise from the exchange of saturation of the cyclohexadiene ring protons with that of other three phenyls as a result of inter- or intra-molecular exchange of the MIB anion through the intermediacy of the phosphonium enolate, **4** (Scheme 6.5). Thus, during the presaturation time (3 sec), exchange of the MIB anions give rise to pronounced saturation transfer signals at the other phenyls of **6** and weaker phenyl transfer signals of **4**. The phenyls of **6** (meta protons at 7.5 ppm) and phenyls of **4** (ortho, meta protons

at 7.8 ppm) show negative transfer signals on irradiating H-3 protons of cyclohexadiene ring (Fig. 6.19).

Furthermore, irradiating the ortho and meta protons of the phenyl signals of the minor compound of **4** at 7.8 ppm, gives negative enhancement at H-2 and H-3 of the cyclohexadiene of **6** (Fig 6.19c). Similarly, upon irradiating the para protons of the phenyl signals of **4** at 7.9 ppm, saturation transfer signals at H-2 and H-4 of the cyclohexadiene of **6** are observed. Thus observation of saturation transfer strongly confirms exchange and equilibrium of ylide, **6** and ion pair **4**.

i) Intramolecular

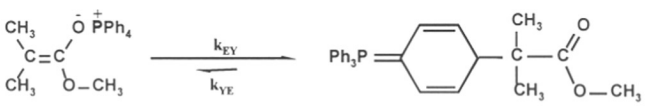

ii) Intermolecular

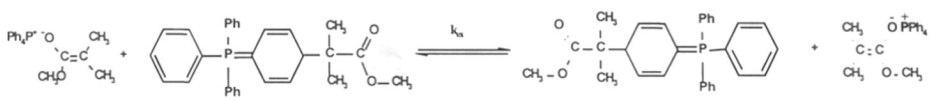

Scheme 6.5: Intra- and intermolecular equilibrium between ionic and ylide structures of tetraphenyl phosphonium enolate

Surprisingly, upon irradiation of the MIB methyl protons of **6** at room temperature, a small positive NOE enhancement (≈1 %) is observed at the phenyl groups in addition to the enhancements at H-2, H-3 and H-4 (Fig. 6.20). If MIB exchange between the cyclohexadiene and the phenyl rings is slow, then irradiation of its α-methyl groups should give only NOE enhancement at the cyclohexadiene protons.

Indeed, at -40° C, irradiation of the methyl protons of the MIB group shows positive NOE enhancements mainly at H-3 and H-4 of the cyclohexadiene ring and not at the three phenyls. At low temperature the rate of exchange is slowed down and saturation transfer is suppressed.

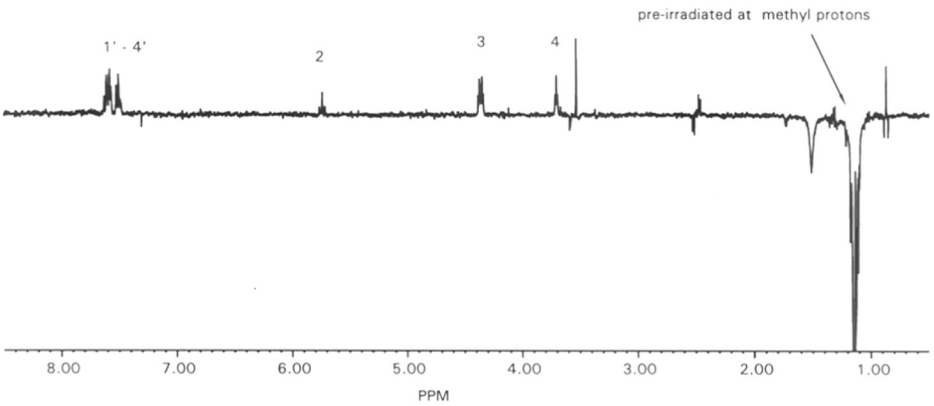

Fig. 6.20: NOE difference spectrum of **4** resulting from irradiation at methyl protons of ester at room temperature.

Determination exchange rate of enolate anion by NOE kinetics:

The observation of a pronounced saturation transfer at room temperature between the cyclohexadiene and the phenyl protons indicates an exchange of the MIB groups between the four phenyl rings with a rate in the order of magnitude of the proton longitudinal relaxation time, $T_1^{-1} \approx 1\ s^{-1}$. In order to determine the exchange rate of the MIB anion, NOE experiments were performed using different presaturation times irradiating at H-2 at 5.74 ppm at room temperature. The presaturation time was varied from 0.1 to 10 s. The change in intensity was plotted against the presaturation time (Fig 6.21) and the best exponential fit of the data points shows that the rate constant of exchange of MIB anion (k_{YE}) from one phenyl to another is 0.72 s^{-1}. This supports the existence of a dynamic equilibrium between the ylide and the enolate (Scheme 6.5).

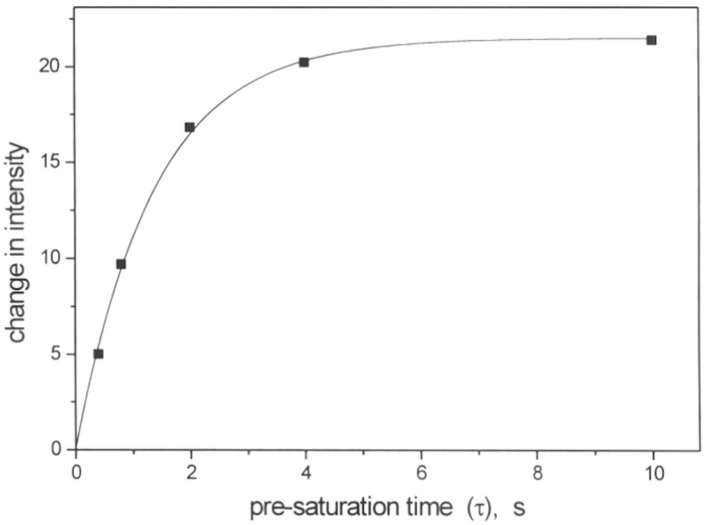

Fig. 6.21: Change in intensity of ortho phenyl protons of 6 during the presaturation of H-2.

The feasibility of ylide and enolate structures are confirmed by semiempirical (PM3) and *ab initio* calculations[45] (Fig. 6.22). The calculations of enolate **4** show that there is a short-range interaction between enolate oxygen and three ortho protons of the phenyl rings (1.7 Å). This would indicate that the existence of ortho substituted ylide intermediate cannot be excluded.

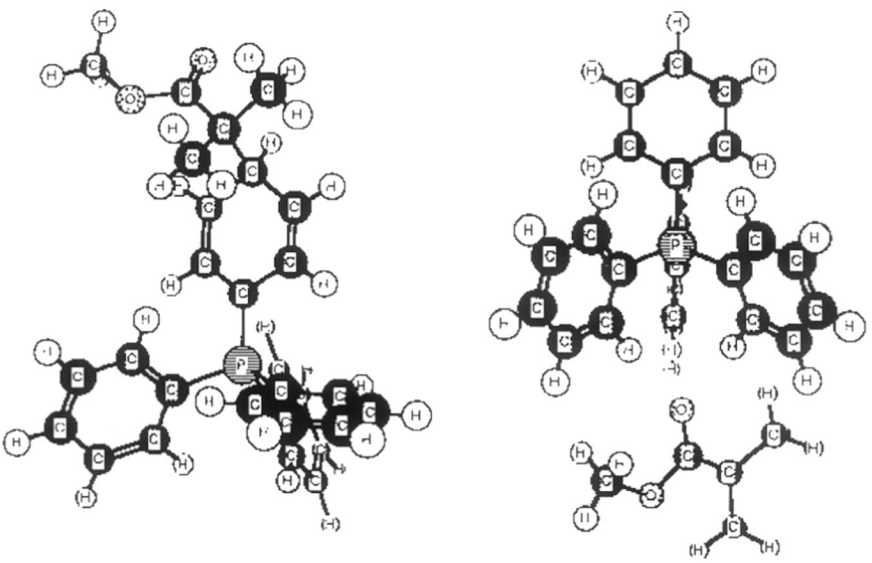

(a) (b)

Fig. 6.22: Structures of a) ylide and b) enolate of teteraphenylphosphonium methyl isobutyrate calculated by *ab initio* method[45].

Since the exchange of MIB anion with other phenyl rings can be inter- or intra-molecular, the nature of exchange is not yet clear. In case of intermolecular exchange the observed rate constant should depend on the concentration. The insertion of monomer can be via ion pair and in case of inramolecular exchange it would be expected to take place during the exchange (Scheme 6.6). The delocalization of π-electrons results to C4-ester bond cleavage and the formation of ion pair. The ion pair again turns to ylide by attacking adjacent phenyl group at para position.

At low temperature, a small decrease in intensity of the enolate signals relative to the ylide signals is observed. ^{13}C and ^{1}H NMR of **6** and **7** do not show any significant change in chemical shifts and line width of the carbons and protons, when decreasing the temperature from +20 °C to -40 °C indicating either a small enthalpy of enolate formation or a presence of still very low fraction of the enolate even at -40 °C.

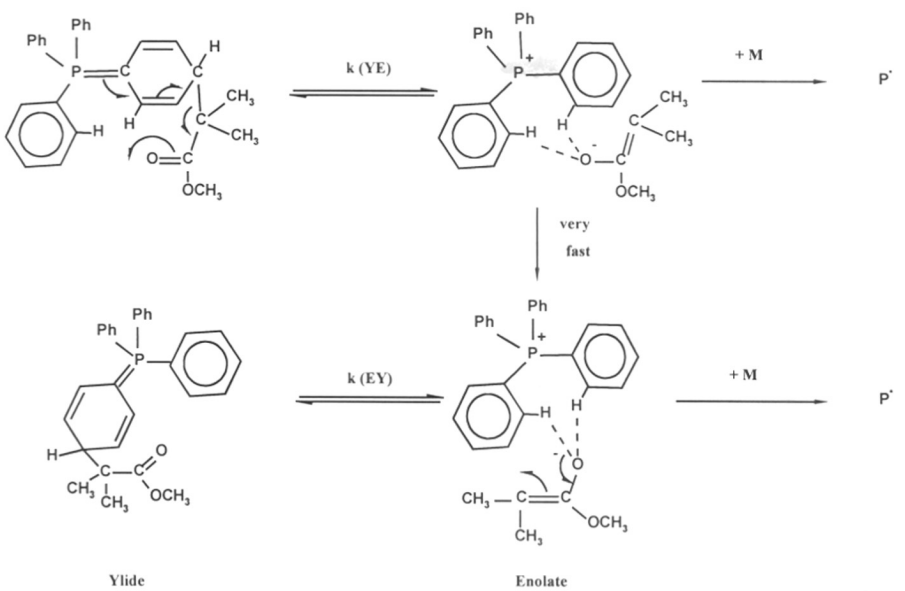

Scheme 6.6: Exchange of ylide MIB group via ion pair

The presence of equilibrium between dormant and active species is also confirmed by the kinetic results of MMA polymerization using tetraphenylphosphonium

triphenylmethanide as initiator in THF at temperatures between -20 and +20 °C. The observed polymerization rate constants were found to be one to two orders of magnitude smaller than those expected for the PMMA,PPh_4 enolate that should show a reactivity somewhat smaller than that of the cryptated PMMA,(Na, 222).

The NOE-saturation transfer experiments show a slow rate of exchange of the MIB anion (k_{YE}=0.72s^{-1}). It has been shown that an equilibrium between species of different reactivity should lead to a considerable broadening of the MWD if the rate of interconversion is slow compared to the rate of propagation ($M_w/M_n = 1 + 1/\beta$ where $\beta = k_{YE}/k_{app}$, and $k_{app} = k_p \cdot \alpha \cdot [I]_0$, and α is the fraction of enolate)[46,47,48]. However, the polymer at room temperature has a narrow MWD ($M_w/M_n \leq 1.1$). Considering the model compound exchange rate (k_{YE} = 0.72 s^{-1}) and the apparent rate constant of polymerization (k_{app} = 3.7 s^{-1}) at 20° C, a low value of β = 0.2 is obtained indicating that the resulting PMMA should possess a broad MWD. This contradiction indicates that the exchange rate for the polymer may be higher due to the steric hindrance exerted by the polymer chain compared to that for the model compound. In fact, when using the model compound, **4/6** as an initiator for MMA polymerization, the reaction proceeds with a large induction period.

A model of the living dimer of tert-butyl methacrylate, di-tert-butyl 2-lithio-2,4,4-trimethylglutarate also gives an ylide compound when treated with tetraphenylphosphonium chloride. However, in NOE experiments the ylide resulting from the dimeric model compound shows only small negative signals of phenyls as a result of saturation transfer. These lower negative signals indicate a less pronounced exchange due to the lower nucleophilicity of the dimeric enolate anion.

6.4 Conclusion

The anionic polymerizaion of methyl methacrylate using tetraphenylphosphonium triphenylmethanide as an initiator proceeds in a living manner even at room temperature. The polymerization follows first-order kinetics with respect to monomer conversion and shows a linear dependence of the number average degree of polymerization on conversion with high initiator efficiencies and

narrow molecular weight distributions ($M_w/M_n < 1.1$). The rate constant depends on the active centre concentration indicating the coexistence of ion pair and free ions and are one to two orders of magnitude smaller than those expected for tetraphenylphosphonium cation. This conforms the presence of large mount of dormant species during polymerization.

Proton, ^{13}C, and ^{31}P NMR of the product of the metathesis reaction between isobutyrate ester enolates and tetraphenylphosphonium chloride in THF indicate the formation of cyclohexadiene phosphor ylide through addition of the ester enolate to one of the phenyl rings. The expected tetraphenylphosphonium enolates are only found in minor quantities (ca. 10 %). Proton NOE emasurements point to the exchange of isobutyrate groups between the phenyl groups which indicates a dynamic equilibrium between the ylide and enolate structures .

The α-phosphonium isobutyrates are models for the chain ends in the anionic polymerizaion of methyl methacrylate in which the enolate and ylide are the propagating and dormant species, respectively.

6.5 References

1. Müller, A. H. E: in *Comprehensive polymer science,* Vol. 3; Allen, G.; Bevington, J. C., Ed., Pergamon, Oxford, **1988**, p387.
2. Warmkessel, J.; Kim, J.; Quirk, R.; Brittain, W. *Polym. Prep. (Am. Chem. Soc., Div. Polym.Chem.* **1994**, 35, 589.*Macromolecules,*
3. Kundel, D.; Müller, A. H. E.; Lochmann, L.; Janata, M. *Makromol. Chem., Macromol. Symp.***1992**, 60, 315.
4. Varshney, S. K.; Jerome, R.; Bayard, P.; Jacobs, C.; Fayt, R.; Teyssie, Ph., *Macromolecules,* **1992**, 25, 4457.
5. Johann, C.; Müller, A. H. E. *Makromol. Chem., Rapid Commun.,* **1981**, 2, 687.
6. Gia, H-B.; McGrath, J. E.; in: *Recent Advances in Anionic Polymerization;* Hogen-Esch, T.; Smid, J., Ed., Elsevier, New York, **1987**, p.173.
7. Lochmann, L.; Kolarik, J.; Doskocilova, D.; Vozka, S.; Trekoval, J. *J. Polym. Sci. Polym. Chem. Ed.* **1979**, 17, 1727.
8. Lochmann, L.; Müller, A. H. E.; *Prepr., IUPAC Intl. Symp. on Macromol.,* Merseburg, Vol. 1, **1987**, 78.
9. Vershney, S. K.; Hautekeer, J. P.; Fayt, R.; Jerome, R.; Teyssie, P. *Macromolecules,* **1990**, 23, 2618.
10. (a) Wang, J. S.; Jerome, R.; Bayard, Ph.; Patin, M.; Teyssie, Ph..; Vuillemin, B.; Heim, Ph. *Macromolecules,* **1994**, 27, 4635. (b) Wang, J. S.; Bayard, Ph.; Jerome, R.; Varshney, S. K.; Teyssie, Ph. *Macromolecules,* **1994**, 27, 4890.

11. Haddleton, D. M.; Muir, A. V. G.; O'Donnell, J. P.; Richards, S. N.; Twose, D. L. *Makromol. Chem., Macromol. Symp.* **1995**, 91, 91

12. Reetz, M. T.; Ostarek, R. J.; *J. Chem. Soc., Chem. Commun.*, **1988**, 213.

13. Reetz, M. T. *Angew. Chem.* **1988**, 100, 1026.

14. Webster, O.W.; Hertler, W. R.; Sogah, D. Y.; Farnham, W. B.; Rajan Babu, T. V. *J. Am. Chem. Soc.*, **1983**, 105, 5706.

15. (a) Sivaram, S.; Dhal, P. K.; Kashikar, S. P.; Khisti, R. S.; Shinde, B. M.; Baskaran, D. *Macromolecules,* **1991**, 24, 1698. (b) Raj, D. J. A.; Wadgaonkar, P. P.; Sivaram, S. *Macromolecules,* **1992**, 25, 2774.

16. Details are given in Chapter 7 of this thesis.

17. Janata, M.; Müller, A. H. E. unpublished results

18. Quirk, R. P. and Bidinger, G. P. *Polym. Bull.* **1989**, 22, 63.

19. (a) Zagala, A. P., Ph.D-Thesis (1996), University of Southern California, Los Angeles, USA. b) Zagala, A. P., Hogen-Esch,T.E, .*Macromolecules,* **1996**, 29, 3038

20. Lohr, G.; Schmitt, B. J.; Schulz, G. V. *Z. Phys. Chem. (Frankfurt am Main), 1972, 78, 177.*

21. Kinetic experiments show presence of termination reaction as the first-order time conversion plots have different slopes (downward curvature). The presence of cyclic β-keto ester product is evidenced by MALDI-TOF spectrum. Baskaran, D.; Müller A. H. E. unpublished results.

22. Initial kinetic experiments were carried out in stirred-tank reactor (capable of mixing reagents <2s) and samples were taken after 3 sec with three seconds interval up to 15 sec. The maroon color of the initiator changed immediately to ogange-red after mixing with MMA solution. The conversion after 3 sec was found to be 100 %.The obtained PMMA had broad MWD.

23. Müller A. H. E.; Zhuang, R.; Yan, D. Y.; Litvinenko, G. *Macromolecules,* **1995**, 28,4326.

24. Jeuck, H.; Müller, A. H. E.; *Makromol. Chem., Rapid Commun.*, **1982**, 3, 121

25. Yakimanski, A.; Müller, A. H. E.; Weiss, H. in preparation (1996)

26. Fuoss, R. M. *J. Am. Chem. Soc.*, **1958**, 80, 5059.

27. Lochmann, L.; Lím, D. J. Organomet. Chem. 1973, 50, 9

28. Lochmann, L.; Rodová, M.; Petránek, J.; Lím, D. *J. Polym. Sci., Polym. Chem. Ed.* **1974**, 12, 2295

29. Lochmann, L.;Trekoval, J. *J. Organomet. Chem.* **1975**, 99, 329

30. Vancea, L.; Bywater, S. *Macromolecules* **1981**, 14, 1776

31. Vancea, L.; Bywater, S. *Macromolecules* **1981**, 14, 1321

32. Seebach, D. *Angew. Chem.* **1988**, 100, 1685

33. Boche, G.; Harms, K.; Marsch, M. *Makromol. Chem., Macromol. Symp.* **1993**, 67, 97

34. Wang, J.S.;Jérôme, R.;Warin, R.;Teyssié, P. *Macromolecules* **1993**, 26, 1402

35. Wang, J.S.;Jérôme, R.;Warin, R.;Zhang, H.;Teyssié *Macromolecules* **1994**, 27, 3376

36. Oki,M.;Nakanishi,H. *Bull. Chem. Soc. Jpn.* **1970**, 43, 2558

37. House,H.O.;Prabhu,A.V.;Phillips,W.V. *J. Org. Chem.* **1976**, 41, 1209

38. Albrigt,T.;Freeman,W.;Schweizer,E. *J. Am. Chem. Soc.* **1975**, 97, 940

39. Simons,W.: "*The Sadtler Guide to Carbon-13 NMR Spectra*", Sadtler Reaserch Laboratories, Philadelphia 1983
40. Tebby.J: "*CRC Handbook of Phosphorousus-31 Nuclear Magnetic Resonance Data*", CRC Press, Boston 1991
41. Ramirez,F.;Rhum,D.;Smith,C. *Tetrahedron* **1965**, 21, 1941
42. Gray, G. *J. Am. Chem. Soc* **1973**, 95, 5092
43. Gray, G. *J. Am. Chem. Soc.* 1973, 95, 7736
44. Betes,R.;Brenner,S.;Cole,C.;Davidson,E.;Forsythe,G.;McCombs,D.;Roth,A. *J. Am. Chem. Soc* **1973**, 95, 926
45. Yakimanski, A.;Müller, A.H.E.;Weiss, H. in preparation
46. Figini, R. V. *Makromol. Chem.* **1964**, 71, 193
47. Figini, R. V. *Makromol. Chem.* **1967**, 107, 170
48. Müller, A.H.E.;Zhuang,R.;Yan,D.Y.;Litvinenko,G. *Macromolecules* **1995**, 28, 4326

7.1 Introduction

The properties of alkyl (meth)acrylate polymers can be tailored for a specific application by controlling their molecular weight, molecular weight distribution, stereochemistry, chain-end functionalization as well as through block copolymer formation with other monomers. Although variety of strategies are available to tailor the physical and chemical properties of acrylic polymers, the anionic polymerization is the methodology most suited for this task.

The controlled anionic polymerization of acrylic monomers is rendered difficult due to the presence of ester group which lead to side reactions with initiator as well as propagating chain-ends[1]. However, several new methods for living anionic polymerization of alkyl (meth)acrylates have been recently reported in literature[2]. The first significant break-through in this area came from Webster and co-workers[3] at Dupont who introduced the Group Transfer Polymerization (GTP) technique. Using silyl ketene acetals as initiator and nucleophile/Lewis acid as catalysts, GTP provides living polymerization of methacrylic acid esters at room temperature. Subsequently, several other initiating systems have been shown to give a controlled polymerization of methacrylic esters at ambient temperature. They include metal-free anions[4], ligand-modified classical anions[5], transition metal containing initiators[6] and aluminum coordinated initiating systems[7].

The metal-free initiators are of great interest owing to their low cost as well as their ability to polymerize primary acrylates at room temperature. Hence, metal-free anionic polymerization offers the potential of an industrially viable method for large scale production of alkyl(meth)acrylate polymers with well-defined molecular properties. Reetz and co-workers[4] used, for the first time, metal-free carbon or nitrogen nucleophiles as initiator for controlled anionic polymerization of n-butylacrylate. They used resonance stabilized malonate derivatives as nucleophile with tetra-n-butylammonium as counterion and synthesized poly (n-butylacrylate) of relatively narrow molecular weight distribution at room temperature. Using this

strategy, several functional metal-free initiators consisting of tetra-n-butylammonium salt of oxazoline, malonate were prepared by us and used for the polymerization of alkyl acrylates[8]. It was found that the polymerization of alkyl acrylates using tetrabutylammonium salts proceeds with a characteristic induction period and often results in a higher number-average molecular weight (M_n) than theoretically calculated M_n from feed ratios of monomer to initiator. Preliminary kinetic results confirmed that these polymerization have a considerable induction period, exhibit non-linear time-conversion plots, and broader MWD's than reported before[9].

Quirk et al[10] used Bu_4N^+ salt of 9-methylfluorene as an initiator for the polymerization of MMA in THF at ambient temperature. At very low initiator concentration, Quirk et al obtained PMMA of broad MWD (M_w/M_n = 2.16) in low yield (24 %). Reetz et al[11] observed a slow initiation of MMA at high concentration of Bu_4N^+ salt of 9-ethylfluorene as initiator at room temperature. The reason for a slow initiation was attributed to aggregation as well as steric shielding of bulky non-metal cation. Recently, Zagala and Hogen-Esch[12] have reported the use of tetraphenylphosphonium cation in the anionic polymerization of MMA in THF. As seen in previous chapter, the detailed NMR studies of a model compound, i.e. enolate (methyl isobutyrate) anion with tetraphenylphosphonium counterion, suggested that the propagating enolates are in equilibrium with dormant phosphorous ylide intermediate[13]. The kinetic results also support the existence of such an equilibrium in the anionic polymerization of MMA in presence of tetraphenylphosphonium counterion in THF[14].

Several intriguing observations, such as, unreacted residual initiator, broad and bimodal molecular weight distributions of the obtained polymer and inconsistent initiator efficiency ($0.2 < f > 1$) are generally associated with metal-free anionic polymerization, thus rendering control of the polymerization rather difficult. This chapter discusses the result of metal-free anionic polymerization of alkyl (meth)acrylates using initiators (Scheme 7.1) containing tetrabutylammonium and tetramethyldiethylguanidinium counter cations in THF.

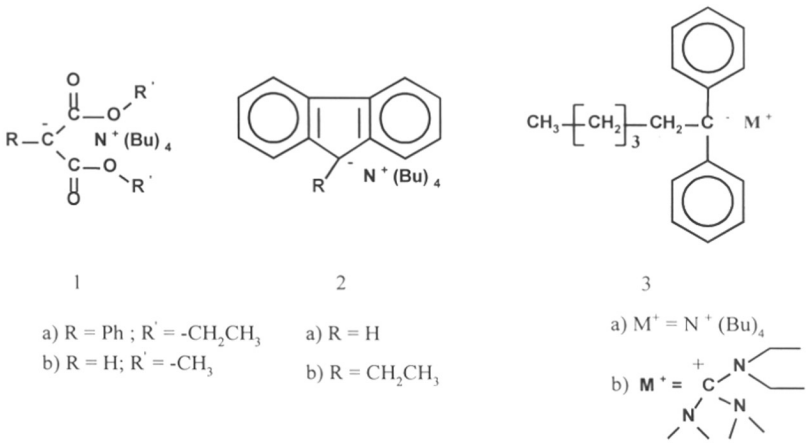

Scheme 7.1: Metal-free anionic initiator used for alkyl (meth)acrylate polymerization

7.2 Experimental Section

7.2.1 Reagents

Methyl methacrylate(MMA, Aldrich), methylacrylate (MA, Aldrich), n-butylacrylate (nBA, Aldrich) and tert-butylacrylate (tBA, Aldrich) were purified as described in Chapter 2. Diethylphenylmalonate (DEPM, Aldrich) and Dimethylmalonate (DMM, Ardrich) were used as received. Fluorene (Fl , Merck, Bombay) was recrystallized in dry n-hexane or THF). 9-ethylfluorene (9EFl, Fluka) was distilled under high vacuum and stored in refrigerator. Tetrahydrofuran (THF, SD fine chemicals, Bombay) was purified as described in Chapter 2. Diethylamine (Fluka), dichlorethane (Aldrich) were distilled over CaH_2. N,N,N',N'-tetramethylurea (Fluka) and oxalyldichloride(Aldrich) were used as received without any further purification. n-BuLi (1.6 M in hexane, Aldrich) was used after determining its actual concentration by double titration. Diphenylethylene (DPE, Aldrich) was titrated with a small amount of n-BuLi and distilled under high vacuum.

Tetra-n-butylammonium hydroxide (TBAOH, 20 % solution in toluene/methanol, SD fine chemicals, Bombay) was used as received after determining its concentration by titration against standard acid solution. Tetra-n-butylammonium chloride (TBACl,

Fluka-USA) was twice recrystallized in THF and dried under dynamic high vacuum for 2 days and stored at room temperature in a Glove-Box. Tetramethyldiethylguanidinium chloride (QC) was synthesized in THF by reacting N,N,N',N'-tetramethylchloroformamidinium chloride with diethylamine as reported in literature[15]. N,N,N',N'-tetramethylchloroformamidinium chloride was prepared by the reaction of N,N,N',N'-tetramethylurea and oxalyldichloride in 1,2-dichloroethane as reported in literature[16]. The pale yellow crystals of QC was found to be insoluble in THF. Fig. 7.1 shows the ^{13}C NMR of QC in $CDCl_3$(100 Mhz, ppm); 11.14 (N-CH_2-CH_3), 38.47 (N-CH_3), 41.74 (N-CH_2-) and 160.8 (C^+, cation).

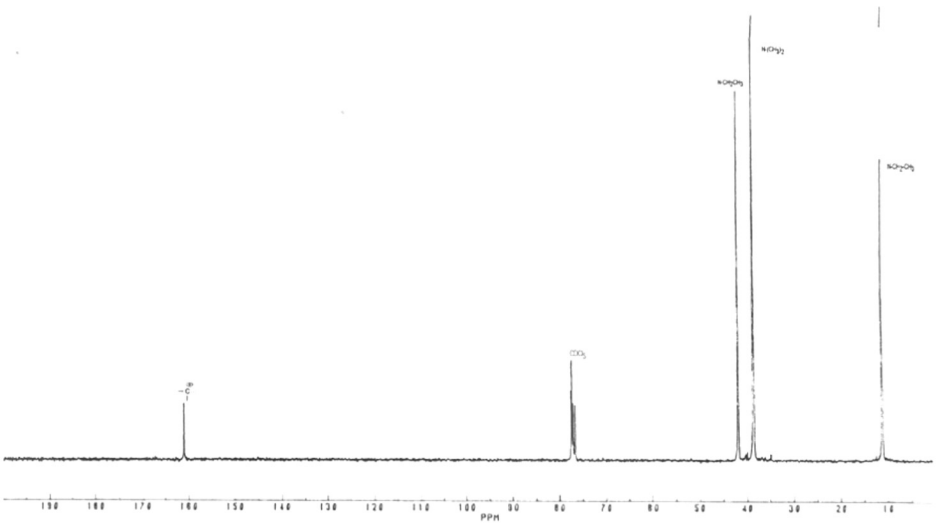

Fig. 7.1: ^{13}C NMR of tetramethyldiethylguanidinium chloride in $CDCl_3$ at 30°C.

7.2.1.1 Initiators

1,1'-Diphenylhexyllithium (DPHLi) initiator was prepared by reacting a known amount of n-BuLi with a slight excess of DPE in THF at -40 °C. Fluourenylpotassium and 9-ethyllfluorenylpotassium were prepared by metalation reaction with potassium mirror in THF under vacuum. The concentration of these initiators was determined by Gilman's double titration method (Chapter 2). Tetrabutylammonium salts of diethylphenylmalonate, dimethylmalonate and fluorene were prepared by deprotonation with Bu_4NOH (TBAOH) as described below:

Dry toluene (50 mL) was transferred into a flame-dried 100 mL round bottom flask under a positive nitrogen pressure using stainless steel cannula. To this flask was added 10 mL of 8.16 mmol of TBAOH in methanol/toluene solvent mixture. While preparing malonate salt having ethoxy ester group such as diethylphenylmanolate, methanol from the TBAOH solution was replaced by adding 10 mL portion of ethanol and distilling slowly methanol as much as possible. This procedure was repeated twice. Then, equimolar amount of desired CH-acid compound (neat or in toluene solution) was added into TBAOH solution. The reaction mixture was stirred for 15 minutes at room temperature. In case of diethylphenylmalonate or dimethylmalonate, no change in color was noticed whereas, in case of fluorene light saffron color developed indicating the formation of anion. Toluene was distilled to one-half of its original volume slowly under vacuum in order to remove water azeotropically at room temperature. It is important to keep the substances in solution during azeotropic distillation.

In order to drive the reaction to completion, 45 mL of dry toluene was added twice and distilled slowly under vacuum. Finally, all the toluene was removed to dryness. Initiators obtained as pale crystals of tetrabutylammonium diethylphenylmalonate (**1a**), white crystals of tetrabutylammonium dimethylmalonate (**1b**) and dark orange crystals of tetrabutylammonium fluorenide (**2a**) were washed 3 to 4 times with 20 mL of dry n-hexane to remove excess or unreacted CH-acid compound. The initiators were characterized by NMR (Fig. 7.2 and 7.3) and stored under N_2 in refrigerator. The initiators were dissolved in known amount of THF and the concentration was determined by hydrolyzing with excess standard HCl acid of known concentrations and back titration of residual HCl with standard NaOH solution using phenolphthalein as indicator.

Tetrabutylammonium diethylphenylmalonate (**1a**): pale crystals; ^{1}H NMR (300 MHz, DMSO-D_6) δ ; 1.0 (t, N-$CH_2CH_2CH_2CH_3$), 1.5 (m, N-$CH_2CH_2CH_2$-), 1.7 (m, N-CH_2CH_2-), 3.4 (m, N-CH_2-), 4.2 (q, -O-CH_2-), 1.25 (t, -O-CH_2CH_3), and 7.4 (m, phenyls). ^{13}C NMR (75.5 MHz, in THF) ppm; 13.8 (N-$CH_2CH_2CH_2CH_3$), 23.1 (N-$CH_2CH_2CH_2$-), 27.1 (N-CH_2CH_2-), 61.5 (N-CH_2-), 81.1 (C$^-$ anion), 171.5 (C=O), 59.2 (-O-CH_2-), 19.2 (-O-CH_2CH_3), phenyl carbons 148.4, 129.4, 135.6, 123.8 ppm.

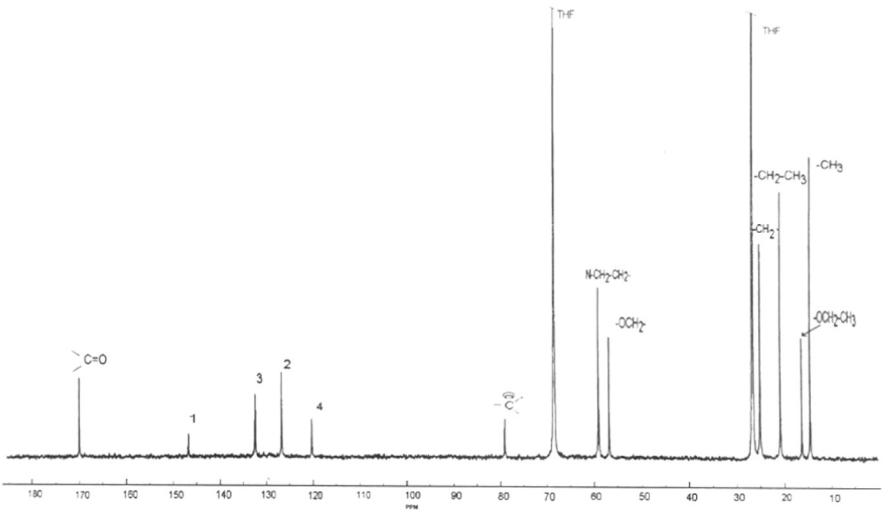

Fig 7.2: ^{13}C NMR of tetrabutylammonium diethylphenylmalonate, **2a** in THF at 30 °C. The initiator was prepared by deprotonation method.

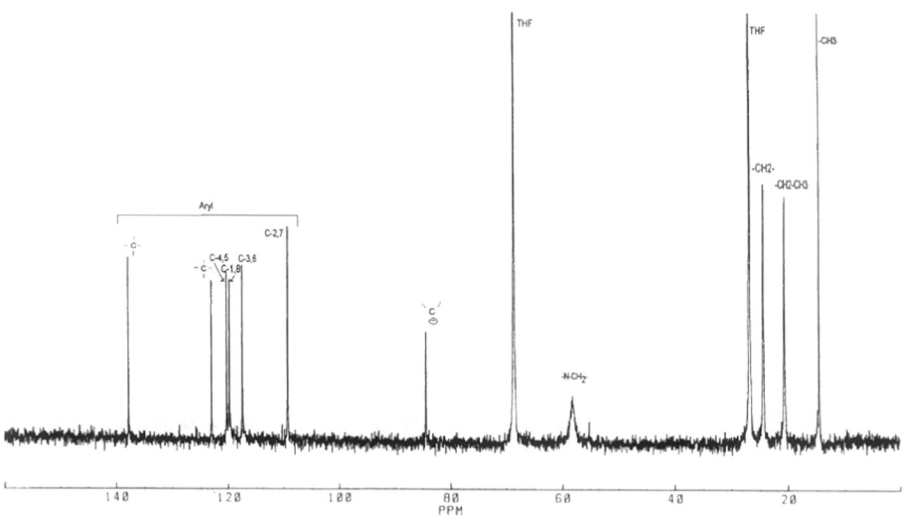

Fig. 7.3: ^{13}C NMR of tetrabutylammoniumfluorenide salt, **2a** in THF prepared by deprotonation method.

Tetrabutylammonium fluorenide (**2a**): dark-orange crystals; ^{1}H NMR (300 MHz, DMSO-D_6) δ ; 0.98 (t, N-$CH_2CH_2CH_2CH_3$), 1.49 (m, N-$CH_2CH_2CH_2$-), 1.7 (m, N-CH_2CH_2-), 3.5 (m, N-

CH_2-), 5.82 (s, CH⁻ anion), 6.38 (t, aryl H-2,7), 6.78 (t, aryl H-3,6), 7.18 (d, aryl H-1,8), 7.78 (d, aryl H-4,5). ^{13}C NMR (75.5 MHz, in THF) PPM; 14.5 (N-$CH_2CH_2CH_2CH_3$), 20.6 (N-$CH_2CH_2CH_2$-), 24.4 (N-CH_2CH_2-), 58.2 (N-CH_2-), 84.4 (CH⁻ anion), 122.9 (C), 119.76 (C-1,8), 109.25 (C-2,7), 117.42 (C-3,6), 120.23 (C-4,5) and 137.7 (C).

Tetrabutylammonium salts of 1,1'-diphenylhexane (DPHTBA), fluorene (FlTBA), and 9-methylfluorene (9MFlTBA) were prepared by reacting its precursor metal salts with dry tetrabutylammonium chloride in THF at low -40 °C. Similarly tetramethyldiethylguanidinium salts of 1.1'-diphenylhexane was prepared by reacting DPHLi with tetramethyldiethylguanidinium chloride (QC). The red color of DPHLi anion changed into maroon color upon reaction with THF solution containing TBACl and to wine-red color upon reaction with tetramethyldiethylguanidinium chloride at -40 °C indicating the exchange of cations from Li^+ to TBA and QC respectively.

7.2.2 Polymerization of Alkyl (meth)acrylates

Batch polymerization was carried out in a flamed glass reactor under pure nitrogen atmosphere as described in Chapter 2. The solvent, initiator solution in THF, and the monomer were transferred by capillary technique or syringe. Required amount of initiator solution in THF was added into the reactor containing 35 mL (or 70 mL) of THF. The purified alkyl (meth)acrylate neat or diluted in THF (1:2 v/v) was added to the initiator solution slowly (1 mL per min) at 30 °C. After 3-5 mins of monomer addition, reaction temperature increased by 10-15 °C. In all cases, the initiator color did not disappear completely and persisted throughout the polymerization. At high concentration of initiator, the reaction mixture was characterized by a pale yellow color for initiator 1a, an orange color for **2a**, slight maroon color for **3a** and slight wine-red color for **3b**. Reaction was terminated after 15 mins and in some cases 2 mins with methanol containing small amount of dil HCl. The residual initiator color disappeared upon addition of termination agent.

Poly (methyl acrylate) (PMA), Poly (n-butylacrylate) (PnBA), Poly (tert-butylacrylate) (PtBA) were recovered by evaporating THF and extracting the polymers in ether. The ether layer was washed twice with small amount of water, once with $NaHCO_3$ solution followed by NaCl solution. Ether layer was then dried by anhydrous $MgSO_4$ and filtered. After evaporating the solvent in roto-evaporator, the polymers (PMA,

PnBA, PtBA) were dried in high vacuum for 3 hours. Poly (methyl methacrylate) (PMMA) was recovered by precipitation in n-hexane and dried under vacuum at 60 ^{0}C for 4 h.Characterization of polymers were carried out by using a Waters GPC 150C equipped with two μ-ultrastyragel linear columns and THF as the eluent at a flow rate of 1 mL min^{-1} at 30 ° C. Standard monodisperse poly(methyl methacrylate)s (Polymer Laboratory) were used for calibration. NMR was recorded on a Bruker 300 MHz Spectrometer using D_2O as internal lock.

7.3 Result and Discussion

7.3.1 Polymerization of Alkyl Acrylates Using Tetrabutylammonium Diethylphenylmalonate Salt

Anionic polymerization of methyacrylate, n-butylacrylate and tert-butylacrylate was performed using tetrabutylammonium diethylphenylmalonate salt (**1a**) and dimethylmalonate salt (**1b**) in THF at 0 °C - 30 °C (Table 7.1). Diluted monomer was added drop by drop to a pale-yellow colored initiator solution. In all cases, after 2-5 min of diluted monomer addition, temperature rose to 40 °C to 45 °C depending on the initiator concentration indicating the presence of considerable induction period. A faint pale-yellow color of the initiator was visible even after complete monomer addition which persisted throughout the polymerization and disappeared only on termination using methanol containing small amount of diluted HCl.

The obtained poly (methacrylate) (PMA), poly (n-butylacrylate)(PnBA) and poly (tert-butylacrylate) (PtBA) are characterized by broad molecular weight distribution. PMA possess very high polydispersity index and lower number average molecular weight (M_n) than the M_n calculated from the feed ratio of moles of monomer and initiator. This indicates the presence of several other secondary reactions leading to loss of control during polymerization.

Table 7.1: Anionic polymerization of acrylate monomers using tetrabutylammonium salt of diethylphenylmalonate(TBADEPM) in THF [a].

Run	Monomer	$[I]_0$ mol/L	$[M]_0$ mol/L	T °C	Yield %	$M_{n,cal}$ [b]	$M_{n,SEC}$ [c]	M_w/M_n [d]
1	MA	8.44	2.00	0	95	20,000	4,000	3.7
2	MA	8.66	1.76	0	85	17,000	3,300	3.7
3	nBA	7.08	1.16	30	92	21,000	23,700	2.73[e]
4	nBA	19.13	11.63	0	96	7,800	8,900	3.36[e]
5	tBA	11.60	0.725	0	96	8,300	38,300	1.69
6	tBA	65.00	1.078	30	100	2,100	6,800	1.76
7	tBA	137.20	1.896	30	95	1,770	7,000	1.62

a) Diluted monomer in THF solution (1:2 v/v) was added drop by drop. After 2-5 mins of induction period, strong rise in temperature (10-15 °C) was noticed in all cases. b) $M_{n,cal}$ = (grams of monomer /moles of initiator). c) obtained using SEC calibrated with standard PMMA. d) broad MWD. e) bi-modal distribution having a shoulder at peak maximum.

In case of PnBA and PtBA, higher number average molecular weight were obtained with lower initiator efficiencies ($0.88 > f > 0.21$). PtBA has comparatively narrow molecular weight distribution ($M_w/M_n = 1.61$) where as PnBA showed a bi-modal distribution (Fig 7.4).

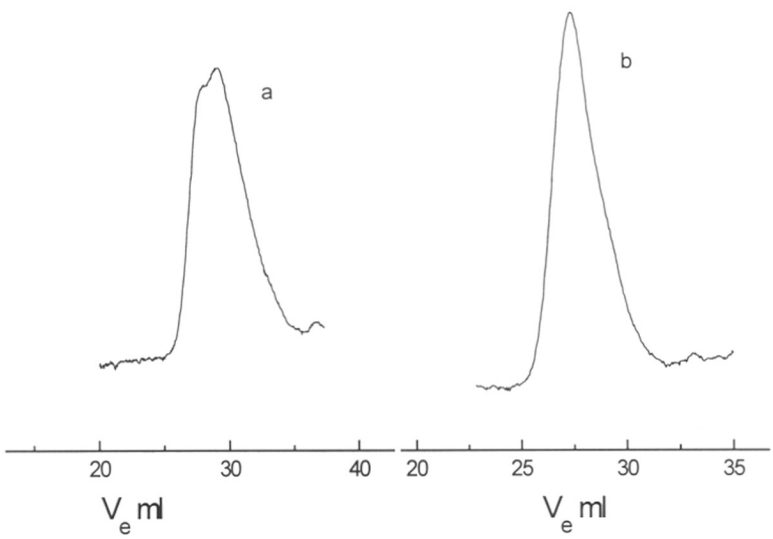

Fig: 7.4: SEC elugrams of polyacrylates synthesized using tetrabutylammonium diethylphenylmalonate, **1a**, as initiated in THF at 30 °C. a) poly (n-butylacrylate), $M_{n,SEC} = 23,700$, $M_w/M_n = 2.73$ and b) poly (tert-butylacrylate), $M_{n,SEC} = 38,300$, $M_w/M_n = 1.69$.

A shoulder at peak maximum were noticed in the SEC elugrams of PnBA. The higher reactivity of tBA and the better stabilization of propagating anion of tBA may be responsible for the observed narrow molecular weight distribution. It is clear from the results that the polymerization of alkyl acrylate using **1a** is uncontrollable and leads to polymer with broad molecular weight distribution with low initiator efficiency.

7.3.2 Polymerization of MMA in Presence of Tetrabutylammonium Counterion

Metal-free anionic polymerization of MMA was performed using tetrabutylammonium fluorenyl (**2a**) and 9-ethylfluorenyl (**2b**) as initiators in THF at 30 °C and the results are shown in Table 7.2. Diluted monomer was added drop by drop to the orange colored initiator solution. The polymerization is characterized by an orange color persisting after initiation indicating incomplete initiation. The appearance of residual initiator color during the polymerization strongly depends on the initiator/monomer concentration.

Table 7.2: Metal-free anionic polymerization of MMA using tetrabutylammonium salts of fluorenide and 9-ethylfluorenide as initiator in THF at 30 °C[a].

Run	$[I]_0$ mol/L	$[M]_0$ mol/L	Yield %	$M_{n,cal}$ [b]	$M_{n,SEC}$ [c]	$M_{w,SEC}$	M_w/M_n [d]	f [e]
Initiator, **2a**, tetrabutylammonium fluorenide								
1[f]	13.80	0.790	100	5,700	4,350	6,280	1.44	1.34
2	10.76	0.659	100	6,100	4,140	5,483	1.32	1.49
3	5.67	0.688	100	12,200	7,060	10,250	1.45	1.72
4	3.80	0.688	100	18,400	10,240	15,470	1.42	1.80
5	12.70	0.766	97	6,000	4,240	6,040	1.42	1.42
Initiator, **2b**, tetrabutylammonium 9-ethylfluorenide								
6	10.00	0.685	96	6,360	6,900	25,410	bimodal	0.92
7	5.50	1.170	>95	21,270	13,470	70,050	bimodal	1.57
8	1.76	0.187	>95	10,640	16,050	23,730	1.47	0.66
9	1.87	0.149	80	11,360	12,240	24,210	1.97	0.92
10	10.20	0.163	100	1,590	5,760	11,170	1.94	0.27
11	2.75	0.425	>95	15,455	20,090	54,340	2.70	0.76

a) Diluted monomer in THF solution (1:2 v/v) was added drop by drop, 1ml/min. After 2-5 mins of induction period, strong rise in temperature (10-15 °C) was noticed in all cases. Residual initiator color persisted throughout the polymerization using 2a. b) $M_{n,cal}$ = (grams of monomer /moles of initiator). c) obtained using SEC calibrated with standard PMMA. d) broad MWD. e) initiator efficiency, $f = M_{n,cal}/M_{n,SEC}$. f) initiator prepared by deprotonation method using TBAOH.

At high initiator concentration the residual initiator color persisted even after complete monomer addition (Table 7.2, run 1-5 using **2a**). Experiments carried out using low initiator concentration of **2b** showed that the color of initiator solution changed slowly to colorless upon addition of MMA after 5 min (Table 7.2, run 7, 8 and 11). In all cases, yields were quantitative except in few runs using **2b** as initiator. However, there was no control on molecular weight. UV quantitation of PMMA prepared using **2a** as initiator indicated much less fluorene present as end group than was used for initiation of polymerization. The number average molecular weights obtained were much less than could be accounted for by the fluorene head groups. This may be due to the formation of other initiating species via back-biting reaction or transfer reactions during the polymerization.

^{1}H NMR of soxhlet extracted PMMA samples obtained using initiator **2a** have additional methoxy signal indicating the formation of Bu_4NOMe. The presence of residual initiator indicates that the attack of initiator to the carbonyl groups may be assumed to be less significant. The methoxide elimination reaction may have resulted from the attack of propagating species on the carbonyl groups of monomer or polymer. It appears that the reactivity of a enolate with non-metal counter cation is much higher than the initiator 1 and 2.

The fast polymerization of MMA is seen during the addition of diluted MMA to THF containing initiator, **2b** at higher concentration (10^{-2} mol/l, Table 7.2, run 10). Addition of a drop of diluted MMA resulted fast local polymerization leading to a high molecular weight PMMA which eventually precipitates and slowly re-dissolves into the polymerization mixture. The polymers obtained using initiator, **2b** have a higher number average molecular weight than the calculated ones. The obtained PMMAs possesses a bimodal or broad molecular weight distribution exhibiting either low or high molecular weight tailings (Fig. 7.5).

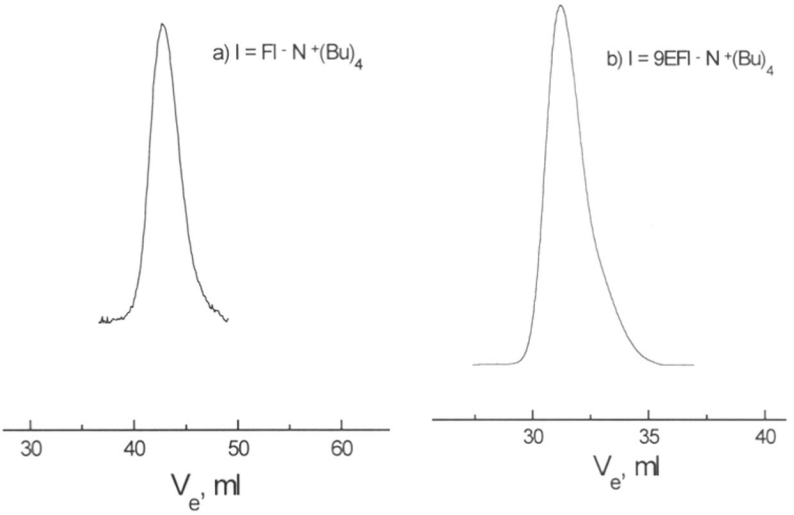

Fig. 7.5: SEC elugrams of PMMA synthesized in THF at 30 °C a) using **2a**, $M_{n,SEC}$ = 4140, M_w/M_n = 1.32 and b) using **2b**, $M_{n,SEC}$ = 16,050 M_w/M_n = 1.47.

In order to confirm the presence of residual initiator, Michael adduct of **2b** and MMA was preformed and the reaction mixture was analyzed by UV/Vis spectrum before and after MMA addition. Absorption of initiator solution before mixing with MMA was considered as zero time intensity. A solution of MMA ($1.17 \cdot 10^{-2}$ mol/l) was added to THF containing, **2b** ($1.1 \cdot 10^{-2}$ mol/l) within 2 sec using nitrogen pressure at 30 °C and the reaction solution was characterized by UV/Vis spectrum with time.

The UV/Vis spectrum of the initiator solution showed broad absorption bands at 376 nm and 512.7 nm in visible region. Fig.7.6 shows a plot of intensity of absorption bands of **2b** in presence of MMA with time. After an initial decrease, no appreciable change in the intensities of these absorption bands are noticed (even after 30 mins). This observation is also consistent with the results obtained by Reetz and co-workers[11] who noticed the persistence of initiator color during polymerization. A slow initiation was considered responsible for the presence of initiator color during polymerization. This confirms that initiation is incomplete and thus raises many questions on the effect of non-metal cation on the initiation process in anionic polymerization.

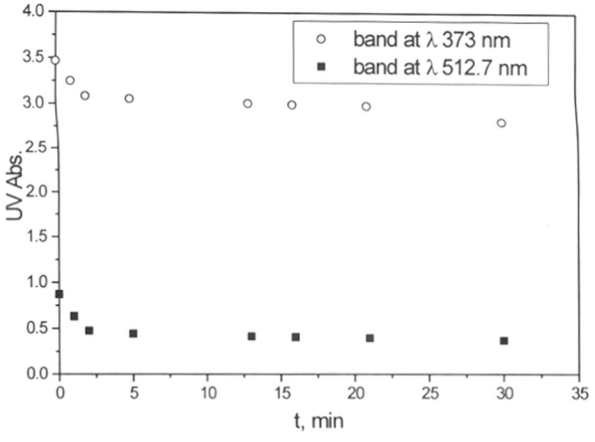

Fig 7.6: Change in intensity of absorption bands of initiator **2b** after mixing with MMA.

7.3.3 The Effect of Counter Cations on the Polymerization of MMA in THF

Anionic polymerization of MMA was performed in presence of tetrabutylammonium, tetramethyldiethylguanidinium and lithium counterion using 1,1'-diphenylhexyl anion as initiator. The initiators were prepared *insitu* by reacting lithium salt of the precursor anion with the THF solution of the corresponding non-metal chlorides at -40 °C as well as at 30 °C. The cation exchange reaction was carried out at 30 °C and showed an immediate disappearance of the color of the initiator, **3a** (maroon) and **3b** (wine-red) whereas at -40 °C the intensity of the initiator color did not change in both the cases. This indicates that the stability of these initiators are very low at higher temperature, probably as a result of Hoffmann elimination. Hence, polymerization was carried out at -40 °C. Polymerization of MMA was done by adding neat MMA into initiator solution at -40 °C. The color of the initiators did not disappear completely even after the complete monomer addition. A slight initiator color persisted throughout the polymerization which disappeared only upon addition of CH_3OH after 2 min. Quantitative conversion (>95 %) was obtained after 2 min indicating fast polymerization in presence of non-metal counterions. The results of the polymerization are given in Table 7.3. Reactions were terminated within 1-2 min.

Table 7.3: Anionic polymerization of MMA[a] using 1,1-diphenylhexyl anion with tetrabutylammonium and tetramethyldiethyl guanidinium as counter ions in THF at -40 °C.

Run	[I] x10^3 mol/l	[M] mol/l	Yield %	$M_{n,cal}$	$M_{n,SEC}$	$M_{w,SEC}$	M_w/M_n [b]	f [c]
Diphenylhexyl tetra-n-butylammonium (**3a**) initiator								
1	6.7	0.340	94	5,080	28,901	48,152	1.66	0.17
2	4.5	0.374	>94	8,311	52,539	1,47,921	2.80	0.16
3	4.5	0.748	100	16,647	15,035	29,171	1.94	1.10
4[d]	4.5	0.374	98	8,311	9,597	37,199	3.87	0.86
Diphenylhexylguanidinium (**3b**) initiator								
5	4.5	0.374	100	8,311	11,644	31,757	2.73	0.71
6	9.71	0.802	100	8,262	9,595	27,716	2.88	0.86

a) neat monomer was added with 10-15 sec. Initiator color (very low in intensity) persisted throughout polymerization. Reaction was terminated with in 2 mins.

b) Bimodal distributions with high-molecular weight tailing

c) Initiator efficiency, $f = M_{ncal} / M_{nSEC}$.

d) MMA was added drop by drop for 1-2 mins.

In both the cases, i.e using TBA^+ or Q^+ counterion, the obtained PMMA possess broad/bimodal distribution with higher number average molecular weight than theoretically calculated ones. The initiator efficiencies are low and inconsistent. A slow addition of monomer (drop by drop) did not improve the results and the SEC elugram showed a very broad, bi-modal distribution of equal intensities (Table 7.3, run 4). Almost in all cases, high molecular weight tailing (shoulder) was observed in their respective SEC elugrams. A typical SEC elugrams of PMMA prepared using various counterion at similar experimental conditions are given for comparison in Fig. 7.7. It can be seen that under similar conditions, the use of lithium counterion (DPHLi initiator) resulted PMMA with narrow molecular weight distribution (M_w/M_n = 1.16) at -40 °C in THF.

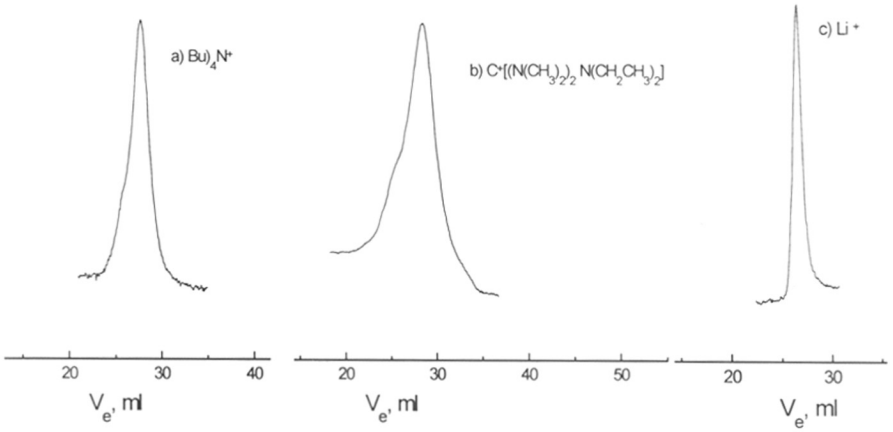

Fig 7.7: SEC elugrams of Polymethylmethacrylate samples synthesized in presence of different countercation in THF at -40 °C. The polymerization of MMA was initiated using 1,1'-diphenylhexyl anion with a) in presence of tetrabutylammonium counterion, b) in presence of tetramethyldiethylguanidinium counterion and c) in presence of lithium counterion.

The observed bimodal distribution and higher number average molecular weight of the polymers (PnBA, PtBA, and PMMA) in presence of ammonium as well as guanidinium cation show the inefficiency of the metal-free anionic polymerization in providing controlled polymerization. Unlike lithium counterion, the residual initiator color was seen in non-metal containing initiating systems depending on the initiator/monomer concentration.

Based on these studies the following observations are note worthy:

1) Persistance of initiator color throughout polymerization indicating incomplete initiation;
2) Quantitative conversion within 2 min indicating a fast polymerization;
3) Bimodal molecular weight distribution of the resulting PMMA as well as poor and inconsistent initiator efficiency.

A possible explanation for the incomplete initiation as well as for lower initiator efficiency comes from the experimental observations that the polymerization is very fast with a characteristic induction period in presence of non-metal counterion. Hence, the course of the polymerization is primarily determined by the rate of mixing (monomer), the apparent rate of initiation and the formation of active centers whose proportions are all set at the initial stages of polymerization.

The slow initiation as well as the presence of induction period (as seen in other initiators, such as, malonate and fluorenyl initiators with TBA^+) can result in an increase in active center concentration during the initial stages of polymerization. This type of situation can also arise when the reactivity and the contribution of contact/solvent separated ion pairs differs to a large extent between the initiator and the propagating anion.

7.3.3.1 Ion-pair Effects in Anionic Polymerization of MMA

The ion-pair effect is the most significant factor in the initiation processes of anionic polymerization. We believe that the main reason for often encountered irreproducibilities in metal-free anionic polymerization is because of the inability to achieve prefect initiation with non-metal necleophiles. This is partly because of the fact that the pK_a values of malonates (~16) and fluorenyls (~23) are lower compared to ester enolate. The pK_a values of ester enolate ($CH_3CO_2CH_2CH_3$) as calculated by Bordwell[19,20] is around 30 to 31. This suggest that the rate of propagation in metal-free anionic polymerization should be greater than the rate of initiation, i.e. $k_p >> k_i$.

Kinetic investigation on the metal-fee anionic polymerization of MMA using tetrakis(-tris-(dimethylamino)-phosphoranylidenamino)-phophonium salt of diphenylhexyl anion at room temperature shows evidences of termination and the obtained PMMA possess broad molecular weight distribution with low initiator efficiency (f = 0.2)[19]. A first-order time conversion plot showed a down-ward curvature indicating the presence of termination. NMR experiments carried out at 30 °C confirm the stability of this initiator for 4 to 5 hours. The plot of number average degree of polymerization, P_n, with converstion, x_p was linear. However, the initiator efficiency, f, was very low (f = 0.20) in all cases irrespective of the initial initiator concentration. Since the experiment was done using flow-tube reactor with shortest mixing time and the stability of the initiator at room temperature is also confirmed by NMR spectroscopy, it appeared that the rest of the initiator is not accounted for the polymerization. Thus, the reactivity of the propagating enolate anion with non-metal counter ion differs considerably from the initiator in terms of charge distribution.

These observation strongly suggest the involvement of cationic charge (as well as size) dependent ion pairing equilibrium in the initiation processes of anionic polymerization of alkyl (meth)acrylate. Chang and Hogen-Esch[20] reported a significant ion-pairing effect on the equilibrium addition of 9-methylfluorenyl (9MeF$^-$ M$^+$) carbanion alkali salts to 1-phenyl-1-(4-pyridyl)ethylene (PPE) in THF using Li^+, Na^+, and Cs^+ as counterions (equation 7.1).

$$9MeF^- M^+ + PPE \underset{THF}{\overset{K}{\rightleftharpoons}} 9MeF\text{-}PPE^- M^+ \qquad (7.1)$$

The nucleophilic addition reaction was characterized using ion-pair equilibrium and dissociation constant. They found that the apparent equilibrium constant K which is equal to $K_{\pm}$ at high concentration of carbanion is strongly dependent on the ionpair dissociation constant of 9-MeF$^-$M$^+$ (K_{d1}) and FPPE$^-$M$^+$ (K_{d2}) as given by the following equation 7.2.

$$K_{\pm} = \frac{K_{d1}}{K_{d2}} \times K_{-} \qquad (7.2)$$

Chang and Hogen-Esch calculated the apparent rate constant, K using the UV/Vis absorption intensity ratios of FPPE- and 9MeF- at different concentrations of PPE. The results obtained showed that the apparent equilibrium constant, K, decreases with increasing cation size. The rate constant of lithium (K_{Li}) is higher than for cesium (K_{Cs}) by a factor of about 13,000 times. Similar ionpairing effects appear to be operative in metal-free anionic polymerization using a bulky non-metal counterion especially such as their aggregation in solution is highly improbable due to larger interionic distances[21]. Hence the equilibrium addition of metal free nucleophiles such as tetrabutylammonium, tetramethyldiethyl guanidinium salts to an acrylate monomer can be analyzed using their ionpairing equilibrium similar to the one reported for 9MeF$^-$ addition to PPE (Scheme 7.2).

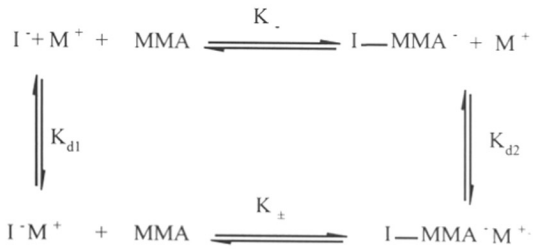

I^- = malonate or fluorenyl or diphenylhexyl anion
$M^+ = N^+(Bu)_4$ or $C^+[(N(CH_3)_2)_2(N(CH_2CH_3)_2)]$

Scheme 7.2: Equilibrium addition of initiator to MMA and their ion-pairing effect

We used higher initiator concentration, 10^{-3} to 10^{-2} M in all the polymerization and hence the degree of dissociation of ionpairs into free ions is negligible. The apparent equilibrium constant, K for the initiation of acrylate monomer follows equation 7.2. Thus, K should strongly depend on the ionpair dissociation constants of propagating metal-free enolate ion pairs.

The apparent equilibrium constant for initiation, K_i, for tetrabutylammonium and guanidinium counterion appears to be very low as one should expect a higher dissociation constant , K_{d2} for bulky non-metal enolate (as it is seen for the other system). The presence of residual initiator in our experiments confirms that the apparent initiation constant is lower compared to propagation. This leads to an incomplete initiation. The broad/bi-modal distribution of the obtained polymers are due to several factors such the competing propagation, inhomogeneous mixing of reagent as well as the presence of induction period. Using lithium as counterion, the equilibrium initiation of MMA is driven to right by the well known electrostatic association of enolate ionpair, MMA^-Li^+ , exhibiting a lower dissociation constant, K_{d2}. Hence, the initiation of MMA polymerization using DPHLi as initiator is faster as the value of K becomes higher compared to other non-metal countion.

7.4 Conclusion

Metal-free anionic polymerization of alkyl (meth)acrylates using tetrabutylammonium as well as tetramethyldiethylguanidinium counterion do not give satisfactory control of molecular weight. The effect of counterion is clearly seen from the result of the polymerization carried out using lithium counterion under identical condition. The inconsistent results such as lower initiator efficiences, broad and bi-modal distribution of the resulting polymers are attributed to the ion-pairing effects on the initiation processes of metal-free anionic polymerization.

7.5 References

1. a) Glusker, D. L.; Galluccis, R. A.; Evans, R. A. *J. Am . Chem. Soc.*, **1964**, 86, 187. b) Schreiber, H. *Makromol. Chem.*, **1956**, 36, 86. c) Kawabata, N.; Tsuruta, T. *Makromol. Chem.* **1965**, 86, 231. d) Fait, B. A., *E. Polym. J.* **167**, 3, 523.
2. Davis, T.; Haddleton, D.; Richards, S. *J. M. S. Rev. Macromol. Chem. Phys.* **1994**, C34, 243.
3. Webster, O.W.; Hertler, W. R.; Sogah, D. Y.; Farnham, W. B.; Rajan Babu, T. V. *J. Am.Chem. Soc.*, **1983**, 105, 5706.
4. a) Reetz, M. T.; Ostarek, R. J. *J. Chem. Soc., Chem. Commun,* **1988**, 213. b) Reetz, M. T. *Angew.Chem.* **1988**, 100, 1026. c) Reetz, M. T.; Hutte, S.; Goddard, R.; Minet, U. *J. Chem. Soc., Chem. Commun.*, **1995**, 275. d) Reetz, M. T.; Hutte, S.; Goddard, R. *Zeitschrift for Naturforschung*, **1995**, 415.
5. a) Varshney, S. K.; Jerome, R.; Bayard, P.; Jacobs, C.; Fayt, R.; Teyssie, Ph., *Macromolecules,* **1992**, 25, 4457. b) Johann, C.; Müller, A. H. E. *Makromol. Chem., Rapid Commun.*, **1981**, 2, 687. c) Gia, H-B.; McGrath, J. E.; in: *Recent Advances in Anionic Polymerization;* Hogen-Esch, T.; Smid, J., Ed., Elsevier, New York, **1987**, p.173. d) Lochmann, L.; Kolarik, J.; Doskocilova, D.; Vozka, S.; Trekoval, J. *J. Polym. Sci. Polym. Chem. Ed.* **1979**, 17, 1727. e) Lochmann, L.; Müller, A. H. E.; *Prepr., IUPAC Intl. Symp. on Macromol.*, Merseburg, Vol. 1, **1987**, 78. f) Vershney, S. K.; Hautekeer, J. P.; Fayt, R.; Jerome, R.; Teyssie, P. *Macromolecules,* **1990**, 23, 2618. g) Wang, J. S.; Jerome, R.; Bayard, Ph.; Patin, M.; Teyssie, Ph..; Vuillemin, B.; Heim, Ph. *Macromolecules,* **1994**, 27, 4635. h) Wang, J. S.; Bayard, Ph.; Jerome, R.; Varshney, S. K.; Teyssie, Ph. *Macromolecules,* **1994**, 27, 4890.
6. a) Kobayashi, S.; Shoda, S.; Iwata, S.; Abe, M. *Polym. News.* **1990**, 5(1), 15. b) Yasuda, H.; Yamamota, H.; Yamashita, M.; Yokata, K.; Nakamura, A.; Miyake, S.; Kai, Y.; Kanehisa, N. *Macromolecules,* **1993**, 26, 7134. c) Yasuda, H.; Yamamoto, H.; Yokota, K.; Miyake, S.; Nakamura, A. *J. Am. Chem. Soc.* **1992**, 114, 4908.
7. a) Kitayama, T.; Shinozaki, T.; Sakamoto, T.; Yamamoto, M.; Hatada, K. *Makromol. Chem., Suppl.* **1989**, 167, 15. b) Ballard, D. G. H.; Bowlers, R. J.; Haddleton, D. M.; Richards, S. N.; Sellens, R.; Twose, D. L. *Macromolecules,* **1992**, 25, 5907.

8. a) Sivaram, S.; Dhal, P. K.; Kashikar, S. P.; Khisti, R. S.; Shinde, B. M.; Baskaran, D. *Macromolecules,* **1991**, 24, 1698 and *Polym. Bull.* **1991**, 25, 77. b) Raj, D. J. A.; Wadgaonkar, P. P.; Sivaram, S. *Macromolecules,* **1992**, 25, 2774. c) Bandermann, F.; Beckelmann, D.; Broska, D.; Fieberg, A.; Roloff, T.; Wolters, D. *Macromol. Chem. Phys.* **1995**, 196, 2335.

9. Janata, M.; Müller, A. H. E. - Kinetics of n-butylacrylate polymerization using tetrabutylammonium ethyldiethylmalonate as initiators (unpublished results).

10. a) Quirk, R. P. and Bidinger, G. P. *Polym. Bull.* **1989**, 22, 63. b) Quirk, R. P. and Kim, J. S. *J. Phys.Org. Chem.* **1995**, 8, 242.

11. Reetz, M. T.; Hutte, S.; Goddard, R. *J. Phys. Org. Chem.* **1995**, 8, 231.

12. a) Zagala, A. P., Ph.D-Thesis (1996), University of Southern California, Los Angeles, USA. b) Zagala, A. P., Hogen-Esch,T.E, .*Macromolecules,* **1996**, 29, 3038. c) Dimov, D. K.; Hogen-Esch, T. E.; Zagala, A. P.; Müller, A. H. E.; Baskaran, D. *Polym. Prep.(ACS),* **1996**, 37(2), 662.

13. Baskaran, D.; Sivaram, S.; Müller, A. H. E. (communicated to *Macromolecules,* 1996)

14. Baskaran, D.; Kolshorn, H.; Müller A. H. E.; Hogen-Esch, T.E. (communicated to *Angew. Chem.* 1996)

15. Kantlehner, W.; Haug, E.; Mergen, W. W.; Speh, P.; Maier, T.; Kapassakalidis, Brauner, H.J. *Synthesis*, **1983**, 904.

16. Fujisawa, T.; Tajima, K.; Sato, T. *Bull. Chem. Soc. Jpn.,* **1983**, 56, 3529.

17. Bordwell, F. G.; Fried, H. E. *J. Org. Chem.* **1981**, 46, 4327.

18. Bordwell, F. G. *Acc. Chem. Res.* **1988**, 21, 456.

19. Baskaran, D.; Müller, A. H. E.-(research under progress).

20. a) Chang, C. J.; and Hogen-Esch, T. E. *Tetrahedron Lett.*, **1976**, 323. b) Hogen-Esch, T. E. in *J. Phys. Inorg. Chem.*, **1977**, 153-266.

21. Hogen-Esch, T. E.; and Smid, J. *J. Am. Chem. Soc.*, **1966**, 88, 307.